https://www.mdc-berlin.de/de/veroeffentlichungstypen/clinical-journal-club

Als gemeinsame Einrichtung von MDC und Charité fördert das Experimental and Clinical Research Center die Zusammenarbeit zwischen Grundlagenwissenschaftlern und klinischen Forschern. Hier werden neue Ansätze für Diagnose, Prävention und Therapie von Herz-Kreislauf- und Stoffwechselerkrankungen, Krebs sowie neurologischen Erkrankungen entwickelt und zeitnah am Patienten eingesetzt. Sie sind eingeladen, um uns beizutreten. Bewerben Sie sich!

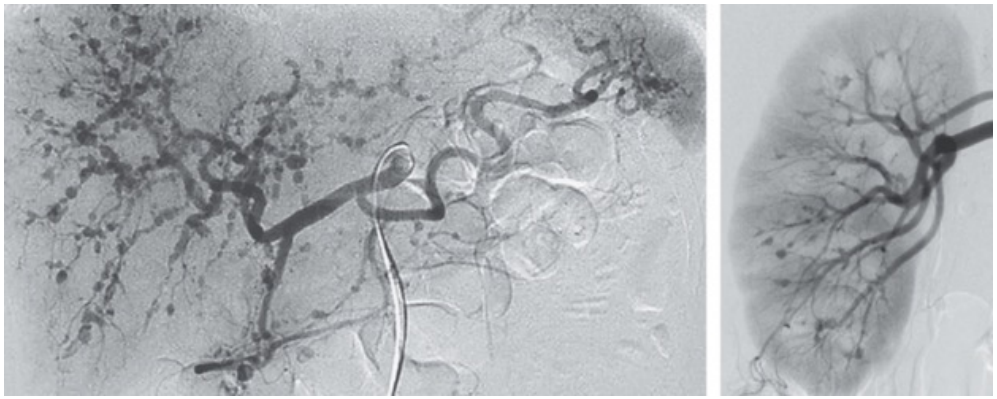

A 62-year-old man presented to the hospital with a 1-month history of muscle aches and weakness in the anterior thighs and the lower posterior aspect of both legs and weight loss of 10 kg. On physical examination, there was numbness of the anterior thighs and posterior lower legs but no skin changes or abdominal tenderness. Laboratory tests showed elevated levels of inflammatory markers. Findings on computed tomography of the chest, abdomen, and pelvis were unremarkable. Tests for antineutrophil cytoplasmic antibodies were negative. Abdominal angiography was performed, shown in the left and right images. What other condition is associated with this patient's diagnosis?

Chronic lymphocytic leukemia

Hepatitits B

HIV

Systemic lupus erythematosus

Tuberculosis

Hepatitis B serologies were negative for this patient. Treatment with oral glucocorticoids and cyclophosphamide was initiated for polyarteritis nodosa. Ten days later, a bowel perforation developed, histopathologic examination of the resected colon showed neutrophilic infiltration and fibrinoid necrosis of the walls of medium-size arteries, as well as disruption of the internal elastic lamina. At follow-up 5 months after presentation, angiography showed resolution of the vascular changes.

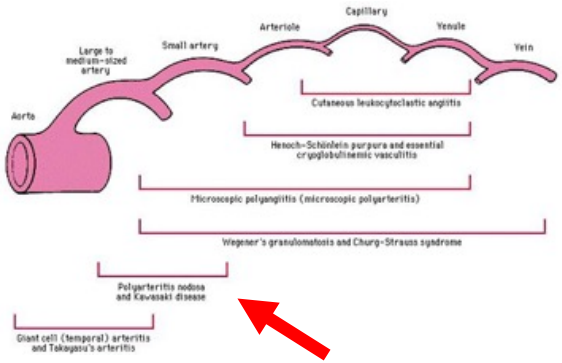

Die Polyarteriitis nodosa, kurz PAN, ist eine Vaskulitis der mittelgroßen Arterien. Sie wird auch als klassische Polyarteriitis nodosa bezeichnet (cPAN), um sie von der mikroskopischen Polyangiitis (mPA) abzugrenzen.

Die Ätiologie ist immer noch ungeklärt (2023), die Polyarteriitis nodosa ist am ehesten als Autoimmunerkrankung aufzufassen. Eine Assoziation besteht zur Hepatitis B, die bei etwa einem Drittel der Patienten vorliegt. Das HBs-Antigen kann bei diesen Fällen in den Läsionen der Polyarteriitis nodosa nachgewiesen werden, was auf einen Immunkomplex-vermittelten Pathomechanismus hinweist.
Darüber hinaus findet sich in weiteren Fällen eine Hepatitis C oder eine HIV-Infektion. Auch im Rahmen einer Haarzellleukämie kann eine PAN auftreten.

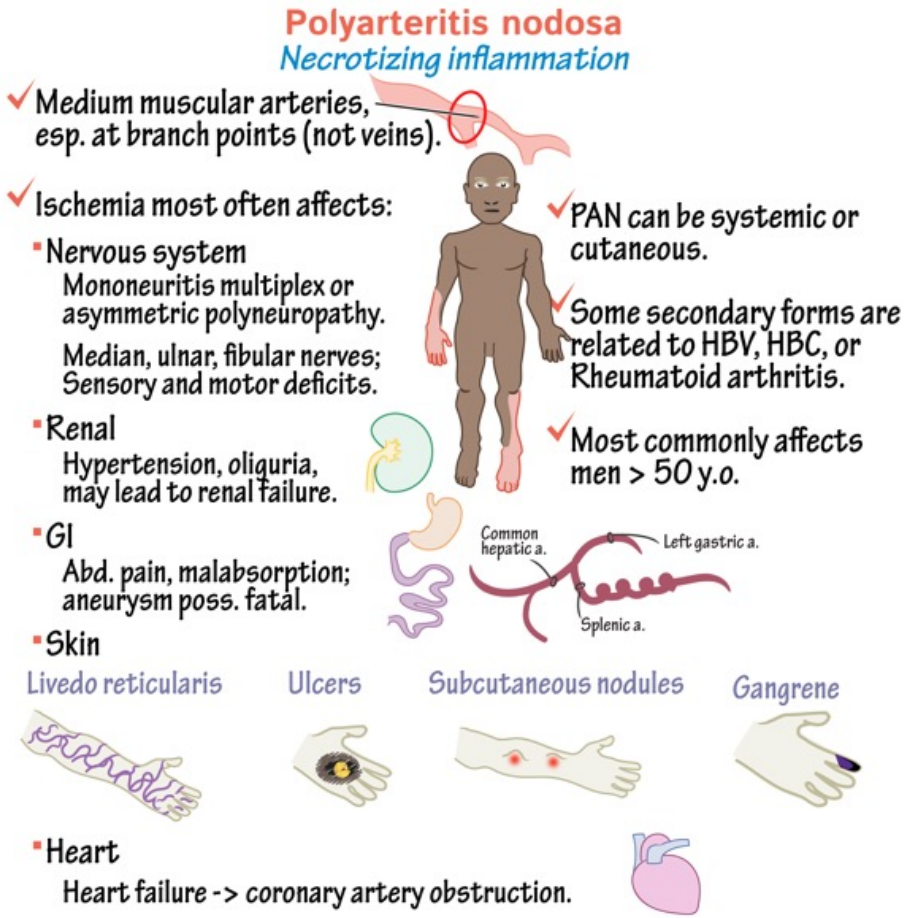

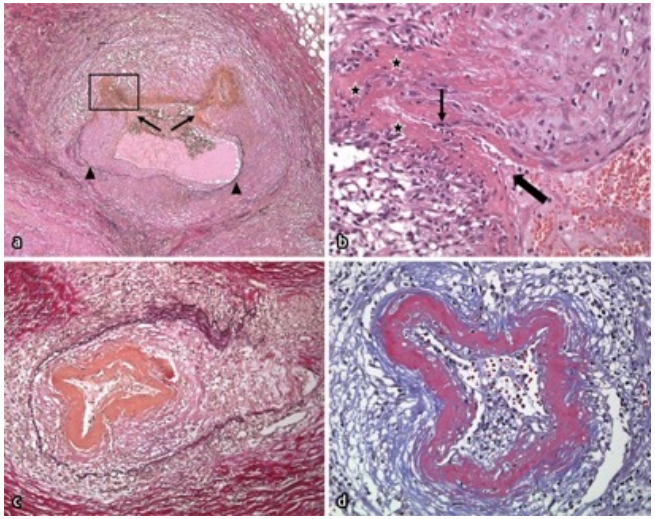
a
b
c
d

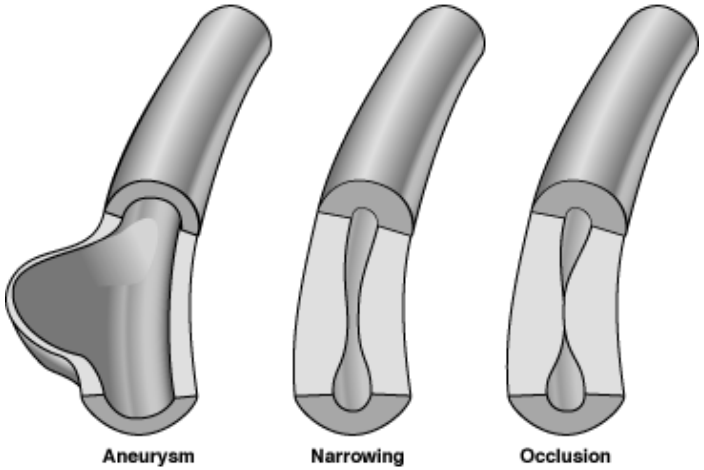
Aneurysm
Narrowing
Occlusion

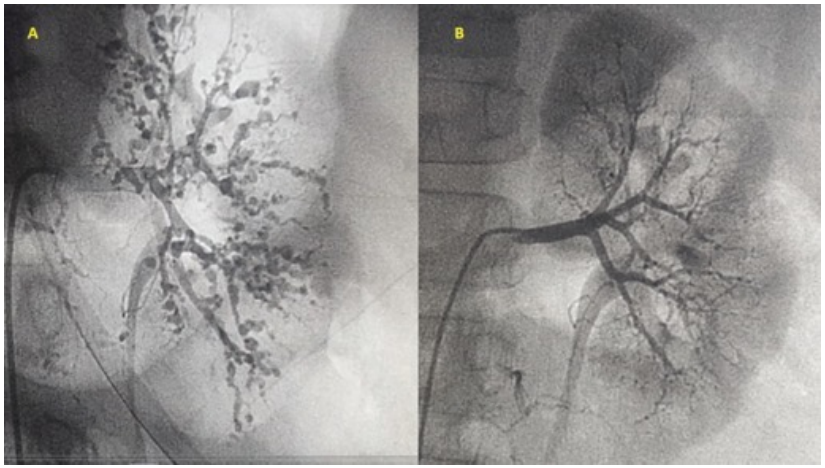
A
B

Falciparum Malaria

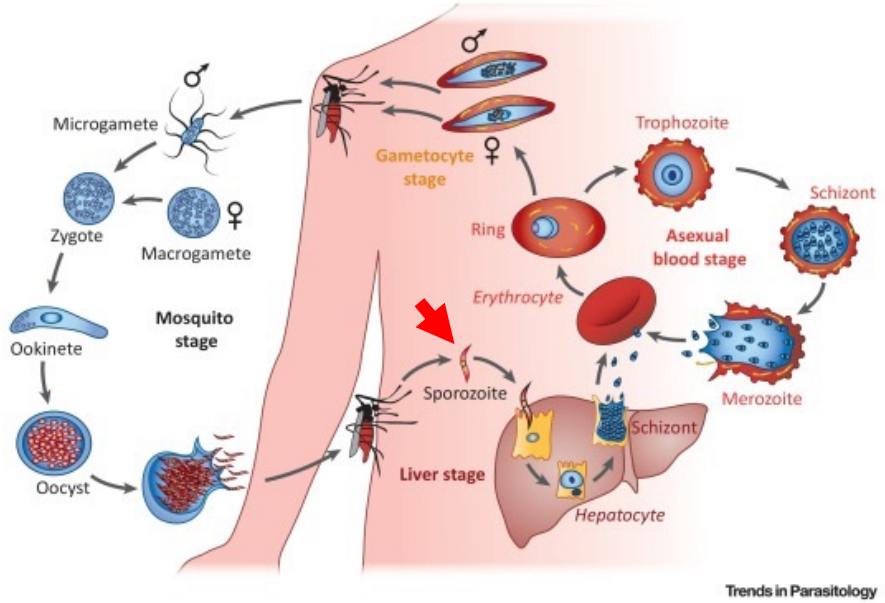

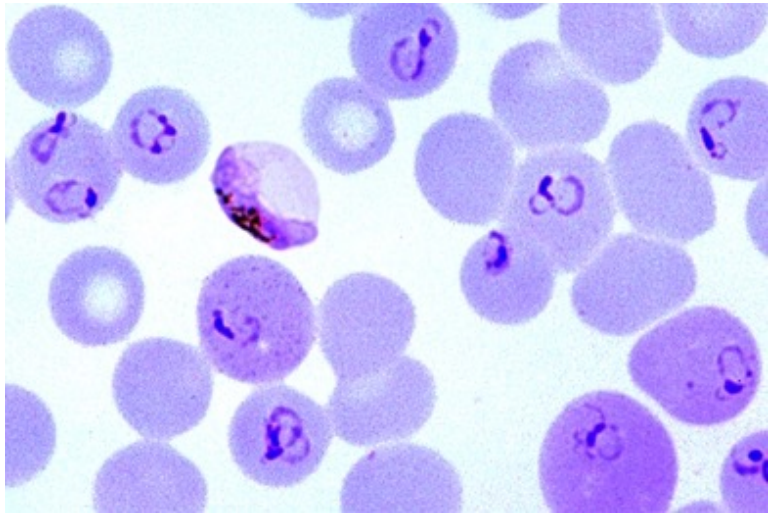

Passive immunity

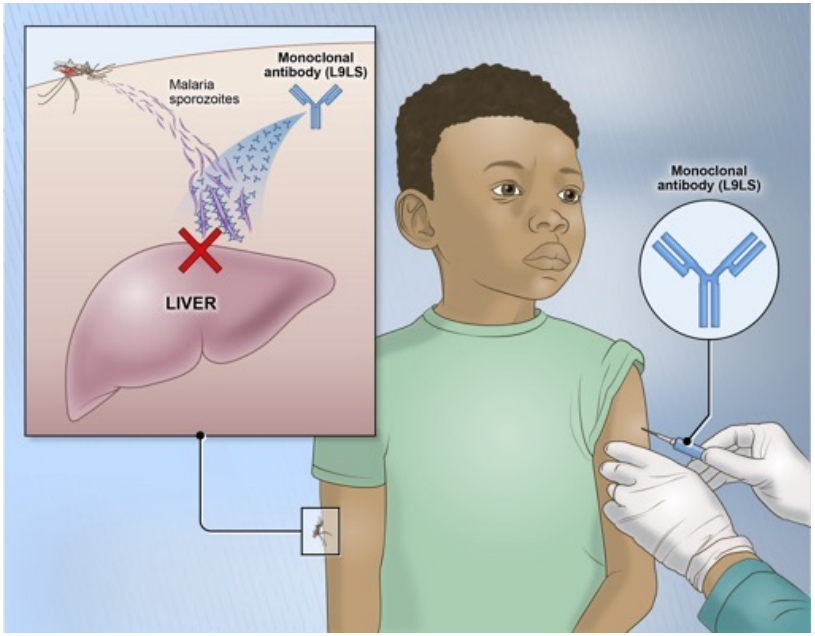

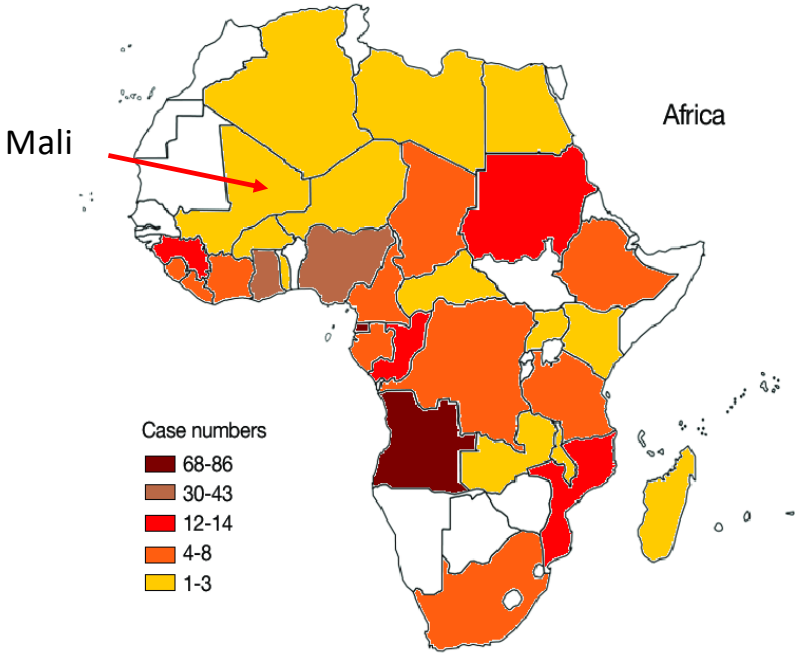

Subcutaneous Administration of a Monoclonal Antibody to Prevent Malaria

Subcutaneous administration of the monoclonal antibody L9LS protected adults against controlled *Plasmodium falciparum* infection in a phase 1 trial. Whether a monoclonal antibody administered subcutaneously can protect children from *P. falciparum* infection in a region where this organism is endemic is unclear. We conducted a phase 2 trial in Mali to assess the safety and efficacy of subcutaneous administration of L9LS in children 6 to 10 years of age over a 6-month malaria season. In part A of the trial, safety was assessed at three dose levels in adults, followed by assessment at two dose levels in children. In part B of the trial, children were randomly assigned, in a 1:1:1 ratio, to receive 150 mg of L9LS, 300 mg of L9LS, or placebo. The primary efficacy end point, assessed in a time-to-event analysis, was the first *P. falciparum* infection, as detected on blood smear performed at least every 2 weeks for 24 weeks. A secondary efficacy end point was the first episode of clinical malaria, as assessed in a time-to-event analysis.

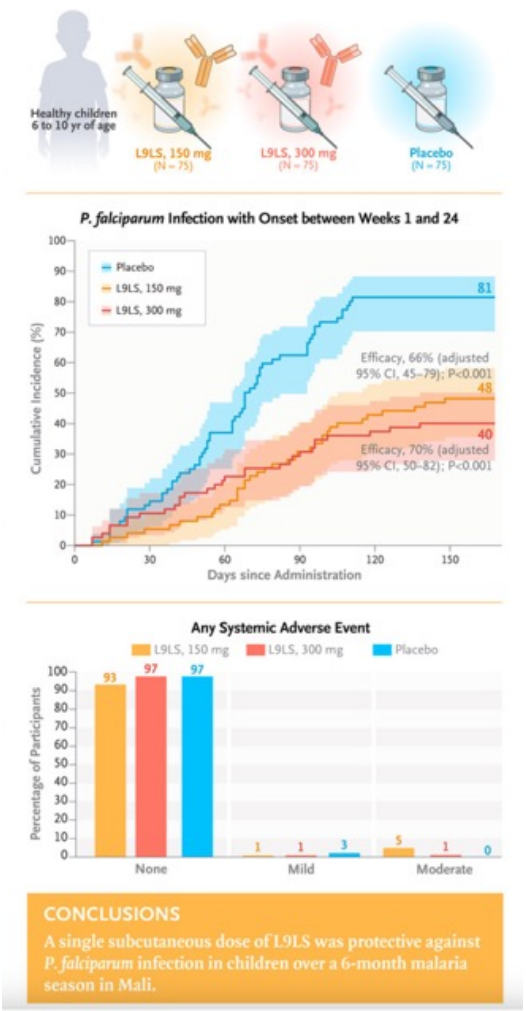

Plasmodium falciparum causes more than 600,000 deaths from malaria annually, mostly among children in Africa. Despite the widespread use of mosquito-control measures, chemoprevention, and case management, little progress has been made in reducing malaria mortality in recent years, a trend that could worsen with increasing resistance to antimalarial drugs and insecticides. Thus, the development of new interventions to reduce malaria mortality is needed.

In 2021, the World Health Organization (WHO) recommended the RTS,S/AS01 vaccine for use in children; four doses of the vaccine had 36% efficacy against malaria over a 4-year period among children 5 to 17 months of age. The WHO also recently endorsed the R21/Matrix-M vaccine for use in children. In locations where monthly seasonal malaria chemoprevention is the standard care during the 4-to-6-month malaria season, a three-dose regimen of the R21/Matrix-M vaccine had 75% efficacy over a 12-month period among children 5 to 36 months of age, and a booster after 12 months was necessary to maintain efficacy. When given seasonally, the RTS,S/AS01 and R21/Matrix-M vaccines have similar efficacy.

In 2021, the World Health Organization (WHO) recommended the RTS,S/AS01 vaccine for use in children; four doses of the vaccine had 36% efficacy against malaria over a 4-year period among children 5 to 17 months of age. The WHO also recommends malaria chemoprevention in high-risk populations, such as infants and young children, children with severe anemia after hospital discharge who are at risk for fatal malaria, and pregnant persons. In a phase 2 trial involving adults in Mali, an intravenous infusion of CIS43LS, a monoclonal antibody with an extended half-life that targets a conserved junctional epitope on the *P. falciparum* circumsporozoite protein (PfCSP), was administered at a dose of 10 mg per kilogram of body weight or 40 mg per kilogram. Over a 6-month malaria season, this monoclonal antibody provided protective efficacy against *P. falciparum* infection of 75.0% and 88.2% at the doses of 10 mg per kilogram and 40 mg per kilogram, respectively.

Methods

Trial Objectives, Participants, and Oversight

We conducted this trial in Kalifabougou and Torodo, Mali, where *P. falciparum* is endemic and is transmitted from July through December.

Trial Product

L9LS is a human IgG1 monoclonal antibody that is produced in accordance with current Good Manufacturing Practices by means of cell-culture expression in a recombinant Chinese hamster ovary-cell line.

Trial Procedures

Age Deescalation and Dose-Escalation Trial (Part A)

For part A, we prespecified that 18 adults would be assigned in open-label fashion to receive L9LS at a dose of 300 mg or 600 mg, administered subcutaneously, or 20 mg per kilogram of body weight, administered intravenously; each group included 6 participants.

Randomized, Placebo-Controlled Trial (Part B)

Children were randomly assigned (in a 1:1:1 ratio) by means of block randomization to receive 150 mg of L9LS, 300 mg of L9LS, or normal saline placebo. L9LS or placebo was administered subcutaneously. Randomization was stratified according to body weight (26 to 30 kg, 20 to 25 kg, or 15 to 19 kg, with 75 participants in each stratum).

The primary efficacy end point was *P. falciparum* blood-stage infection (regardless of the presence of symptoms) as detected by means of microscopic examination of thick blood-smear samples obtained at least every 2 weeks during scheduled trial visits and unscheduled illness visits.

Clinical malaria (a secondary efficacy end point) was detected during scheduled and unscheduled visits. The first definition of clinical malaria (definition 1) was a body temperature of at least 37.5°C or a history of fever in the previous 24 hours and *P. falciparum* asexual parasitemia of more than 5000 parasites per cubic millimeter.

Characteristics of the Participants at Baseline in the Efficacy Trial (Part B).

Characteristic	L9LS, 150 mg (N=75)	L9LS, 300 mg (N=75)	Placebo (N=75)
Median age (range) — yr	8 (6–10)	8 (6–10)	7 (6–10)
Sex — no. (%)			
Female	31 (41)	33 (44)	36 (48)
Male	44 (59)	42 (56)	39 (52)
Median weight (range) — kg	24 (16–30)	22 (16–30)	23 (15–30)
Site — no. (%)			
Kalifabougou	56 (75)	49 (65)	52 (69)
Torodo	19 (25)	26 (35)	23 (31)
Any plasmodium species detected on blood-smear examination at enrollment — no. (%)	14 (19)	13 (17)	12 (16)
Plasmodium falciparum	12 (16)	13 (17)	12 (16)
P. malariae	2 (3)	0	0
P. ovale	0	0	0
Median interval between administration of artemether–lumefantrine and L9LS or placebo (range) — days	7 (7–12)	7 (6–10)	7 (7–12)
Hemoglobin genotype — no. (%)			
Hemoglobin AA	57 (76)	62 (83)	64 (85)
Hemoglobin AS	11 (15)	7 (9)	6 (8)
Hemoglobin AC	6 (8)	6 (8)	5 (7)
Hemoglobin CC	1 (1)	0	0
Hemoglobin SC	0	0	0

Efficacy against *P. falciparum* Infection

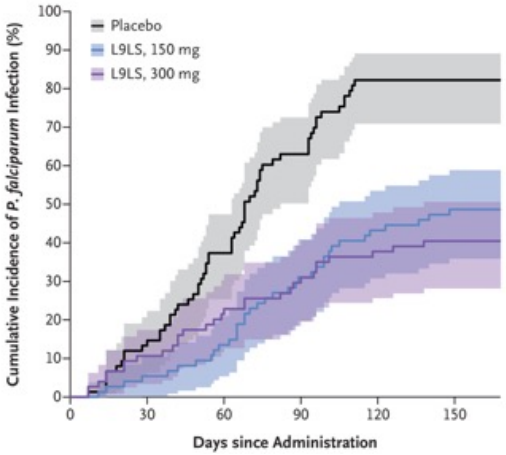

Efficacy against Clinical Malaria.

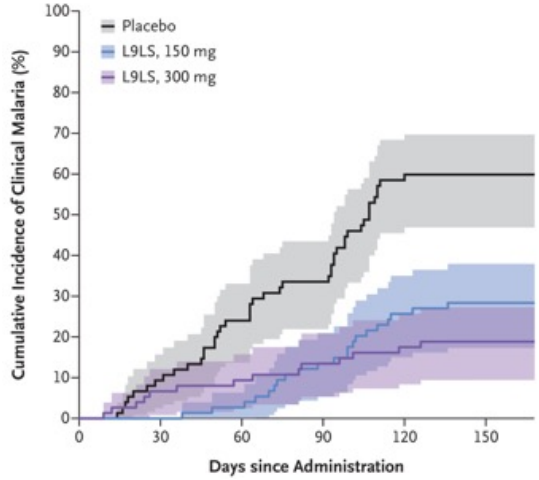

Solicited Maximum Local and Systemic Reactogenicity Events within 7 Days after Administration of L9LS or Placebo in the Efficacy Trial (Part B).

Symptom and Severity†	L9LS, 150 mg (N=75)	L9LS, 300 mg (N=75)	Placebo (N=75)
	number of participants (percent)		
Local reactogenicity events‡			
Pain			
None	74 (99)	75 (100)	74 (99)
Mild	1 (1)	0	1 (1)
Pruritus			
None	75 (100)	75 (100)	74 (99)
Mild	0	0	1 (1)
Swelling			
None	74 (99)	72 (96)	75 (100)
Mild	1 (1)	3 (4)	0
Any local symptom			
None	73 (97)	72 (96)	73 (97)
Mild	2 (3)	3 (4)	2 (3)
Systemic reactogenicity events§			
Fever			
None	72 (96)	75 (100)	74 (99)
Mild	1 (1)	0	1 (1)
Moderate	2 (3)	0	0
Headache			
None	73 (97)	74 (99)	74 (99)
Mild	0	0	1 (1)
Moderate	2 (3)	1 (1)	0
Chills			
None	75 (100)	74 (99)	75 (100)
Mild	0	1 (1)	0
Any systemic symptom			
None	70 (93)	73 (97)	73 (97)
Mild	1 (1)	1 (1)	2 (3)
Moderate	4 (5)	1 (1)	0

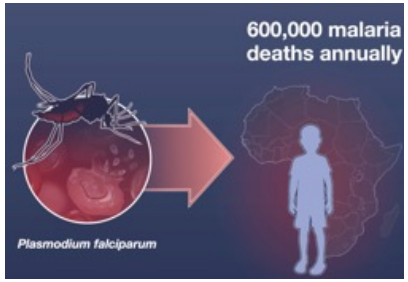

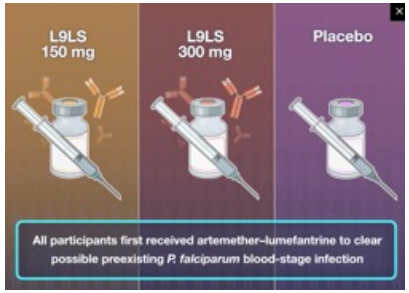

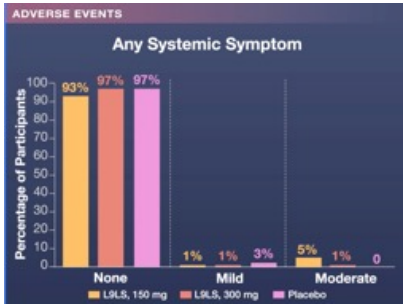

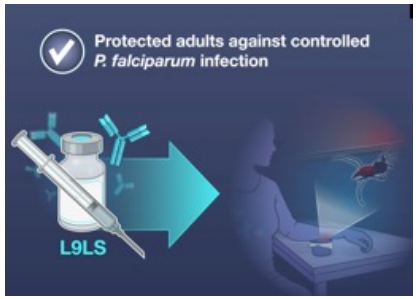

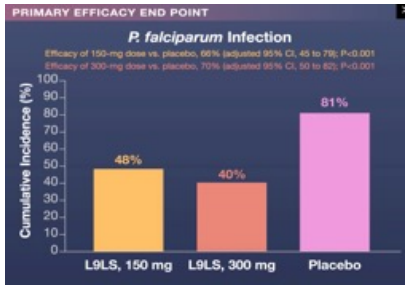

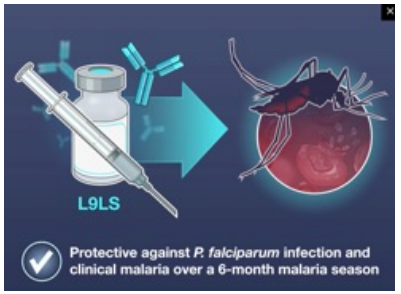

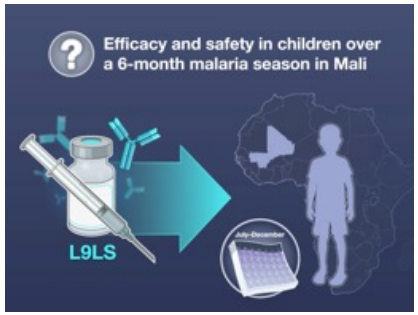

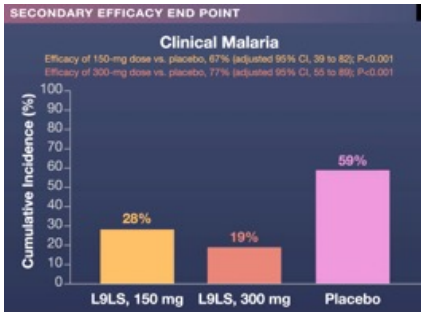

LIMITATIONS AND REMAINING QUESTIONS

Further study is necessary to understand the following:

- The efficacy of administering L9LS with an antimalarial drug to mitigate the risk of preexisting and early infections, particularly in high-transmission areas.
- The efficacy and safety of antimalarial monoclonal antibodies in infants and young children, children with severe anemia after hospital discharge, and pregnant persons.

Reverse cholesterol transport via HDL

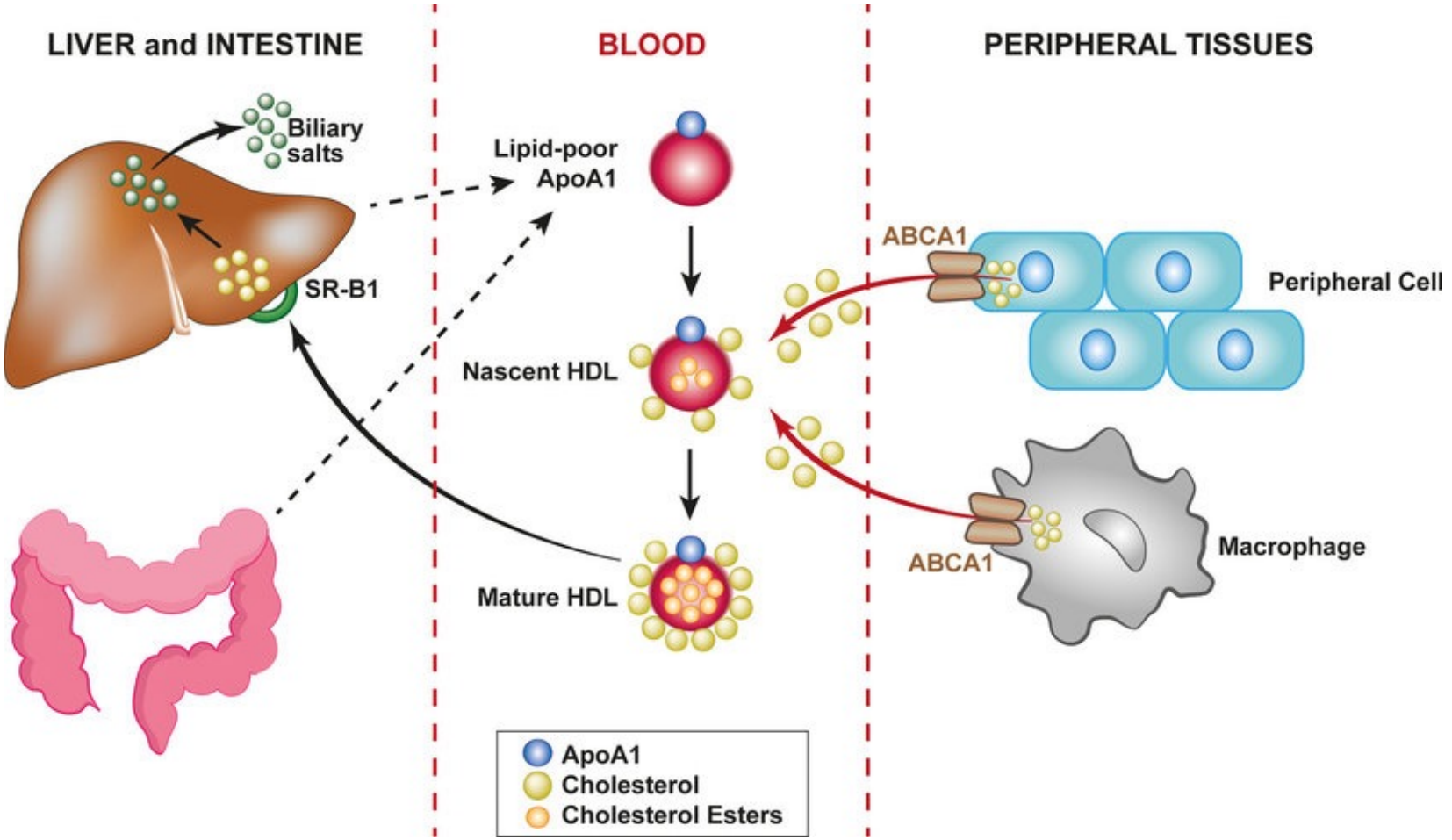

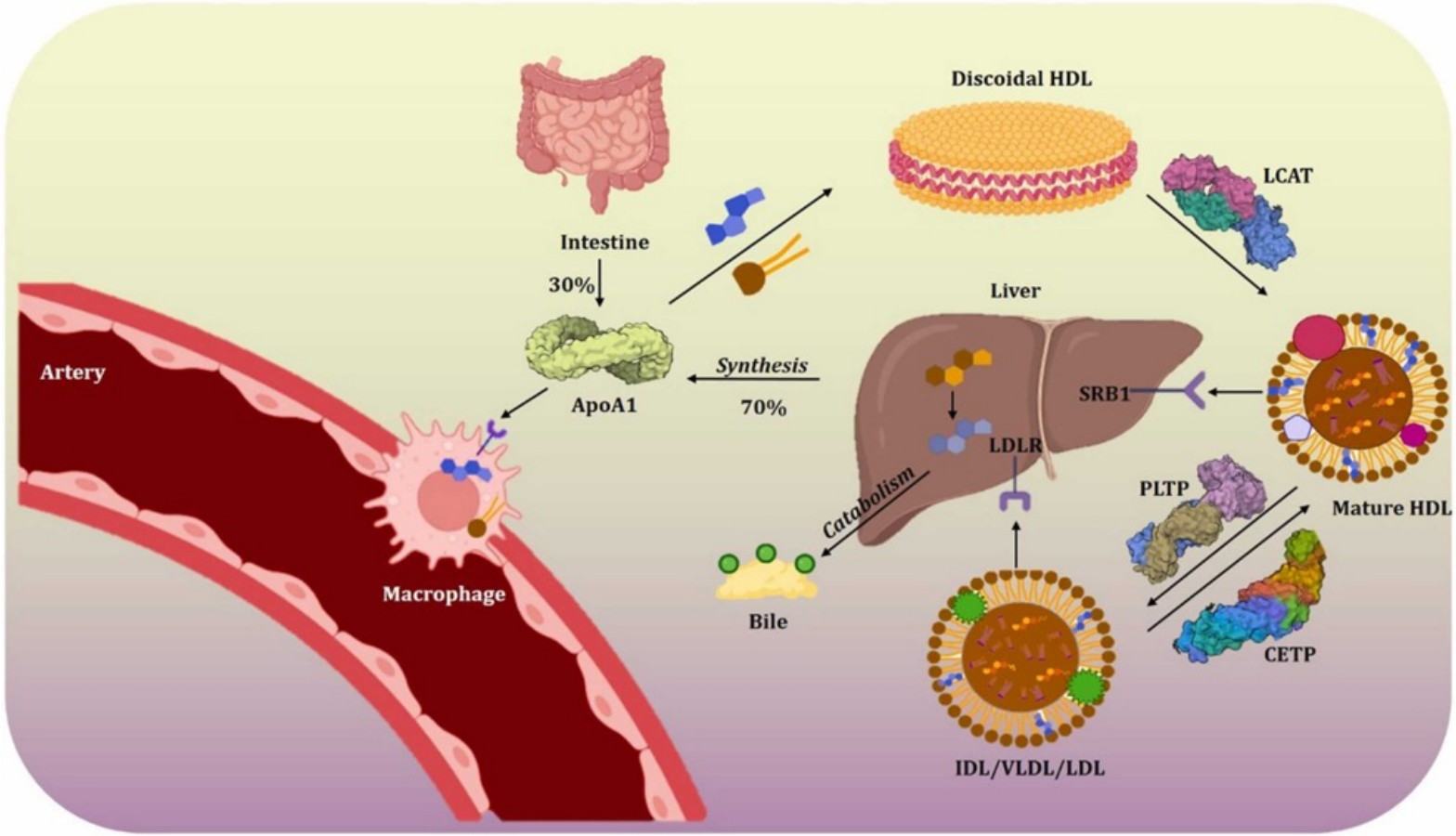
Discoidal HDL
LCAT
Intestine
30%
Liver
Synthesis
70%
ApoA1
Artery
SRB1
LDLR
Catabolism
PLTP
Mature HDL
Macrophage
Bile
CETP
IDL/VLDL/LDL

Apolipoprotein A1 Infusions and Cardiovascular Outcomes after Acute Myocardial Infarction

Cardiovascular events frequently recur after acute myocardial infarction, and low cholesterol efflux — a process mediated by apolipoprotein A1, which is the main protein in high-density lipoprotein — has been associated with an increased risk of cardiovascular events. CSL112 is human apolipoprotein A1 derived from plasma that increases cholesterol efflux capacity. Whether infusions of CSL112 can reduce the risk of recurrent cardiovascular events after acute myocardial infarction is unclear. We conducted an international, double-blind, placebo-controlled trial involving patients with acute myocardial infarction, multivessel coronary artery disease, and additional cardiovascular risk factors. Patients were randomly assigned to receive either four weekly infusions of 6 g of CSL112 or matching placebo, with the first infusion administered within 5 days after the first medical contact for the acute myocardial infarction. The primary end point was a composite of myocardial infarction, stroke, or death from cardiovascular causes from randomization through 90 days of follow-up.

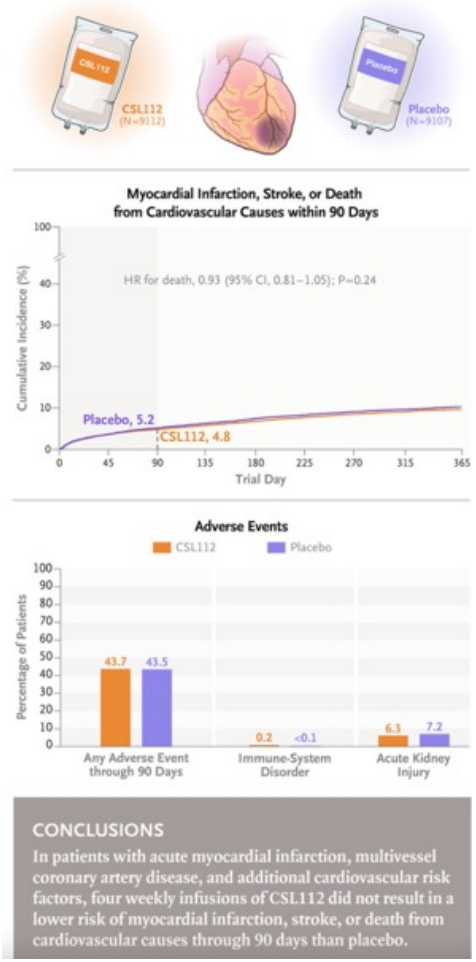

Reverse cholesterol transport is the mechanism by which excess cholesterol, such as atherosclerotic plaque, is removed from peripheral tissues and transported to the liver for excretion in the bile. The initial step in reverse cholesterol transport involves cholesterol efflux, which is mediated predominantly by apolipoprotein A1, the main protein in high-density lipoproteins (HDLs). Patients with acute coronary syndromes have an impaired cholesterol efflux capacity, which has been independently associated with a higher incidence of major adverse cardiovascular events, including a higher incidence of both short-term (30-day) and long-term death from any cause in patients who have had an acute myocardial infarction event.

CSL112 is human plasma–derived apolipoprotein A1 that is formulated with phosphatidylcholine to form disk-shaped particles that are suitable for intravenous infusion. In previous studies, a 6-g dose of CSL112 resulted in immediate and robust increases in apolipoprotein A1 levels (to twice the baseline level) and cholesterol efflux capacity (to four times that of baseline). A dosing regimen of four weekly infusions was chosen to maximize exposure but minimize accumulation in a logistically practical way during the weeks after acute myocardial infarction. We hypothesized that CSL112 administered weekly for 4 weeks beginning immediately after the occurrence of acute myocardial infarction would reduce the risk of myocardial infarction, stroke, and death from cardiovascular causes.

Baseline Characteristics of the Patients.

Characteristic	CSL112 (N=9112)	Placebo (N=9107)
Age		
Mean — yr	65.6±10.1	65.4±10.2
≥65 yr — no. (%)	5418 (59.5)	5341 (58.6)
Male sex — no. (%)	6786 (74.5)	6721 (73.8)
Race or ethnic group — no. (%)†		
White	7769 (85.3)	7698 (84.5)
Asian	743 (8.2)	781 (8.6)
Black	181 (2.0)	181 (2.0)
Other	373 (4.1)	402 (4.4)
Hispanic or Latino	1566 (17.2)	1596 (17.5)
Geographic region — no. (%)		
Western Europe	2459 (27.0)	2455 (27.0)
Central and eastern Europe	3134 (34.4)	3136 (34.4)
Latin America	1456 (16.0)	1453 (16.0)
North America	1178 (12.9)	1175 (12.9)
Asia Pacific	885 (9.7)	888 (9.8)
Body-mass index‡	29.02±4.99	29.08±5.16
Current smoker — no. (%)	2367 (26.0)	2378 (26.1)
Medical history — no. (%)		
Diabetes requiring pharmacotherapy	6280 (68.9)	6246 (68.6)
Peripheral artery disease	1140 (12.5)	1161 (12.7)
Previous myocardial infarction	3325 (36.5)	3353 (36.8)
Previous coronary revascularization	3504 (38.5)	3500 (38.4)
Heart failure	896 (9.8)	951 (10.4)
Ischemic stroke	468 (5.1)	491 (5.4)
Hypertension	7263 (79.7)	7210 (79.2)
Hypercholesterolemia	5839 (64.1)	5781 (63.5)
Type of index myocardial infarction — no. (%)		
STEMI	4606 (50.5)	4600 (50.5)
NSTEMI	4506 (49.5)	4507 (49.5)
Procedure performed for index myocardial infarction — no. (%)		
Coronary angiography	8869 (97.3)	8868 (97.4)
Percutaneous coronary intervention	8037 (88.2)	7997 (87.8)
Medications at randomization — no. (%)		
Aspirin	8489 (93.2)	8473 (93.0)
P2Y12 inhibitor or other antiplatelet agent	8508 (93.4)	8490 (93.2)
HMG-CoA reductase inhibitor, a statin	8429 (92.5)	8424 (92.5)
High-intensity statin therapy§	6871 (75.4)	6890 (75.7)
Median lipid value (IQR) — mg/dl¶		
Total cholesterol	160 (133–192)	159 (133–190)
LDL cholesterol	84 (61–112)	84 (62–111)
HDL cholesterol	39 (33–46)	39 (33–47)
Triglycerides	156 (117–212)	153 (117–208)
Renal function — no. (%)‖		
Normal, eGFR ≥90 ml/min/1.73 m^2	2260 (24.8)	2256 (24.8)
Mild impairment, eGFR ≥60 to <90 ml/min/1.73 m^2	4496 (49.3)	4436 (48.7)
Moderate impairment, eGFR ≥30 to <60 ml/min/1.73 m^2	2017 (22.1)	2134 (23.4)
Severe impairment, eGFR <30 ml/min/1.73 m^2	60 (0.7)	45 (0.5)

Primary and Secondary Efficacy End Points

End Point	CSL112 (N=9112)	Placebo (N=9107)	Hazard Ratio (95% CI)
Primary end point — no. of patients (%)			
Composite of myocardial infarction, stroke, or death from cardiovascular causes through 90 days†	439 (4.8)	472 (5.2)	0.93 (0.81–1.05)
Myocardial infarction through 90 days	312 (3.5)	342 (3.8)	0.91 (0.78–1.06)
Stroke through 90 days	57 (0.6)	49 (0.5)	1.15 (0.79–1.69)
Death from cardiovascular causes through 90 days	107 (1.2)	128 (1.4)	0.83 (0.64–1.07)
Key secondary efficacy end points			
No. of hospitalizations for coronary, cerebral, or peripheral ischemia at 90 days (mean rate over 90 days)	433 (0.045)	442 (0.047)	0.97 (0.84–1.12)‡
Composite of myocardial infarction, stroke, or death from cardiovascular causes through 180 days — no. of patients (%)	622 (6.9)	683 (7.6)	0.91 (0.81–1.01)
Myocardial infarction, stroke, or death from cardiovascular causes through 365 days — no. of patients (%)	885 (9.8)	944 (10.5)	0.93 (0.85–1.02)
Other secondary efficacy end points — no. of patients (%)			
Death from any cause at 365 days	341 (3.8)	345 (3.8)	0.98 (0.84–1.14)
Myocardial infarction through 180 days	450 (5.0)	513 (5.7)	0.87 (0.77–0.99)
Myocardial infarction through 365 days	638 (7.2)	705 (7.9)	0.90 (0.81–1.00)
Stroke through 180 days	81 (0.9)	71 (0.8)	1.13 (0.82–1.56)
Stroke through 365 days	115 (1.3)	109 (1.2)	1.05 (0.89–1.36)
Death from cardiovascular causes through 180 days	150 (1.7)	169 (1.9)	0.88 (0.71–1.10)
Death from cardiovascular causes through 365 days	230 (2.6)	242 (2.7)	0.94 (0.79–1.13)

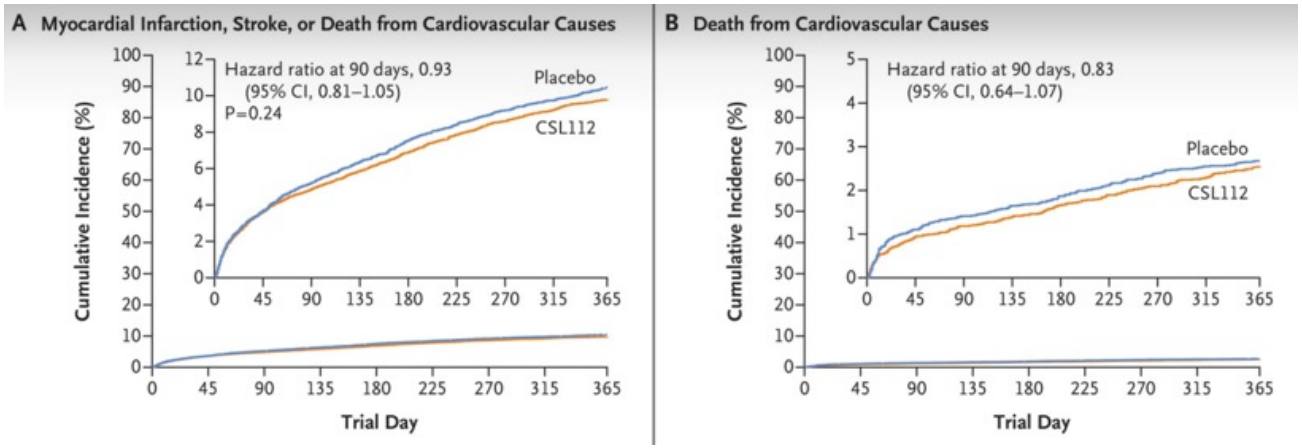

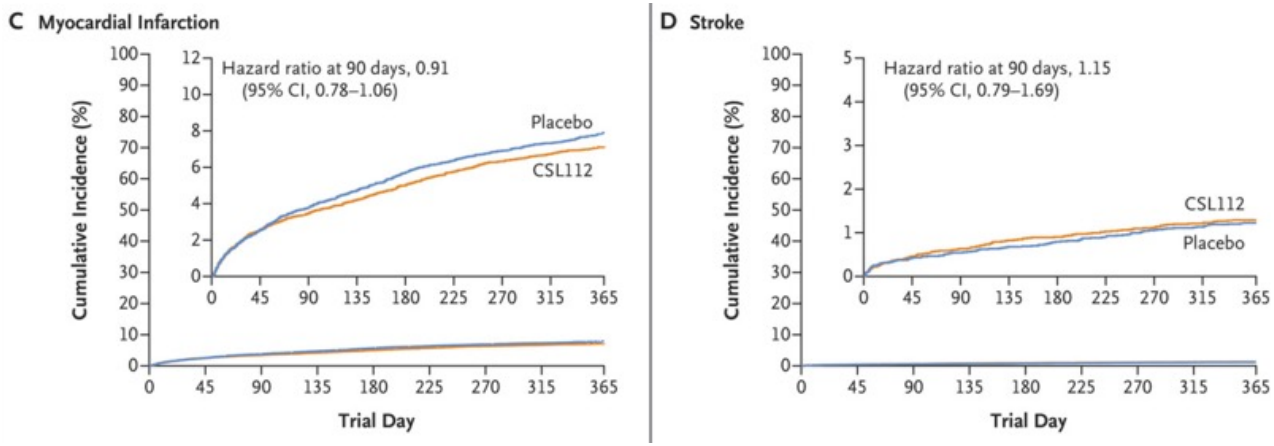

Primary Efficacy End Point and Individual Components of the Primary End Point.

Panel A shows the cumulative incidence of a composite of myocardial infarction, stroke, or death from cardiovascular causes through 90 days (primary end point) and through 180 and 365 days (key secondary end points).

Panels B, C, and D show the cumulative incidence of the individual components of the composite end point through 365 days. All assessments were performed in a time-to-first-event analysis. The insets show the data on an enlarged y axis.

Investigator-Reported Adverse Events.

Event	CSL112 (N=9010)	Placebo (N=9027)	P Value†
	no. of patients (%)		
Any adverse event from the beginning of the treatment period through 90 days	3938 (43.7)	3927 (43.5)	0.79
Serious adverse events	1514 (16.8)	1557 (17.2)	0.43
Cardiac disorders	513 (5.7)	514 (5.7)	1.00
Infections and infestations	394 (4.4)	401 (4.4)	0.83
Gastrointestinal disorders	168 (1.9)	176 (1.9)	0.70
Renal and urinary disorders	151 (1.7)	138 (1.5)	0.44
Respiratory, thoracic, and mediastinal disorders	116 (1.3)	120 (1.3)	0.84
Nonfatal adverse events leading to permanent discontinuation of the investigational product, irrespective of seriousness	221 (2.5)	214 (2.4)	0.73
Renal and urinary disorders	39 (0.4)	51 (0.6)	0.24
Infections and infestations	35 (0.4)	33 (0.4)	0.81
Skin and subcutaneous tissue disorders	31 (0.3)	24 (0.3)	0.35
Investigations	29 (0.3)	19 (0.2)	0.15
Immune-system disorders	14 (0.2)	4 (<0.1)	0.02
Prespecified adverse events of special interest, irrespective of seriousness			
Hypersensitivity‡	214 (2.4)	206 (2.3)	0.69
Serious hypersensitivity events‡	17 (0.2)	15 (0.2)	0.73
Acute kidney injury§	570 (6.3)	650 (7.2)	0.02
Potential hepatic injury¶	39 (0.4)	25 (0.3)	0.08
New or worsening heart failure‖	281 (3.1)	262 (2.9)	0.41

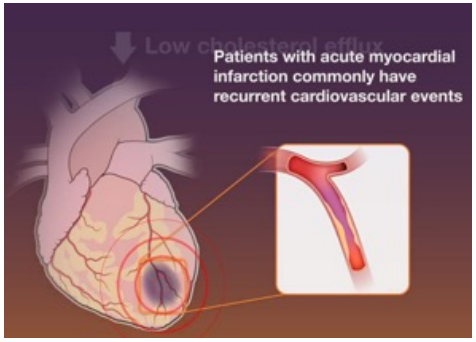
Low cholesterol efflux
Patients with acute myocardial infarction commonly have recurrent cardiovascular events

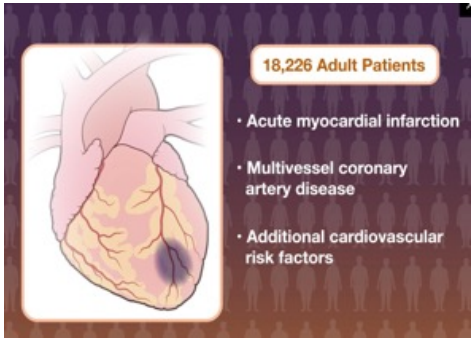
18,226 Adult Patients
• Acute myocardial infarction
• Multivessel coronary artery disease
• Additional cardiovascular risk factors

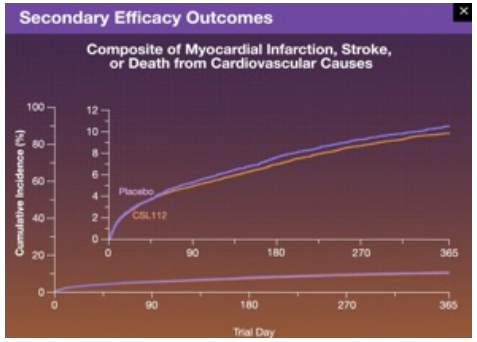
Secondary Efficacy Outcomes
Composite of Myocardial Infarction, Stroke, or Death from Cardiovascular Causes
Cumulative Incidence (%)
Placebo
CSL112
Trial Day

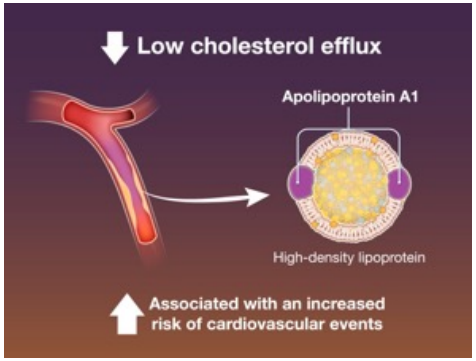
Low cholesterol efflux
Apolipoprotein A1
High-density lipoprotein
Associated with an increased risk of cardiovascular events


4 Weekly Infusions
CSL112
Placebo
N=9112
N=9107
First infusion given within 5 days after first medical contact for the index myocardial infarction

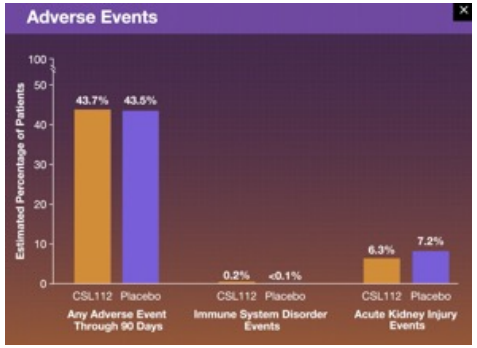
Adverse Events
Estimated Percentage of Patients
43.7%
43.5%
0.2%
<0.1%
6.3%
7.2%
CSL112 Placebo
Any Adverse Event Through 90 Days
Immune System Disorder Events
Acute Kidney Injury Events


CSL112
Human plasma–derived apolipoprotein A1
Would lower the risk of recurrent cardiovascular events after acute myocardial infarction

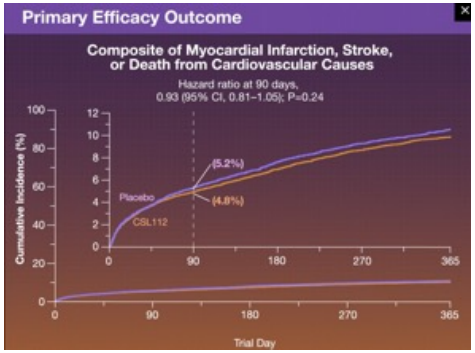
Primary Efficacy Outcome
Composite of Myocardial Infarction, Stroke, or Death from Cardiovascular Causes
Hazard ratio at 90 days, 0.93 (95% CI, 0.81–1.05); P=0.24
Cumulative Incidence (%)
(5.2%)
(4.8%)
Placebo
CSL112
Trial Day

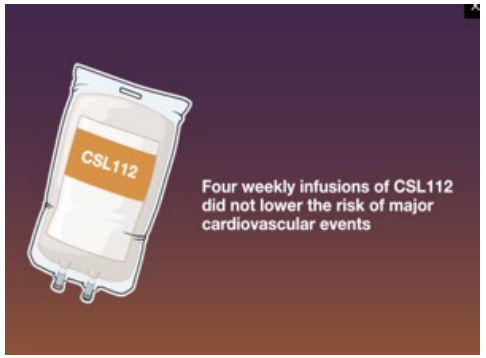
CSL112
Four weekly infusions of CSL112 did not lower the risk of major cardiovascular events

Bei der Transkatheter-Aortenklappen-Implantation (TAVI) wird eine Ersatzklappe in zusammengefalteter Form an der Spitze eines Katheter-Schlauchs zum Herzen eingeführt und dort an der richtigen Stelle zur Entfaltung gebracht. Der gesamte Vorgang erfolgt unter permanenter Röntgenüberwachung an hochauflösenden Monitoren.

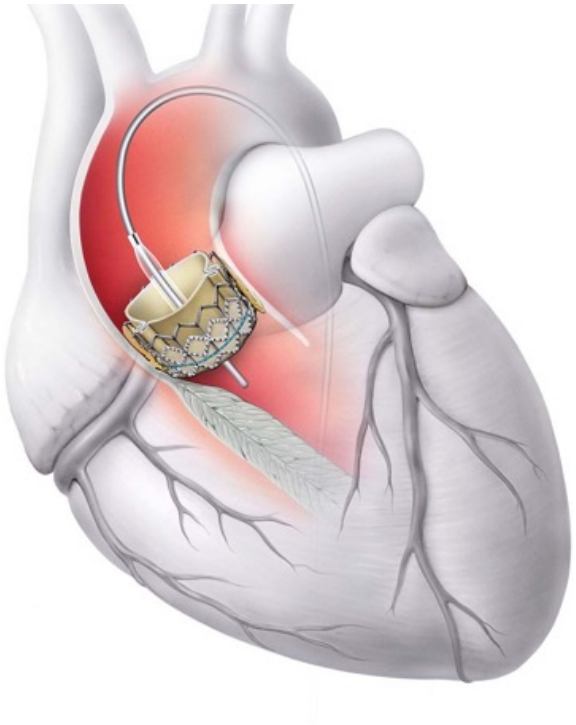

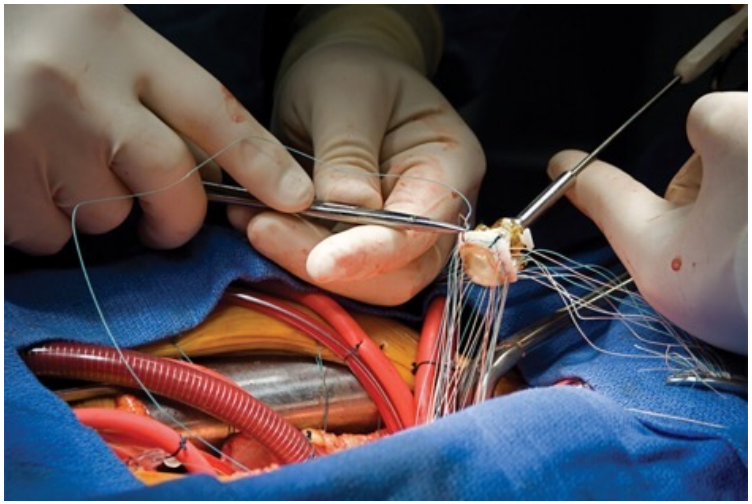

Surigal aortic valve replacement (SAVR). Das operative Vorgehen besteht darin, sämtliche Aortenwandanteile inklusive der Sinus aortae wegzuschneiden, die Klappen- und Ringanteile aber zu belassen. Die Abgänge der Koronararterien werden als sogenannte Buttons (Knöpfe) isoliert. Der gesamte Klappenapparat wird nun innerhalb einer Rohrprothese mit oder ohne ausgebildete Sinus implantiert und der Ring durch U-Nähte stabilisiert (Verfahren nach David).

Transcatheter or Surgical Treatment of Aortic-Valve Stenosis

Among low-risk patients with severe, symptomatic aortic stenosis who are eligible for both transcatheter aortic-valve implantation (TAVI) and surgical aortic-valve replacement (SAVR), data are lacking on the appropriate treatment strategy in routine clinical practice. In this randomized noninferiority trial conducted at 38 sites in Germany, we assigned patients with severe aortic stenosis who were at low or intermediate surgical risk to undergo either TAVI or SAVR. Percutaneous- and surgical-valve prostheses were selected according to operator discretion. The primary outcome was a composite of death from any cause or fatal or nonfatal stroke at 1 year.

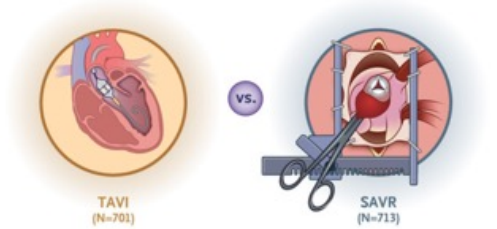

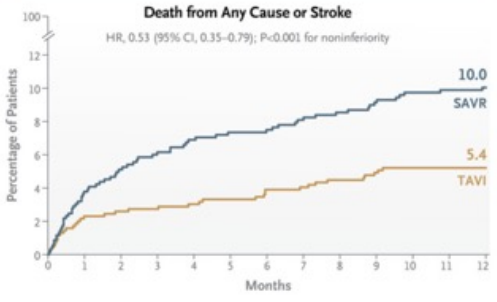

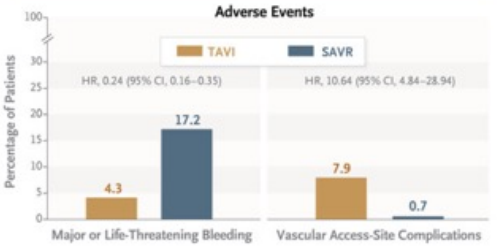

CONCLUSIONS

In patients with severe, symptomatic aortic-valve stenosis and low or intermediate surgical risk, TAVI was noninferior to SAVR with respect to a composite outcome of death or stroke at 1 year.

Transcatheter aortic-valve implantation (TAVI) is increasingly performed in patients with severe, symptomatic aortic-valve stenosis. In younger patients at low surgical risk, both TAVI and surgical aortic-valve replacement (SAVR) may be applicable, although the appropriate treatment strategy in this population remains subject to the considerations of individual heart teams. TAVI has evolved as a treatment option for younger and lower-risk patients and is increasingly used in clinical practice. However, these trials were sponsored by industry and tested specific transcatheter heart-valve devices in selected patient populations, which limits the applicability of the results to inform routine clinical practice. Insufficient evidence remains regarding the comparison of TAVI and SAVR in a patient population mirroring the real-world setting in which operators have unrestricted access to several contemporary transcatheter heart-valve devices. A pragmatic clinical trial comparing TAVI with SAVR should allow for valve selection by the local heart team on the basis of individual patient anatomical and medical considerations after randomization to the treatment strategy.
To address these issues, we designed the pragmatic DEDICATE trial (Randomized, Multicenter, Event-Driven Trial of TAVI versus SAVR in Patients with Symptomatic Severe Aortic-Valve Stenosis) to compare the two procedures in patients who were at low or intermediate surgical risk and who were eligible for both treatment strategies in a real-world setting.

Characteristic	TAVI (N=701)	SAVR (N=713)
Demographic		
Age — yr	74.3±4.6	74.6±4.2
Male sex — no./total no. (%)	390/696 (56.0)	400/698 (57.3)
Medical history		
Median body-mass index (IQR)†	28.1 (25.3–31.9)	28.1 (25.4–31.2)
Median STS-PROM score (IQR) — %‡	1.8 (1.2–2.4)	1.9 (1.2–2.5)
Score on EuroSCORE II — %§	2.1±1.4	2.1±1.8
Median frailty score (IQR)¶	3.0 (2.0–4.0)	3.0 (2.0–3.0)
Left ventricular ejection fraction — %	57.8±9.8	57.7±9.3
Cardiovascular risk factors — no./total no. (%)		
Hypertension	588/694 (84.7)	605/694 (87.2)
Dyslipidemia	378/691 (54.7)	383/689 (55.6)
Diabetes mellitus	235/695 (33.8)	229/698 (32.8)
Coexisting illness — no./total no. (%)		
Coronary artery disease	238/694 (34.3)	266/697 (38.2)
Cerebrovascular disease	27/676 (4.0)	31/693 (4.5)
Peripheral vascular disease	34/694 (4.9)	45/697 (6.5)
Previous myocardial infarction	36/696 (5.2)	52/697 (7.5)
Previous stroke	42/692 (6.1)	42/696 (6.0)
Atrial fibrillation	201/695 (28.9)	191/697 (27.4)
COPD	101/695 (14.5)	118/697 (16.9)
Pulmonary hypertension	84/693 (12.1)	73/686 (10.6)
NYHA class ≥3	321/695 (46.2)	318/697 (45.6)
Permanent pacemaker	37/696 (5.3)	35/698 (5.0)
Left bundle-branch block	53/678 (7.8)	54/682 (7.9)
Right bundle-branch block	65/678 (9.6)	65/682 (9.5)

Primary and Secondary Outcomes at 1 Year (Intention-to-Treat Population).

Outcome	TAVI (N=701)		SAVR (N=713)		Hazard Ratio (95% CI)
	no. of events	*% of patients*	*no. of events*	*% of patients*	
Primary outcome					
Death from any cause or stroke†	37	5.4	68	10.0	0.53 (0.35–0.79)
Secondary outcomes					
Death from any cause	18	2.6	42	6.2	0.43 (0.24–0.73)
Stroke	20	2.9	32	4.7	0.61 (0.35–1.06)
Stroke or TIA	28	4.1	35	5.1	0.78 (0.47–1.27)
Disabling stroke	9	1.3	21	3.1	0.42 (0.19–0.88)
Death from any cause or disabling stroke	26	3.8	57	8.4	0.45 (0.28–0.70)
Cardiovascular death	14	2.0	30	4.4	0.47 (0.24–0.86)
Myocardial infarction	7	1.0	14	2.1	0.51 (0.20–1.19)
New-onset atrial fibrillation	86	12.4	211	30.8	0.36 (0.28–0.46)
New-onset left bundle-branch block	222	32.0	120	17.5	2.03 (1.63–2.54)
New permanent pacemaker implantation	82	11.8	47	6.7	1.81 (1.27–2.61)
Prosthetic-valve dysfunction	11	1.6	4	0.6	2.44 (0.87–8.15)
Prosthetic-valve endocarditis	4	0.6	7	0.9	0.66 (0.18–2.19)
Prosthetic-valve thrombosis	5	0.7	2	0.3	2.09 (0.50–11.64)
Aortic-valve reintervention	4	0.6	2	0.3	1.70 (0.38–9.78)
Major or life-threatening or disabling bleeding	30	4.3	119	17.2	0.24 (0.16–0.35)
Acute kidney injury of stage II or III‡	9	1.3	17	2.5	0.56 (0.24–1.21)
Vascular access-site complication	55	7.9	5	0.7	10.64 (4.84–28.94)
Rehospitalization for cardiovascular cause	84	12.2	91	13.3	0.89 (0.66–1.20)

A Stroke or Death from Any Cause

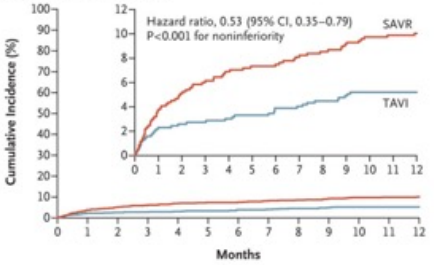

B Death from Any Cause

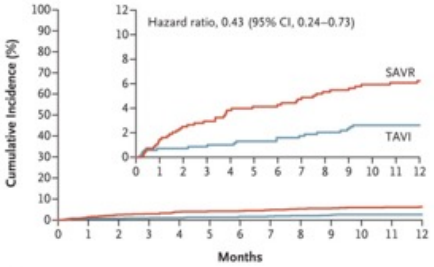

C Stroke

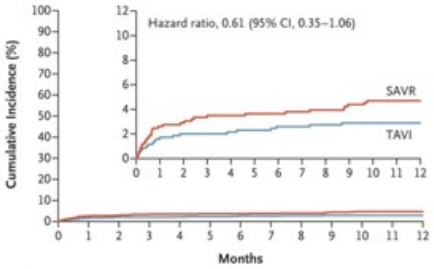

Subgroup	TAVI	SAVR	Hazard Ratio for Death or Strok
	no. of patients with event/total no.		
Overall	37/701	68/713	
Age			
<75 yr	18/359	30/345	
≥75 yr	19/337	38/354	
Sex			
Male	21/390	35/400	
Female	16/306	33/298	
Body-mass index			
<25	8/163	17/159	
25 to <30	12/277	26/293	
≥30	17/255	25/246	
STS-PROM score			
≤2%	15/387	23/378	
>2 to ≤4%	18/282	36/284	
>4%	4/27	9/35	
NYHA class			
≤2	20/374	30/379	
>2	17/321	38/318	
Coronary artery disease			
Yes	15/238	26/266	
No	22/456	42/431	
Previous myocardial infarction			
Yes	1/36	7/52	
No	36/660	61/645	
Previous stroke			
Yes	2/42	5/42	
No	35/650	62/654	
Cerebrovascular disease			
Yes	2/27	6/31	
No	35/649	60/662	
Peripheral vascular disease			
Yes	2/34	6/45	
No	35/660	61/652	
COPD			
Yes	4/101	15/118	
No	33/594	52/579	
Left ventricular ejection fraction			
<55%	7/165	18/179	
≥55 to <60%	11/165	18/181	
≥60%	19/336	29/306	
Aortic-valve mean gradient			
<40 mm Hg	11/243	33/291	
≥40 mm Hg	26/458	35/422	
Glomerular filtration rate			
<60 ml/min/1.73 m^2	13/210	33/194	
≥60 ml/min/1.73 m^2	23/469	35/493	
Covid-19 lockdown at admittance			
Yes	1/38	5/40	
No	36/663	63/673	
Date of randomization			
Before March 1, 2020	18/374	32/365	
On or after March 1, 2020	19/327	36/348	

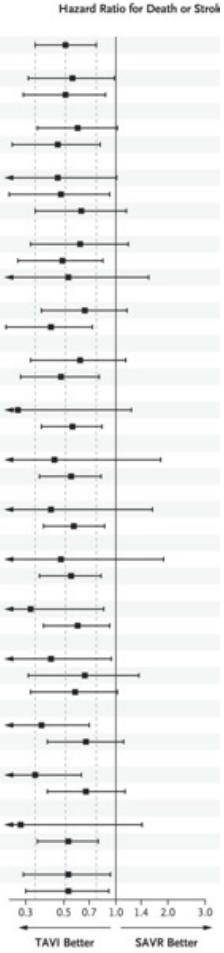

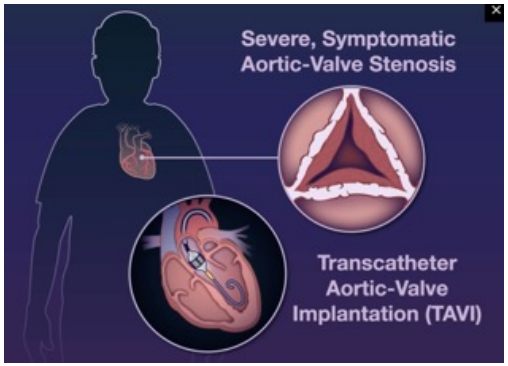
Severe, Symptomatic
Aortic-Valve Stenosis
Transcatheter
Aortic-Valve
Implantation (TAVI)

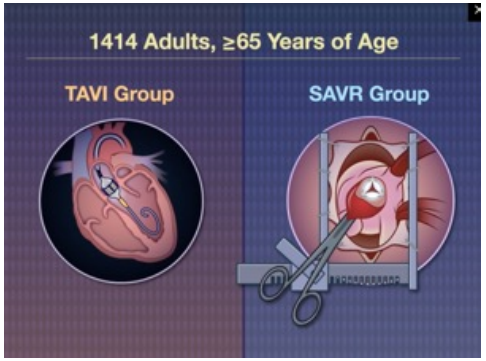
1414 Adults, ≥65 Years of Age
TAVI Group
SAVR Group

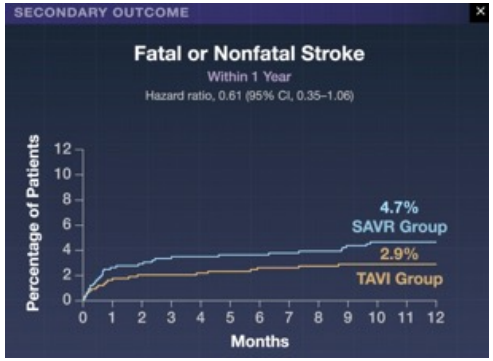
SECONDARY OUTCOME
Fatal or Nonfatal Stroke
Within 1 Year
Hazard ratio, 0.61 (95% CI, 0.35–1.06)
Percentage of Patients
0 2 4 6 8 10 12
4.7%
SAVR Group
2.9%
TAVI Group
0 1 2 3 4 5 6 7 8 9 10 11 12
Months

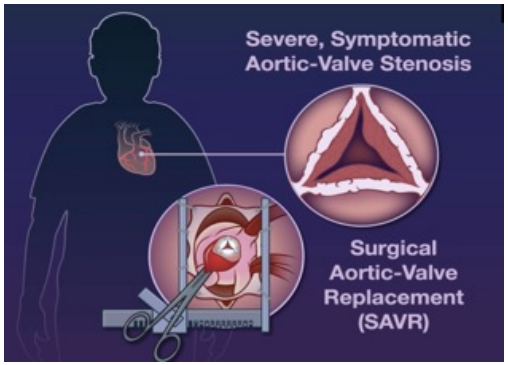
Severe, Symptomatic
Aortic-Valve Stenosis
Surgical
Aortic-Valve
Replacement
(SAVR)

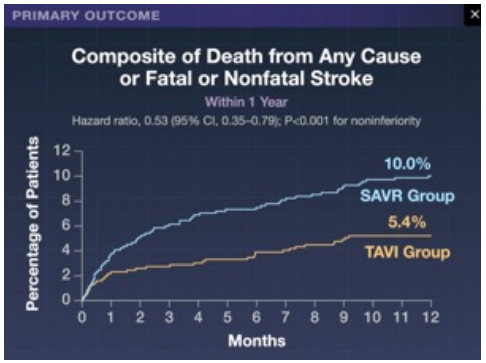
PRIMARY OUTCOME
Composite of Death from Any Cause
or Fatal or Nonfatal Stroke
Within 1 Year
Hazard ratio, 0.53 (95% CI, 0.35–0.79); P<0.001 for noninferiority
Percentage of Patients
0 2 4 6 8 10 12
10.0%
SAVR Group
5.4%
TAVI Group
0 1 2 3 4 5 6 7 8 9 10 11 12
Months

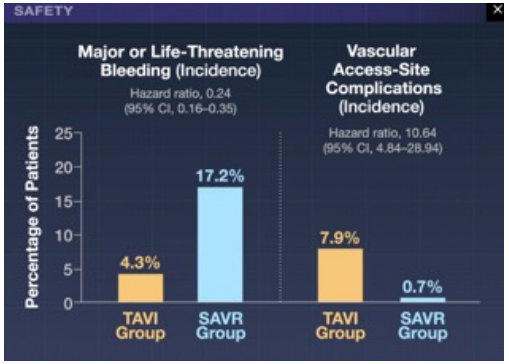
SAFETY
Major or Life-Threatening
Bleeding (Incidence)
Hazard ratio, 0.24
(95% CI, 0.16–0.35)
Vascular
Access-Site
Complications
(Incidence)
Hazard ratio, 10.64
(95% CI, 4.84–28.94)
Percentage of Patients
0 5 10 15 20 25
4.3%
17.2%
7.9%
0.7%
TAVI
Group
SAVR
Group
TAVI
Group
SAVR
Group

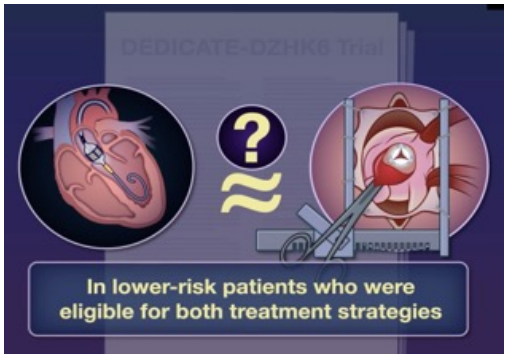
DEDICATE-DZHK6 Trial
?
In lower-risk patients who were
eligible for both treatment strategies


SECONDARY OUTCOME
Death from Any Cause
Within 1 Year
Hazard ratio, 0.43 (95% CI, 0.24–0.73)
Percentage of Patients
0 2 4 6 8 10 12
6.2%
SAVR Group
2.6%
TAVI Group
0 1 2 3 4 5 6 7 8 9 10 11 12
Months

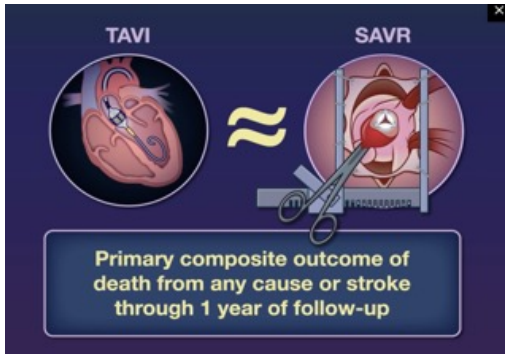
TAVI
SAVR
Primary composite outcome of
death from any cause or stroke
through 1 year of follow-up

Die thrombotisch-thrombozytopenische Purpura (TTP) ist eine schwere Erkrankung, bei der sich im ganzen Körper kleine Blutgerinnsel bilden. Diese blockieren die Blutversorgung lebenswichtiger Organe wie des Gehirns, des Herzens und der Nieren. Die Symptome hängen davon ab, wo die Blutgerinnsel entstehen.

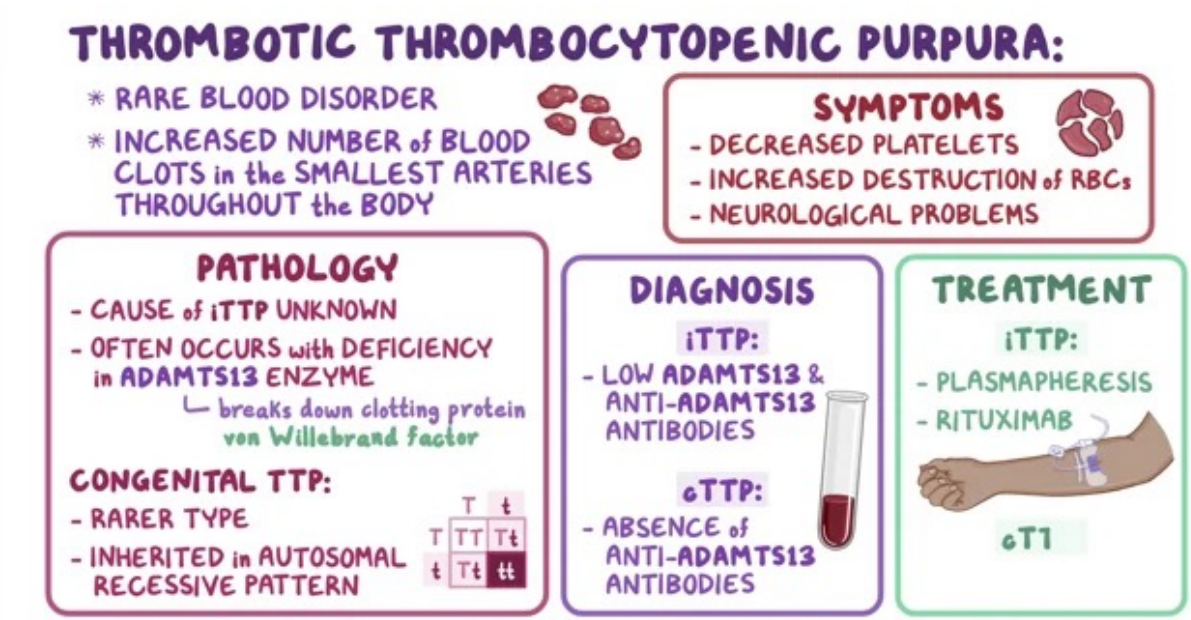

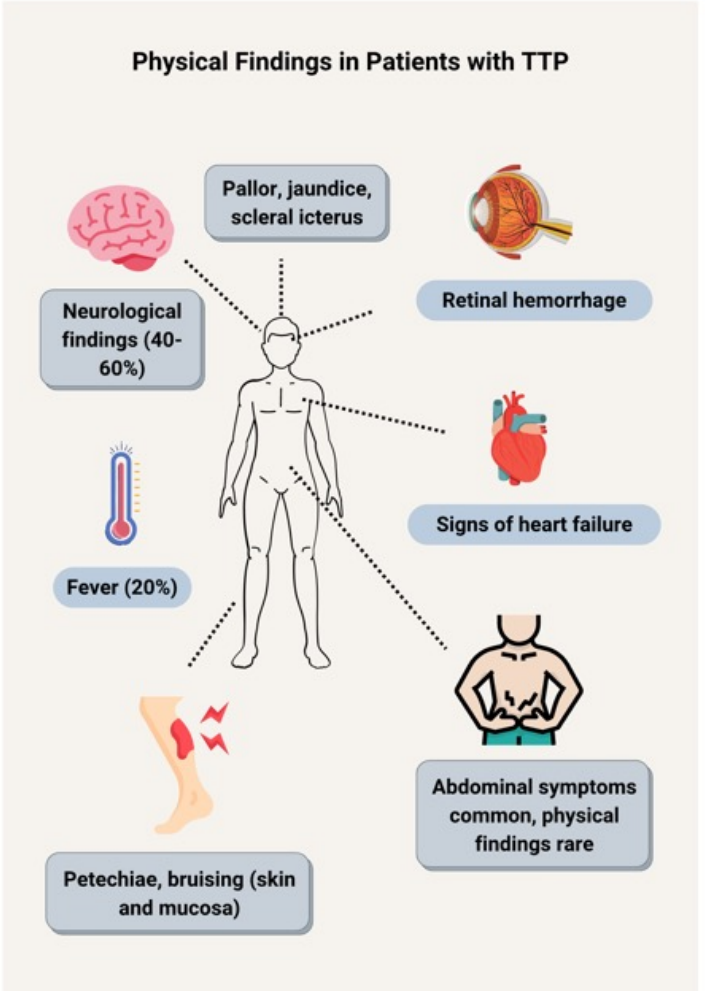

Thrombotische **Mikroangiopathie**, abgekürzt als **TMA**, ist ein pathologischer Zustand, der aufgrund einer Verletzung des Endothels zu Thrombosen in Kapillaren und Arteriolen führt.

UL-vWF steht für "Unusually Large von-Willebrand-Factor". UL-vWF ist das von den Endothelzellen und den Thrombozyten produzierte vWF-Multimer. Es wird im zirkulierenden Blut durch die Metalloprotease ADAMTS-13 in kleinere Dimere gespalten. Die Spaltung erzeugt einen kleineren von-Willebrand-Faktor, der im normalen Blutfluss nicht zu einer Adhäsion und Aggregation d er Thrombozyten führt.
siehe auch: Thrombotisch-thrombozytopenische Purpura.

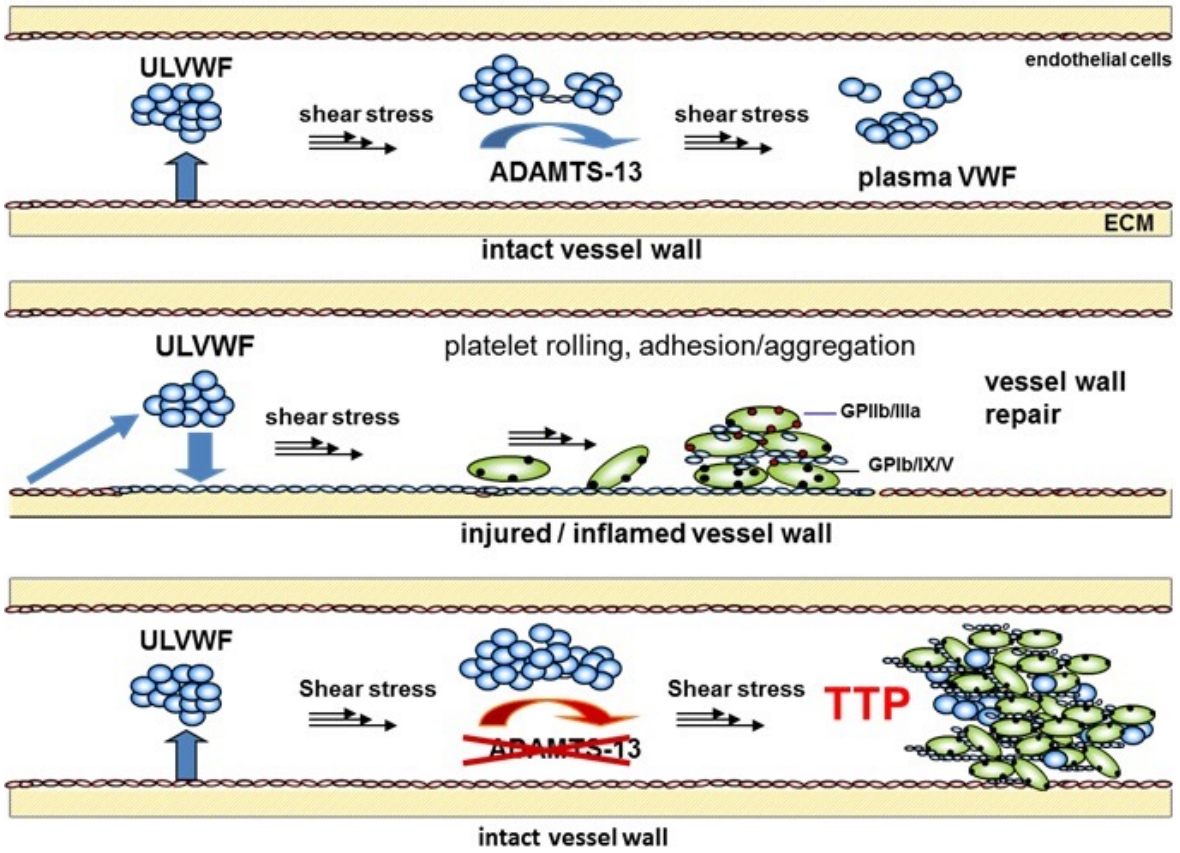

Recombinant ADAMTS13 in Congenital Thrombotic Thrombocytopenic Purpura

Congenital thrombotic thrombocytopenic purpura (TTP) results from severe hereditary deficiency of ADAMTS13. The efficacy and safety of recombinant ADAMTS13 and standard therapy (plasma-derived products) administered as routine prophylaxis or on-demand treatment in patients with congenital TTP is not known. In this phase 3, open-label, crossover trial, we randomly assigned patients in a 1:1 ratio to two 6-month periods of prophylaxis with recombinant ADAMTS13 (40 IU per kilogram of body weight, administered intravenously) or standard therapy, followed by the alternate treatment; thereafter, all the patients received recombinant ADAMTS13 for an additional 6 months. The trigger for this interim analysis was trial completion by at least 30 patients. The primary outcome was acute TTP events. Manifestations of TTP, safety, and pharmacokinetics were assessed. Patients who had an acute TTP event could receive on-demand treatment.

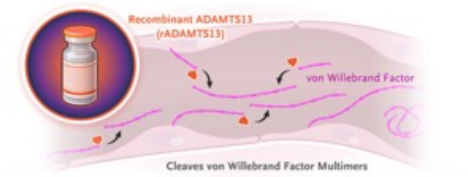

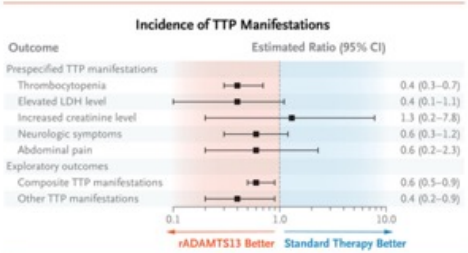

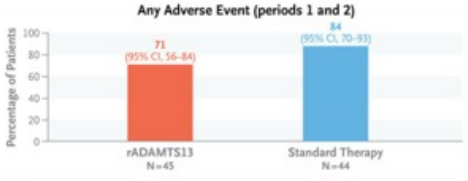

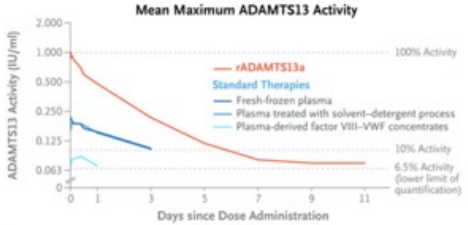

CONCLUSIONS

Among patients with congenital TTP, rADAMTS13 was an effective prophylactic therapeutic approach with an acceptable side-effect profile.

Congenital thrombotic thrombocytopenic purpura (TTP) is an ultrarare thrombotic microangiopathy (prevalence, ≥0.5 cases per million population). Congenital TTP results from severe hereditary deficiency (<10% of normal activity) of ADAMTS13 (a disintegrin and metalloproteinase with thrombospondin motifs 13), leading to accumulation of ultralarge von Willebrand factor multimers with high platelet-binding activity. Spontaneous formation of platelet-rich microthrombi and organ ischemia lead to acute symptoms and long-term organ damage with associated illness and premature death; platelet consumption manifests as thrombocytopenia, a hallmark of congenital TTP.

Current standard therapy involves ADAMTS13 replacement through prophylactic or on-demand infusions of fresh-frozen plasma, plasma that had been treated with a solvent–detergent process, or ADAMTS13-containing plasma-derived factor VIII–von Willebrand factor concentrates. These products are reliant on donor plasma and provide limited ADAMTS13 replacement. Prophylaxis requires lengthy, burdensome infusions in the hospital; allergic reactions to plasma, which can be severe and treatment-limiting, are prevalent. Here, we present the results from a preplanned interim analysis of a phase 3, randomized, controlled, crossover trial in which adults and children with congenital TTP received recombinant ADAMTS13 (TAK-755; Takeda Pharmaceuticals U.S.A.) or standard therapy for prophylactic and on-demand treatment.

Outcome Measures

The primary outcome was acute TTP events among patients receiving prophylaxis with recombinant ADAMTS13 or standard therapy (periods 1, 2, and 3) in the modified full analysis population, as defined in Figure S1. An acute TTP event was defined as a decrease in the platelet count by at least 50% from baseline or to less than 100,000 per microliter and an elevation of the lactate dehydrogenase (LDH) level to more than 2 times the baseline value or more than 2 times the upper limit of the normal range (ULN) (Table S2). Only new acute TTP events occurring during prophylactic treatment contributed to this outcome.

Secondary efficacy outcomes included TTP manifestations (e.g., thrombocytopenia [a decrease in the platelet count by ≥25% from baseline or to <150,000 per microliter], an elevated LDH level [to >1.5 times the baseline value or >1.5 times the ULN], an increased creatinine level [to >1.5 times the baseline value], neurologic symptoms, and abdominal pain). Safety was assessed in terms of adverse events that started or worsened after the first dose of trial treatment, serious adverse events (including relatedness to treatment), and recombinant ADAMTS13 immunogenicity according to the presence of binding and inhibitory antibodies to ADAMTS13 (assessed every 4 weeks). Serious adverse events were defined as events that were fatal or life threatening, resulted in or prolonged hospitalization, resulted in a persistent or clinically significant disability.

Characteristic	Recombinant ADAMTS13→ Standard Therapy (N=21)	Standard Therapy→ Recombinant ADAMTS13 (N=27)	Total (N=48)
Age			
Median (range) — yr	42 (3–54)	27 (5–68)	33 (3–68)
Distribution — no. (%)			
≥18 yr	16 (76)	20 (74)	36 (75)
12 to <18 yr	1 (5)	3 (11)	4 (8)
6 to <12 yr	1 (5)	3 (11)	4 (8)
<6 yr	3 (14)	1 (4)	4 (8)
Sex — no. (%)			
Male	9 (43)	11 (41)	20 (42)
Female	12 (57)	16 (59)	28 (58)
Median BMI (range)†	27.3 (15.3–37.7)	22.7 (15.1–33.3)	24.1 (15.1–37.7)
Race — no. (%)‡			
Asian	2 (10)	3 (11)	5 (10)
Black or African American	0	1 (4)	1 (2)
White	15 (71)	17 (63)	32 (67)
Multiple	0	1 (4)	1 (2)
Not reported	4 (19)	5 (19)	9 (19)
Median age at diagnosis (range) — yr	20 (0–50)	4 (0–58)	10 (0–58)
Blood group — no. (%)			
A	9 (43)	5 (19)	14 (29)
B	4 (19)	3 (11)	7 (15)
AB	2 (10)	5 (19)	7 (15)
O	6 (29)	14 (52)	20 (42)
Acute TTP event in the 12 mo before enrollment — no. (%)	5 (24)	3 (11)	8 (17)
Subacute TTP event in the 12 mo before enrollment — no. (%)	2 (10)	3 (11)	5 (10)
Pretrial treatments for congenital TTP — no. (%)§	21 (100)	26 (96)	47 (98)
Fresh-frozen plasma	16 (76)	17 (63)	33 (69)
Plasma treated with solvent–detergent process	5 (24)	6 (22)	11 (23)
Plasma-derived factor VIII–von Willebrand factor concentrates	0	3 (11)	3 (6)

Summary of Adverse Events in Patients of All Ages in the Safety Analysis Population.

Adverse Event	Periods 1 and 2: Recombinant ADAMTS13 (N=45)			Periods 1 and 2: Standard Therapy (N=44)			Period 3: Recombinant ADAMTS13 (N=36)		
	No. of Patients	Percentage of Patients (95% CI)	No. of Events	No. of Patients	Percentage of Patients (95% CI)	No. of Events	No. of Patients	Percentage of Patients (95% CI)	No. of Events
Any adverse event	32	71 (56–84)	229	37	84 (70–93)	278	26	72 (55–86)	176
Adverse event related to recombinant ADAMTS13 or standard therapy†	4	9 (3–21)	10	21	48 (33–63)	37	1	3 (0–15)	6
Adverse events by maximum severity									
Mild	17	38 (24–54)		14	32 (19–48)		13	36 (21–54)	
Moderate	12	27 (15–42)		17	39 (24–55)		8	22 (10–39)	
Severe	3	7 (1–18)		6	14 (5–27)		5	14 (5–30)	
Hypersensitivity adverse event‡	0	0 (0–8)	0	16	36 (22–52)	24§	0	0 (0–10)	0
Any serious adverse event	1	2 (0–12)	1	7	16 (7–30)	7	4	11 (3–26)	5
Serious adverse event related to recombinant ADAMTS13 or standard therapy†	0	0 (0–8)	0	1	2 (0–12)	1	0	0 (0–10)	0
Adverse event leading to trial discontinuation	0	0 (0–8)	0	0	0 (0–8)	0	0	0 (0–10)	0
Adverse event leading to trial-drug discontinuation	0	0 (0–8)	0	1	2 (0–12)	1	0	0 (0–10)	0
Adverse event leading to trial-drug interruption	0	0 (0–8)	0	7	16 (7–30)	8	0	0 (0–10)	0
Adverse event leading to death	0	0 (0–8)	0	0	0 (0–8)	0	0	0 (0–10)	0

Outcome	rADAMTS13	Standard Therapy	Estimated Ratio (95% CI)
	least-squares mean annualized incidence rate (95% CI)		
Prespecified TTP manifestations			
Thrombocytopenia	0.74 (0.37–1.50)	1.73 (0.92–3.23)	0.4 (0.3–0.7)
Elevated LDH level	0.26 (0.10–0.72)	0.74 (0.38–1.44)	0.4 (0.1–1.1)
Increased creatinine level	0.10 (0.02–0.47)	0.08 (0.02–0.36)	1.3 (0.2–7.8)
Neurologic symptoms	0.18 (0.06–0.51)	0.29 (0.11–0.78)	0.6 (0.3–1.2)
Abdominal pain	0.11 (0.03–0.39)	0.17 (0.06–0.52)	0.6 (0.2–2.3)
Exploratory outcomes			
Composite TTP manifestations	2.28 (1.35–3.88)	3.68 (2.23–6.08)	0.6 (0.5–0.9)
Other TTP manifestations	0.32 (0.14–0.72)	0.81 (0.44–1.49)	0.4 (0.2–0.9)

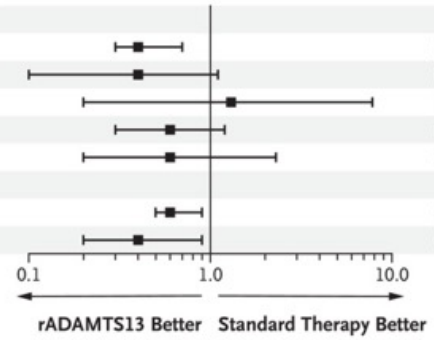

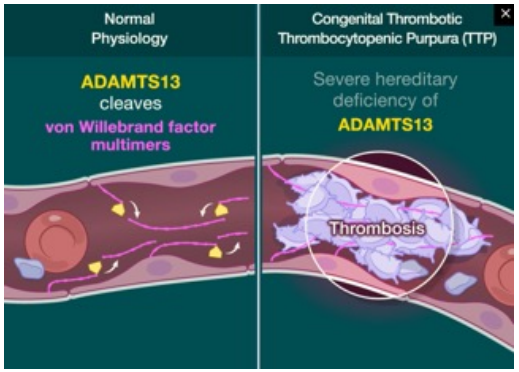
Normal Physiology
Congenital Thrombotic Thrombocytopenic Purpura (TTP)
ADAMTS13
cleaves
von Willebrand factor multimers
Severe hereditary deficiency of
ADAMTS13
Thrombosis


rADAMTS13
Standard Therapy
Plasma-Derived Products
6 Mo
6 Mo
6 Mo
6 Mo
6 Mo
6 Mo


Secondary Outcome
Mean Maximum ADAMTS13 Activity after Infusion
rADAMTS13
101% of normal levels
95% CI, 92–109
Standard Therapy
19% of normal levels
95% CI, 15–22

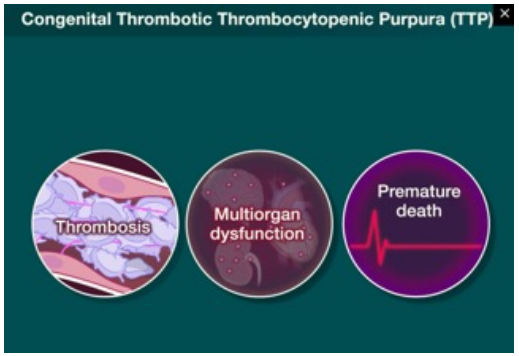
Congenital Thrombotic Thrombocytopenic Purpura (TTP)
Thrombosis
Multiorgan dysfunction
Premature death

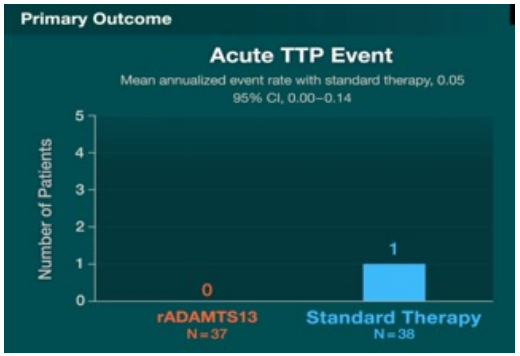
Primary Outcome
Acute TTP Event
Mean annualized event rate with standard therapy, 0.05
95% CI, 0.00–0.14
Number of Patients
0
1
rADAMTS13
N=37
Standard Therapy
N=38

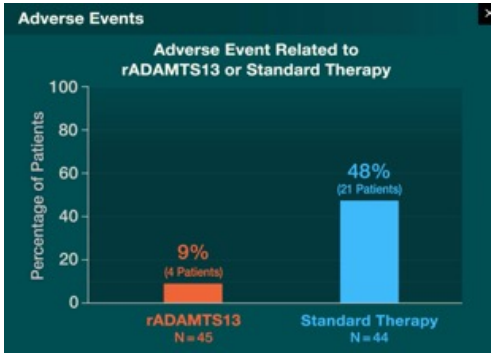
Adverse Events
Adverse Event Related to rADAMTS13 or Standard Therapy
Percentage of Patients
9%
(4 Patients)
48%
(21 Patients)
rADAMTS13
N=45
Standard Therapy
N=44

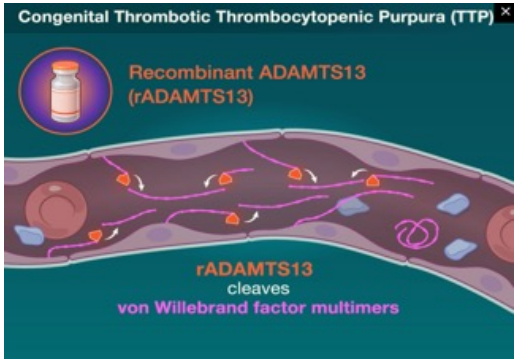
Congenital Thrombotic Thrombocytopenic Purpura (TTP)
Recombinant ADAMTS13
(rADAMTS13)
rADAMTS13
cleaves
von Willebrand factor multimers

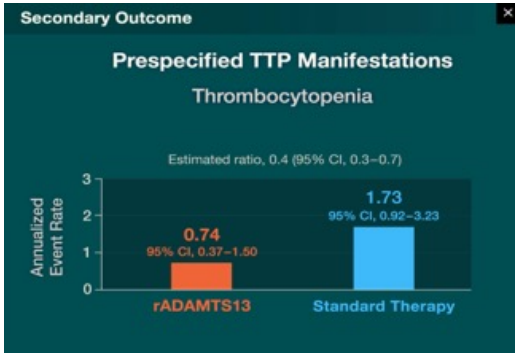
Secondary Outcome
Prespecified TTP Manifestations
Thrombocytopenia
Estimated ratio, 0.4 (95% CI, 0.3–0.7)
Annualized Event Rate
0.74
95% CI, 0.37–1.50
1.73
95% CI, 0.92–3.23
rADAMTS13
Standard Therapy

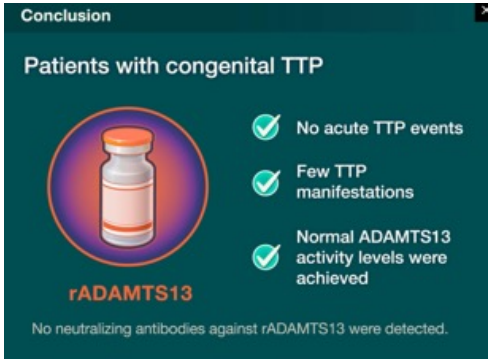
Conclusion
Patients with congenital TTP
rADAMTS13
No acute TTP events
Few TTP manifestations
Normal ADAMTS13 activity levels were achieved
No neutralizing antibodies against rADAMTS13 were detected.

REVIEW ARTICLE

Cryptococcal Disease in Diverse Hosts

The fungus cryptococcus is the most common cause of adult meningitis in parts of the world with high rates of human immunodeficiency virus (HIV) infection and persists in many areas where antiretroviral therapy (ART) is widely available. The fungus is responsible for up to 180,000 deaths each year worldwide and accounts for up to 68% of HIV-related cases of meningitis. In resource-rich regions, increasing use of immunomodulatory therapy and underlying natural susceptibility have led to a change in epidemiologic factors such that deaths in non–HIV-infected patients account for approximately one third of the deaths related to cryptococcal meningitis or meningoencephalitis. With the advent of vaccines to prevent bacterial meningitides such as those from *Streptococcus pneumoniae* and *Haemophilus influenzae*, cryptococcal meningitis has become one of the most common causes of meningitis in the United States..

Mycologic Features

Cryptococcus is a basidiomycetous yeast that is unique among pathogens in humans in that it has an immune-shielding polysaccharide capsule and a cell-wall laccase with broad immunomodulatory properties, which together predispose the organism to neurotropism. The cryptococcus genus is currently undergoing reevaluation but is generally considered to consist of two species complexes, *Cryptococcus neoformans* and *C. gattii*, each of which can be further divided into several molecular genotypes (*C. neoformans*: VNI through VNIV and VNB; and *C. gattii*: VGI through VGVI).

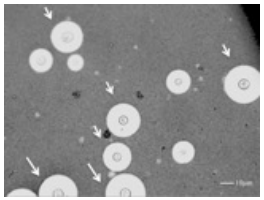

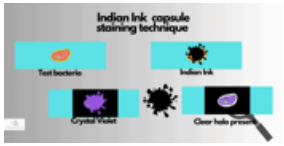

CRYPTOCOCCAL DISEASE IN DIVERSE HOSTS

- Worldwide, cryptococcal meningitis kills up to 180,000 persons annually and is the most common cause of nonviral meningitis in the United States.
- Besides patients with immunosuppression due to human immunodeficiency virus (HIV) infection, chemotherapy, or immunotherapy, the cryptococcus fungus increasingly causes disease in apparently healthy persons, often without signs such as fevers, which results in diagnostic delays and poor outcomes.
- Despite HIV control in developing countries, expected reductions in the prevalence of cryptococcal disease remain elusive, and therapy is hampered by an inability to secure cost-effective drugs such as flucytosine.
- Prompt diagnosis, fungicidal therapy, and intracerebral pressure control are key for successful treatment of cryptococcal meningitis.
- Inflammatory syndromes such as the immune reconstitution and postinfectious inflammatory response syndromes are major causes of clinical deterioration and may necessitate the use of additional adjunctive therapeutic agents.
- Ending Cryptococcal Meningitis Deaths by 2030 is a strategic framework that must be implemented worldwide in order to reduce deaths from cryptococcal meningitis, with a focus on screening, health care worker education, and shorter, more effective therapies.

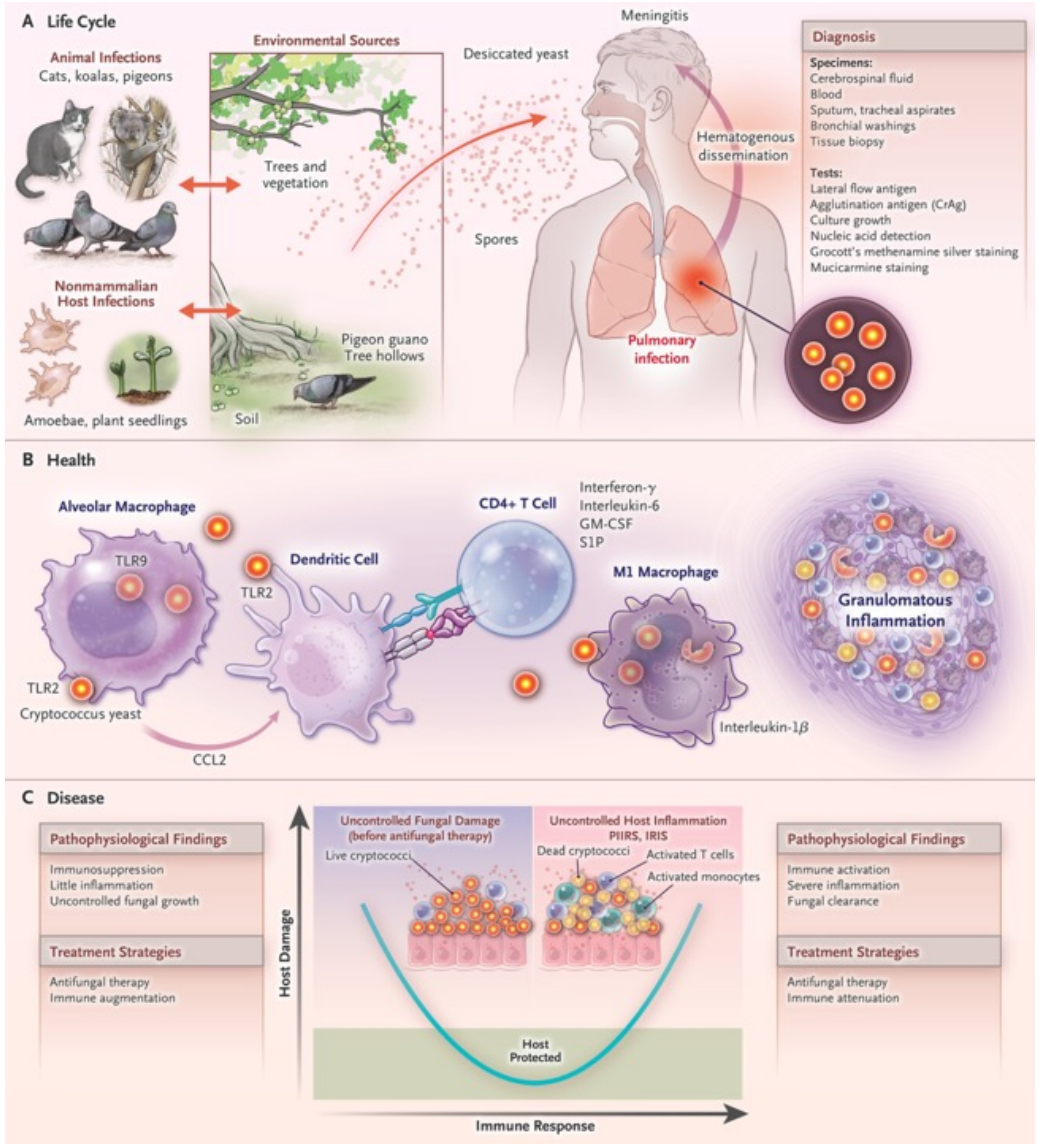

Cryptococcal Life Cycle and Immune Responses.

Cryptococcal yeasts inhabit a number of environmental niches, causing infections in animals and nonmammalian hosts, as well as in humans (Panel A). Infection in humans occurs after the inhalation of desiccated yeast or spores. In healthy persons, responses may be varied, but organisms are recognized by alveolar macrophages by means of pattern-recognition receptors, including toll-like receptors 2 and 9 (TLR2 and TLR9) (Panel B). Activated macrophages then release cytokines such as CCL2 to recruit monocytes and dendritic cells to the lung, which are capable of breaking down fungi and presenting antigen to CD4+ T cells. Activated type 1 helper T cells secrete interferon-γ, interleukin-6, sphingosine-1-phosphate (S1P), and granulocyte–macrophage colony-stimulating factor (GM-CSF), which help to recruit and differentiate classical (M1) macrophages, and these, in turn, facilitate fungal killing and produce cytokines, including interleukin-1β. Secreted cytokines and chemokines activate leukocytes to encapsulate and eliminate cryptococcal organisms within granulomatous lesions. The absence or dysfunction of a healthy immune response may lead to uncontrolled fungal growth, resulting in fungal damage (Panel C, left side of parabola). However, some patients have a skewed hyperimmune response to the pathogen, causing inflammatory damage to the host tissue even after microbiologic control (Panel C, right side of parabola). CrAg denotes cryptococcal antigen, IRIS immune reconstitution inflammatory syndrome, and PIIRS postinfectious inflammatory response syndrome.

Performance Characteristics of Cryptococcal Diagnostic Assays in Cerebrospinal Fluid (CSF) from Persons with Suspected Meningitis.

Diagnostic Test	Sensitivity	Specificity	Positive Predictive Value	Negative Predictive Value
			percent	
Cryptococcal antigen lateral flow immunochromatographic assay	99.3	99.1	99.5	98.7
CSF culture†	90.0	100	100	85.3
100 mm^3	94.2	100	100	91.2
10 mm^3	82.4	100	100	75.8
India ink microscopy	86.1	97.3	98.2	80.2
Cryptococcal antigen latex agglutination assay				
Meridian	97.8	85.9	92.6	95.5
IMMY	97.0	100	100	95.3
Metagenomic next-generation sequencing	93.5	96.0	87.8	98.0
PCR assay‡	82.0	98.0	98.0	79.0

Current Approaches to Treatment According to Patient Group and Resource Availability.

Treatment Phase and Patient Group	Duration
Induction therapy	
In HIV-coinfected patients in resource-rich settings: liposomal amphotericin B, 3–4 mg/kg daily, plus flucytosine, 25 mg/kg 4 times per day	2 wk
In HIV-coinfected patients in resource-limited settings	
Liposomal amphotericin B, 10 mg/kg as a single dose, plus flucytosine, 100 mg/kg/day, and fluconazole, 1200 mg/day	2 wk of flucytosine and fluconazole
Liposomal amphotericin B, 3–6 mg/kg/day, or amphotericin B deoxycholate, 0.7–1.0 mg/kg/day, plus flucytosine, 100 mg/kg/day (for both oral and intravenous formulations)	1 wk
Alternative induction therapy in resource-limited settings	
If flucytosine is not available: amphotericin B deoxycholate, 0.7–1 mg/kg/day given intravenously, plus fluconazole, 800–1200 mg/day	2 wk, although 1 wk of amphotericin B deoxycholate is better than none
If amphotericin B deoxycholate is not available: fluconazole, 1200 mg/day, plus flucytosine, 100 mg/kg/day given orally, if available	2 wk
In organ-transplant recipients: liposomal amphotericin B, 3 mg/kg daily, plus flucytosine, 100 mg/kg daily	2 wk
In previously healthy patients or those who have not received a transplant: liposomal amphotericin B, 3–5 mg/kg daily, or amphotericin B deoxycholate, 0.7–1.0 mg/kg daily, plus flucytosine, 100 mg/kg daily in 4 divided doses	4–6 wk or 2 wk after negative CSF, and flucytosine for first 2 wk
Consolidation therapy	8 wk
Fluconazole, 400–800 mg/day†	
Maintenance therapy	
Fluconazole, 200 mg/day; in HIV-infected patients, start ART at 4–6 wk, and consider discontinuing maintenance therapy after a minimum of 1 yr if CD4+ cell count is >100/mm^3 and HIV viral load is suppressed	12–18 mo

Related Inflammatory Syndromes

There has been a growing appreciation of the role of infection-related inflammatory syndromes in diverse infectious diseases. Intracranial infections such as cryptococcal meningitis are particularly susceptible to these sequelae because of the subsequent swelling within the restricted confines of the skull. For example, the cryptococcal immune reconstitution inflammatory syndrome (IRIS) in HIV-associated disease was found to have an incidence of 4 to 5% in the Ambition trial. The syndrome occurs 1 to 2 months after cryptococcal meningitis has been diagnosed, usually after the early initiation of ART (<4 weeks after diagnosis). Risk factors for cryptococcal IRIS include a high initial CSF fungal burden and low initial markers of inflammation, including blood CD4+ counts, CSF cells, and inflammatory markers such as interferon-γ, which are rapidly corrected after ART initiation.

Framework for Cryptococcal Inflammatory Syndromes.

Phase and Immunologic Characteristics	Evidence in Patients
During active cryptococcal infection	
Paucity of appropriate inflammation for cryptococcosis	Decreased TNF-α, GM-CSF, interferon-γ, TNF-α, and interleukin-6 in CSF[17,83]
Compartment-specific cytokine profile†	Elevated plasma interleukin-5 and interleukin-7[84]; elevated CSF interferon-γ, interleukin-4, interleukin-17, CXCL10, CCL3, and CCL2[85]
Before ART	
Inappropriate (Th2 cell) responses resulting in poor antigen clearance before ART in patients with HIV infection	Elevated interleukin-4; higher baseline cryptococcal antigen in patients with and those without HIV infection[86]
Elevated CSF chemokine expression	Elevated CSF CCL2, and CCL3[87]
Humoral system: decreased specific antibody levels	Decreased plasma IgM, Lam-IgG, and GXM-IgM[88]
Increasing proinflammatory signaling from APCs because of persistent antigen burden and failure to clear antigen	Elevated interleukin-6 from macrophages[89] and elevated CRP and interleukin-7 from APCs
Interaction between host genetic factors and pathogen; LTA4H SNPs associated with MCP-1 production and risk of IRIS among persons without HIV infection	LTA4H SNPs increase risk of non-HIV–associated IRIS[86]
IRIS	
Effective response of innate and adaptive immune systems	Elevated Th1 and Th17 cytokines; elevated innate cytokines: interleukin-8 and GM-CSF; with or without CSF pleocytosis; with or without elevated CSF protein; negative CSF culture; elevated interleukin-6+ and TNF-α+ monocytes[90]; in non-HIV–associated IRIS, increased interleukin-1Ra, interleukin-7, CCL2, and TNF-α,[86]
Neuronal-cell activation and damage	Elevated CSF FGF-2[85]
Aberrant innate cell trafficking	Trafficking of proinflammatory monocytes and CD4+ T cells into CSF[91]
PIIRS	
Release of fungal antigens after fungal lysis, aberrant CNS T-cell and monocyte activation and migration, or neuronal-cell damage	Negative CSF fungal cultures; elevated CSF protein and pleocytosis; elevated soluble interleukin-2 receptor; elevated CSF interleukin-6; increased HLA-DR+CD4+ and CD8+ T cells in CSF[92]; and increased NFL1[18]

Future Directions and Major Unsolved Problems

The emergence of new paradigms in cryptococcal disease is likely to lead to new actionable strategies for a disease that still kills a substantial number of patients despite therapy. For HIV-associated disease, screening and preventive strategies at the time of HIV diagnosis, facilitated by more sensitive diagnostic testing, including a semiquantitative cryptococcal antigen test currently in development, offer the promise of early, cost-effective oral preemptive treatment strategies that may prevent symptomatic infections.

Summary

The Ending Cryptococcal Meningitis Deaths by 2030 Strategic Framework recommends priorities to reduce morbidity and mortality from cryptococcal meningitis; implementation should be a global effort. Focusing on preventing or reducing cryptococcal disease in HIV-infected and non–HIV-infected populations requires further investment in the development of adjunctive therapies, new compounds, and a vaccine, as well as in continuing to educate health care providers in order to minimize diagnostic delays.

Double Corneal Arcus

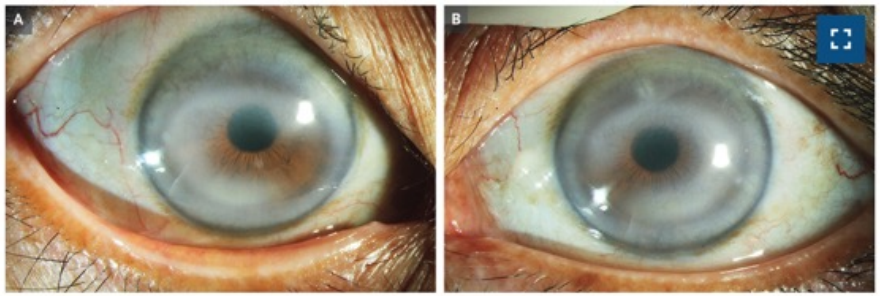

A 63-year-old woman who had presented to the ophthalmology clinic for evaluation of cataracts was found to have white-yellow rings in both eyes. Over the past few years, she had noticed mild worsening of her vision. She reported no history of keratitis or ocular trauma. A lipid panel had been normal at a health maintenance visit 6 weeks before presentation. On ophthalmologic examination, peripheral opacities were observed in the lens of each eye, a finding consistent with age-related cataracts. A funduscopic examination was normal. Visual acuity was 20/30 in each eye. On slit-lamp examination, two concentric white-yellow rings were seen in each cornea (Panel A shows the right eye, and Panel B the left eye). No corneal thinning or inflammation was apparent. A diagnosis of double corneal arcus was made. Corneal arcus (also known as arcus senilis) is an annular opacity that results from lipid deposition. It typically manifests as a single, peripheral ring but may rarely manifest as a double ring, as seen in this patient. Corneal arcus is a consequence of normal aging in older patients and may be associated with hypercholesterolemia in younger patients. The patient was counseled that the double corneal arcus was a benign finding and that her decreased visual acuity was related to the cataracts.

Acute Promyelocytic Leukemia

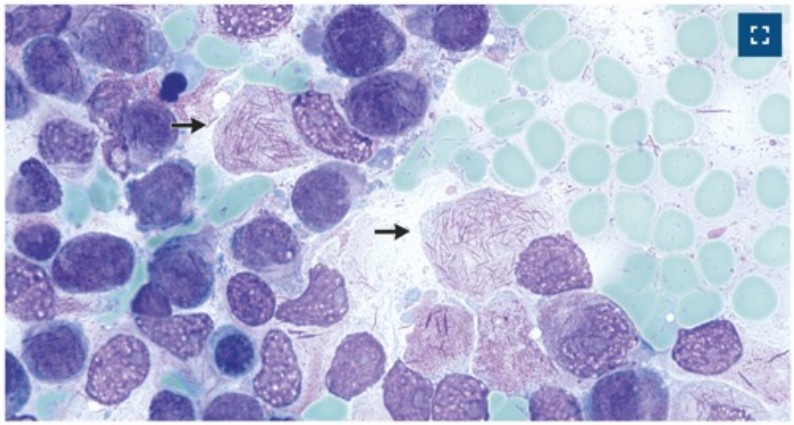

A 47-year-old man presented to the hospital with a 2-day history of weakness and fever. His blood pressure was 64/47 mm Hg, heart rate 110 beats per minute, and temperature 39.0°C. On physical examination, the patient had swelling and redness of the left thigh, which aroused concern about the presence of an abscess. Laboratory studies showed pancytopenia and extreme elevation of the D-dimer level. Promyelocytic blast cells with intracellular Auer rods — needle-shaped cytoplasmic structures specific for myeloid neoplasms — were seen on a peripheral-blood smear. Owing to concern about acute promyelocytic leukemia and sepsis, the patient was admitted to the intensive care unit. Induction chemotherapy with all-*trans* retinoic acid and prednisolone was initiated. A bone marrow biopsy showed promyelocytes with abundant intracellular Auer rods in formations that resembled bundles of sticks (arrows). Genetic analysis for chromosomal translocation identified a PML–RARA fusion gene. A diagnosis of acute promyelocytic leukemia was confirmed. Two days after the start of treatment, differentiation syndrome developed. The hospital course was further complicated by the presence of disseminated intravascular coagulation and *Staphylococcus aureus* bacteremia with leg abscesses. After molecular complete remission had been attained, consolidation chemotherapy that included arsenic trioxide was administered. On hospital day 72, the patient was discharged.

Das PML-Protein ist ein Tumorsuppressorprotein, das für den Aufbau einer Reihe von Kernstrukturen, den so genannten PML-Kernkörpern, erforderlich ist, die sich im Chromatin des Zellkerns bilden.

Cytogenetics morphological

Classic translocation t(15;17)(q24;q21). The translocation may be overlooked in traditional karyotyping. Interphase FISH is indicated, preferably urgent (within 8 hours) on bone marrow aspirate cells (see Figure 1). Although primary anomaly in most cases, t(15;17) can also occur in rare occurrences at acutisation (of promyelocytic type, of course) of a CML with the usual t(9;22).

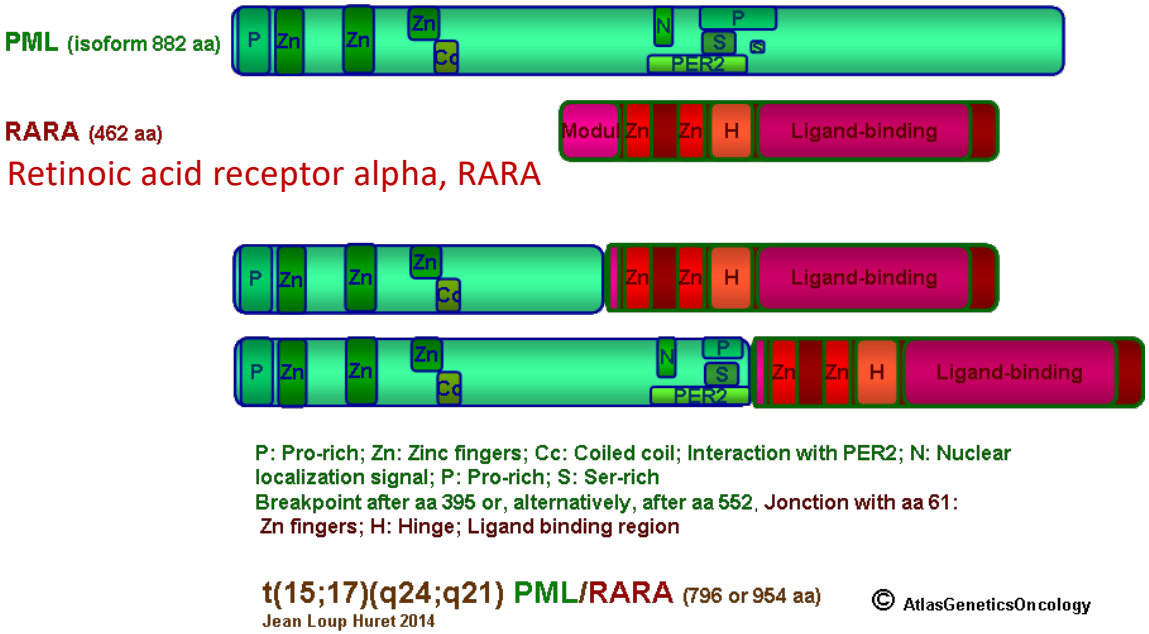

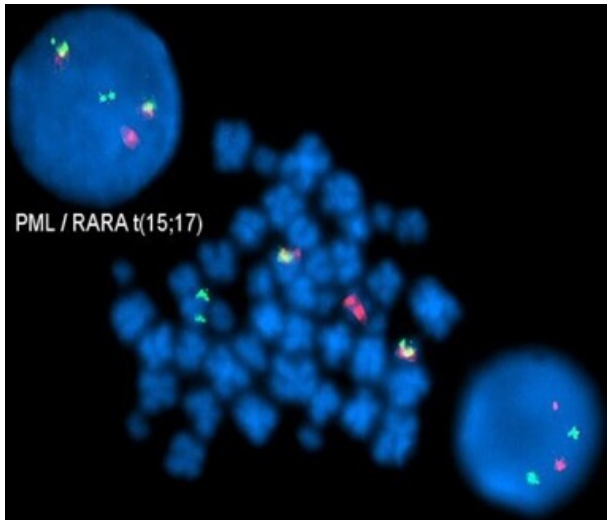

Auerstäbchen sind kleine, stäbchenförmige, azurophile Granula, die man im Rahmen von Leukämien im Zytoplasma von Myeloblasten und Promyelozyten findet. Auerstäbchen finden sich in etwa 30 % der Fälle bei der akuten myeloischen Leukämie (AML) sowie im Rahmen von myelodysplastischen Syndromen.
Es handelt sich um irreguläre Zellorganellen, die lysosomale Enzyme enthalten und Zeichen einer Reifungsstörung der Zelle sind.
Zellen, die multiple Auerstäbchen in Bündeln aufweisen, bezeichnet man als Faggot-Zellen.

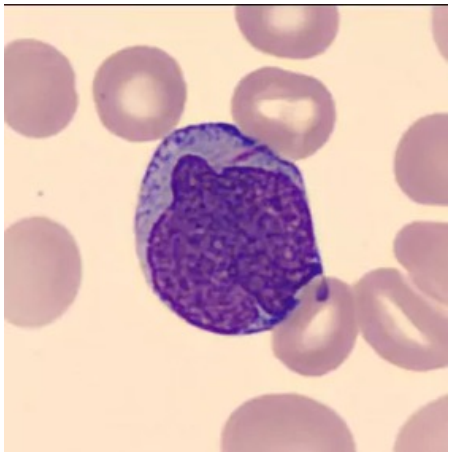

Differentiation Syndrome is a complication of all-trans retinoic acid (ATRA) therapy in patients with acute promyelocytic leukemia (APML). It appears clinically as acute end-organ damage with peripheral edema, hypotension, acute renal failure, and interstitial pulmonary infiltrates.

CLINICAL PROBLEM-SOLVING

The Meat of the Matter

A 32-year-old woman with no clinically significant medical history presented to the emergency department in the winter with a 10-day history of shortness of breath, fevers, and cough. She also reported sore throat and myalgias but no chest pain. Her symptoms did not abate with a 5-day course of azithromycin. She had no pertinent travel or sick contacts and owned no pets. She took a multivitamin daily but no other medications. She reported no tobacco, alcohol, or illicit substance use.

The blood pressure was 117/82 mm Hg, the heart rate 106 beats per minute, and the body temperature 39.3°C. The oxygen saturation while the patient was breathing room air was 85% as measured by pulse oximetry. She was ill-appearing and in mild respiratory distress. Bibasilar crackles were heard on lung auscultation. There was right upper quadrant tenderness without hepatomegaly. Her gastrocnemius muscles were swollen and tender on light palpation in both legs. The remainder of the examination was unremarkable.

The hemoglobin level was 12 g per deciliter, the hematocrit level 35.4%, the white-cell count 1.7×10^3 per microliter without left shift, and the platelet count 96×10^3 per microliter. The serum creatinine level was 0.8 mg per deciliter. The aspartate aminotransferase level was 252 U per liter (normal range, 5 to 34), the alanine aminotransferase level 386 U per liter (normal range, 5 to 55), and the alkaline phosphatase level 253 U per liter (normal range, 40 to 150); bilirubin levels were normal. (One year earlier, a complete blood count with differential and a complete metabolic panel were within normal limits.) The C-reactive protein level was 4.94 mg per deciliter (normal range, 0.1 to 0.5), the ferritin level 4862 µg per liter (normal range, 11 to 307), and the creatine kinase level 203 U per liter (normal range, 29 to 168). Other serum chemical values were normal. A serum specimen was negative for human chorionic gonadotropin. Two sets of blood cultures were obtained; the patient's sputum production was too low to allow a culture to be obtained. Her score on the Pneumonia Severity Index (PSI) was 42.

PSI/PORT Score: Pneumonia Severity Index for CAP
Estimates mortality for adult patients with community-acquired pneumonia.

Age		years
Sex	Female -10	Male 0
Nursing home resident	No 0	Yes +10
Neoplastic disease	No 0	Yes +30
Liver disease history	No 0	Yes +20
CHF history	No 0	Yes +10
Cerebrovascular disease history	No 0	Yes +10
Renal disease history	No 0	Yes +10
Altered mental status	No 0	Yes +20
Respiratory rate ≥30 breaths/min	No 0	Yes +20
Systolic blood pressure <90 mmHg	No 0	Yes +20
Temperature <35°C (95°F) or >39.9°C (103.8°F)	No 0	Yes +15
Pulse ≥125 beats/min	No 0	Yes +10
pH <7.35	No 0	Yes +30
BUN ≥30 mg/dL or ≥11 mmol/L	No 0	Yes +20
Sodium <130 mmol/L	No 0	Yes +20
Glucose ≥250 mg/dL or ≥14 mmol/L	No 0	Yes +10
Hematocrit <30%	No 0	Yes +10
Partial pressure of oxygen <60 mmHg or <8 kPa	No 0	Yes +10
Pleural effusion on x-ray	No 0	Yes +10

Chest Radiography on Admission.

Radiography showed a small right pleural effusion without consolidations or infiltrates.

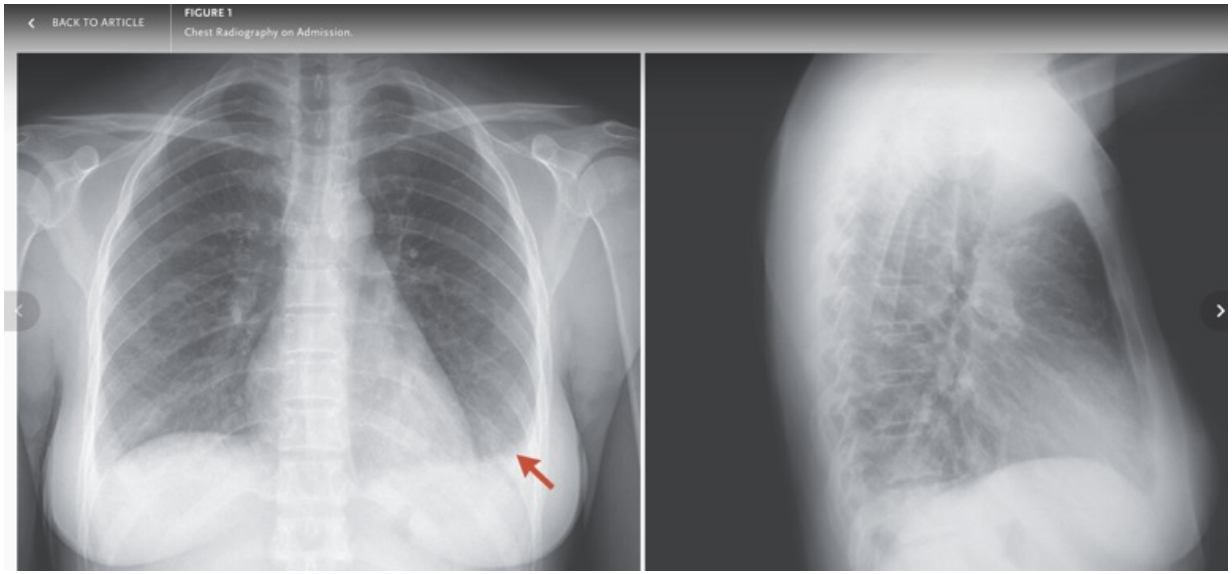

She was admitted to the hospital.

Ceftriaxone was initiated for CAP. Fourth-generation human immunodeficiency virus (HIV) antigen–antibody assay, assessment of HIV viral load, a BioFire polymerase-chain-reaction (PCR) respiratory panel (includes viruses [e.g., SARS-CoV-2], M. pneumoniae, and Bordetella pertussis and B. parapertussis), and urinary antigen testing for S. pneumoniae and Legionella pneumophila were negative. Computed tomographic angiography (CTA) of the chest showed bibasilar consolidations, peribronchiolar nodularity, and septal thickening. Venous Doppler ultrasonography of the legs showed no thrombosis. Computed tomography of the abdomen and pelvis showed no liver or spleen abnormalities. Transthoracic echocardiography revealed an ejection fraction of 60 to 65% without valvular or wall-motion abnormalities.

After 2 days of treatment with ceftriaxone, the patient's oxygen requirement increased. Antibiotic coverage was broadened to include vancomycin and piperacillin–tazobactam to cover methicillin-resistant *S. aureus* (MRSA), *Pseudomonas aeruginosa*, and anaerobes. Bronchoscopy with transbronchial biopsy was considered but deferred because of the patient's escalating oxygen requirements and the associated procedural risks. Microbial cell-free DNA (cfDNA) testing of plasma was performed.

The patient's friend, in speaking with the infectious diseases team, recalled that the patient recently prepared a deer carcass that was harvested during her boyfriend's hunting trip in Alabama. She cooked the venison and served and ate it 20 days before admission. None of the other persons who consumed the cooked meat were reported to be ill.

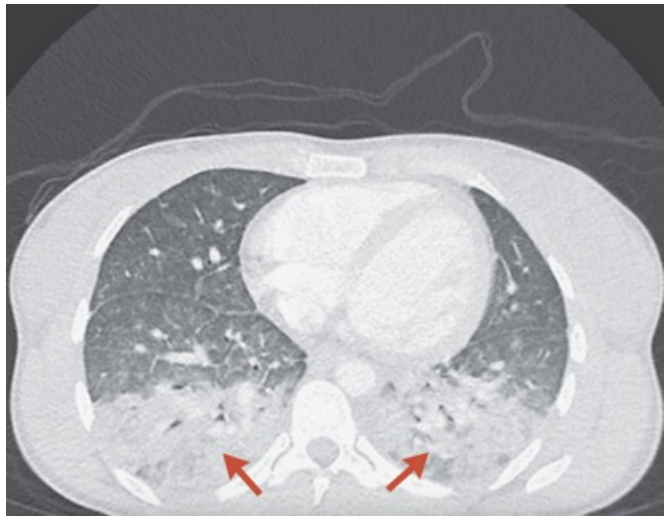

Computed Tomography of the Chest on Hospital Day 2.
Computed tomography showed bibasilar-dependent consolidations, peribronchial nodularities, and septal thickening.

The venison exposure prompted suspicion of zoonotic infections. Serologic testing for *C. burnetii*, *Brucella melitensis*, and *T. gondii* was sent. Doxycycline was initiated as treatment for possible *C. burnetii* infection.
C. burnetii IgM and IgG serologic testing was negative. Testing for brucella IgM was negative, and testing for brucella IgG was equivocal. On hospital day 5, serologic testing for *T. gondii* IgM and IgG was positive, and a sample was sent to the Dr. Jack S. Remington Laboratory for Specialty Diagnostics for confirmatory testing. Testing of blood for *T. gondii* by PCR assay was ordered. Intravenous trimethoprim–sulfamethoxazole was initiated for suspected acute pneumonic toxoplasmosis. Her condition continued to deteriorate, resulting in intubation on hospital day 7. Bronchoscopy with alveolar lavage was performed. The pulmonary team did not perform transbronchial biopsy because of procedural risks. A liver biopsy was performed in the context of elevated levels of liver enzymes and ferritin.

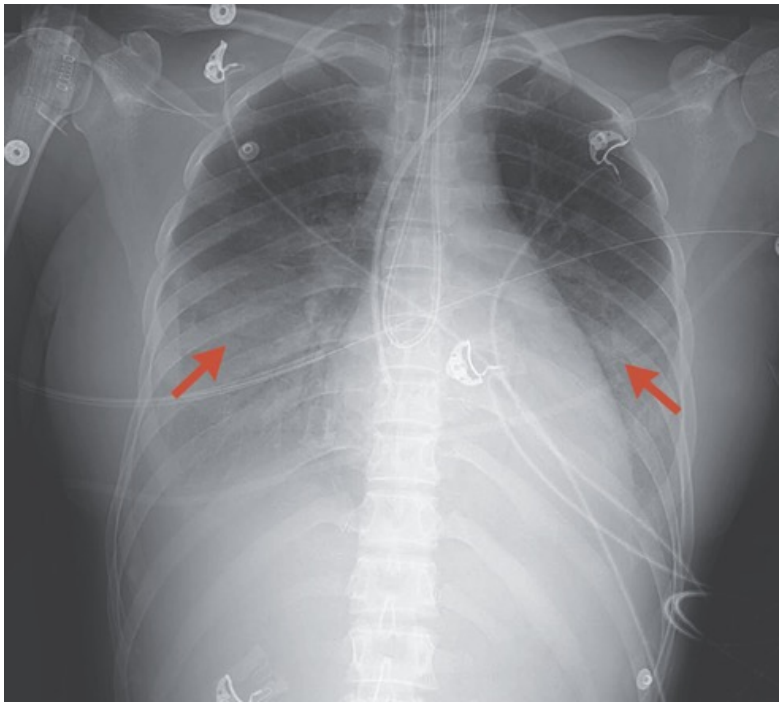

On hospital day 8, tests for microbial cfDNA in plasma returned positive for *T. gondii* with more than 316,000 DNA molecules per milliliter (normal value, <10). The next day, immunohistochemical analysis of the liver-biopsy sample revealed *T. gondii* antigens and a qualitative PCR assay for *T. gondii* in whole blood was positive. Trimethoprim–sulfamethoxazole was continued, and all other antimicrobials were stopped.

On hospital day 9, after 4 days of treatment with intravenous trimethoprim–sulfamethoxazole, the patient was extubated. Her regimen was changed to pyrimethamine, sulfadiazine, and folinic acid when these drugs were made available 12 days later. The reference laboratory confirmed serologic features of an acute toxoplasma infection (high positive toxoplasma IgG dye test; high levels of IgM, IgA, and IgE; and very low IgG avidity). The *T. gondii* PCR assay of the sample obtained during the bronchoscopy with alveolar lavage showed 64,400 copies per milliliter. The liver biopsy and a sample of the venison procured from the freezer of the patient's boyfriend were positive for *T. gondii* by PCR assay. Epidemiologic concerns about virulent Amazonian strains of *T. gondii* potentially being present in the United States prompted genotyping of the venison at the French National Reference Center for Toxoplasmosis. The genotyping result favored an atypical strain of haplogroup 12 that had previously been reported in the Wisconsin outbreak of toxoplasmosis and was distinct from the Amazonian strains. A comprehensive immunodeficiency evaluation — including a lymphocyte subset panel, immunoglobulin and subclasses panel, measurement of total complement levels, and measurement of antibody titers to tetanus, diphtheria, and *S. pneumoniae* — was normal. There were no genetic defects in the TAP1, PI3 kinase, interferon-γ, or interleukin-12 pathways.

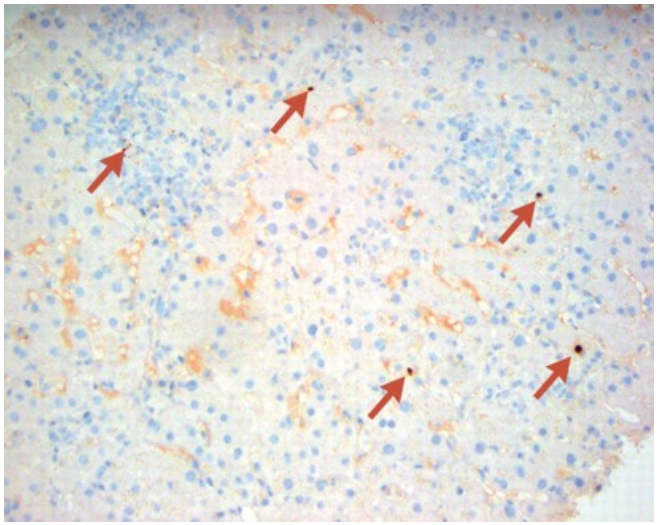

Findings on Liver Biopsy.
Immunohistochemical analysis showed *Toxoplasma gondii* antigens.

Commentary

Pneumonia is a major cause of hospitalization and death among adults in the United States. In a study evaluating 2320 patients hospitalized for CAP in five U.S. hospitals, 21% received intensive care, and overall mortality was 2%. In addition to a thorough history and physical examination, the ATS–IDSA 2019 CAP guidelines recommend comprehensive initial testing in hospitalized patients, including blood and sputum cultures, influenza PCR assay if influenza is circulating in the community, and legionella and pneumococcal urinary antigen tests. In the study above, all the patients underwent standard-care diagnostic testing, yet a pathogen was identified in only 38% of cases, most commonly a virus. The CURB-65 or PSI scores are recommended to assess disease severity and guide decisions about hospitalization. Recommended initial treatment includes a beta-lactam and a macrolide or fluoroquinolone to cover bacterial CAP pathogens, including, but not limited to, *S. pneumoniae*, haemophilus, *C. pneumoniae*, mycoplasma, and legionella. The addition of MRSA or pseudomonal coverage is based on risk factors, such as previous infection with either organism or recent hospitalization with receipt of intravenous antibiotics in the previous 90 days.

Toxoplasma gondii ist ein weltweit vorkommender, intrazellulärer Gewebsparasit und Erreger der Toxoplasmose. Der Erreger ist obligat zweiwirtig. Die sexuelle Vermehrung findet im felinen Endwirt statt. Die asexuelle Vermehrung des Erregers erfolgt in Zwischenwirten. Als Zwischenwirt können nahezu alle Säugetiere dienen.

Endwirt von Toxoplasma gondii sind Hauskatzen. In deren Gastrointestinaltrakt werden folgende Entwicklungsstadien durchlaufen:[1]

- Die Infektion der Hauskatze erfolgt durch Aufnahme von Zysten bei dem Verzehr erbeuteter kleiner Säugetiere. Hierbei handelt es sich um durch Matrixstrukturen ummantelte Ansammlungen mehrerer hundert bis tausend Einzelparasiten (Bradyzoiten, s.u.).
- Im Darmlumen wird die Zystenwand enzymatisch aufgelöst, wobei die darin enthaltenen Bradyzoiten freigesetzt werden. Diese invadieren dann die felinen Enterozyten, vorwiegend im terminalen Ileum. Dort teilen sie sich durch Schizogonie mehrfach unter Bildung eines großen Schizonten, aus dem mehrere Merozoiten hervorgehen. Die Merozoiten werden anschließend nach Zellruptur ins Darmlumen freigesetzt und befallen weitere Zellen, um sich erneut schizogon zu vermehren.
- Nach Durchlaufen mehrerer derartiger Teilungszyklen werden über einen kurzen Zeitraum auch sexuelle Formen gebildet, die als Mikro- und Makrogameten bezeichnet werden. Sie fusionieren und bilden die Oozysten, ca. 10 µm große, rundliche Dauerformen. Oozysten werden nur über einen kurzen Zeitraum nach Infektion der Katze (1 bis 3 Wochen) zu Tausenden über den Kot ausgeschieden.[2]
- die Oozyste sporuliert innerhalb von 1 bis 5 Tagen nach Ausscheidung unter Bildung zweier Sporozysten, bestehend aus einer Sporozystenwand und jeweils 4 länglichen Sporozoiten. Das entstehende Gesamtgebilde wird nun als reife Oozyste bezeichnet. Sie ist durch eine Oozystenwand umschlossen, die ihr eine hohe Umweltresistenz verleiht.

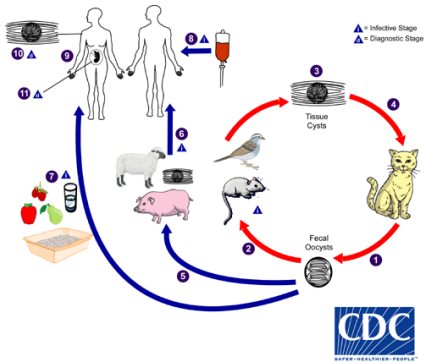

Symptomatik
Bei gesunden, immunkompetenten Menschen verläuft eine Erstinfektion meistens asymptomatisch oder unter Ausbildung unspezifischer Allgemeinsymptome wie Müdigkeit, Kopfschmerzen oder leichtem Fieber. Selten kommt es zu Lymphadenopathie (Piringer-Lymphadenitis), makulopapulösen Exanthemen, Chorioretinitis, Myalgien oder Durchfällen.
Bei immunkompromittierten Menschen (z.B. bei HIV-Infektion) kann es bei Erstinfektion oder auch durch Reaktivierung im Körper verbleibender Oozysten zu schweren Verläufen mit Organschädigung (Myokarditis, Enzephalitis, Hepatitis) und Pneumonie kommen.
Durch die Infektion des Embryos im Mutterleib kann es beim Neugeborenen zu einem Hydrocephalus, einer Chorioretinitis, Kalzifikationen des ZNS, Mikrocephalie, Hepatosplenomegalie sowie zu einer Thrombozytopenie kommen. Bleibende Schäden umfassen Blindheit und mentale Retardierung. Fulminante Embryopathien können zum Abort führen.

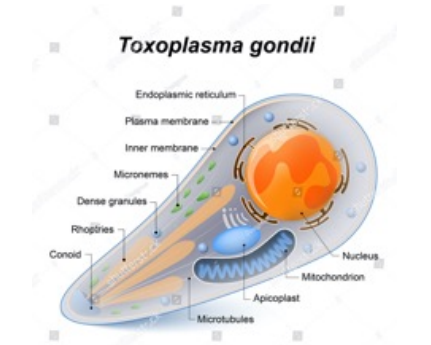

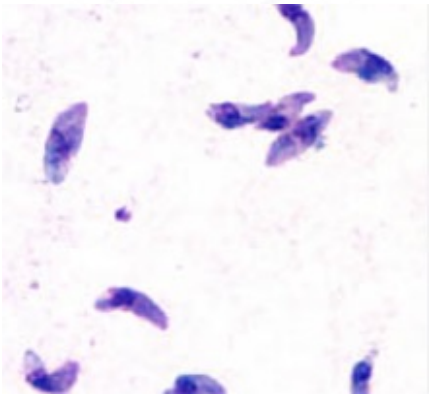

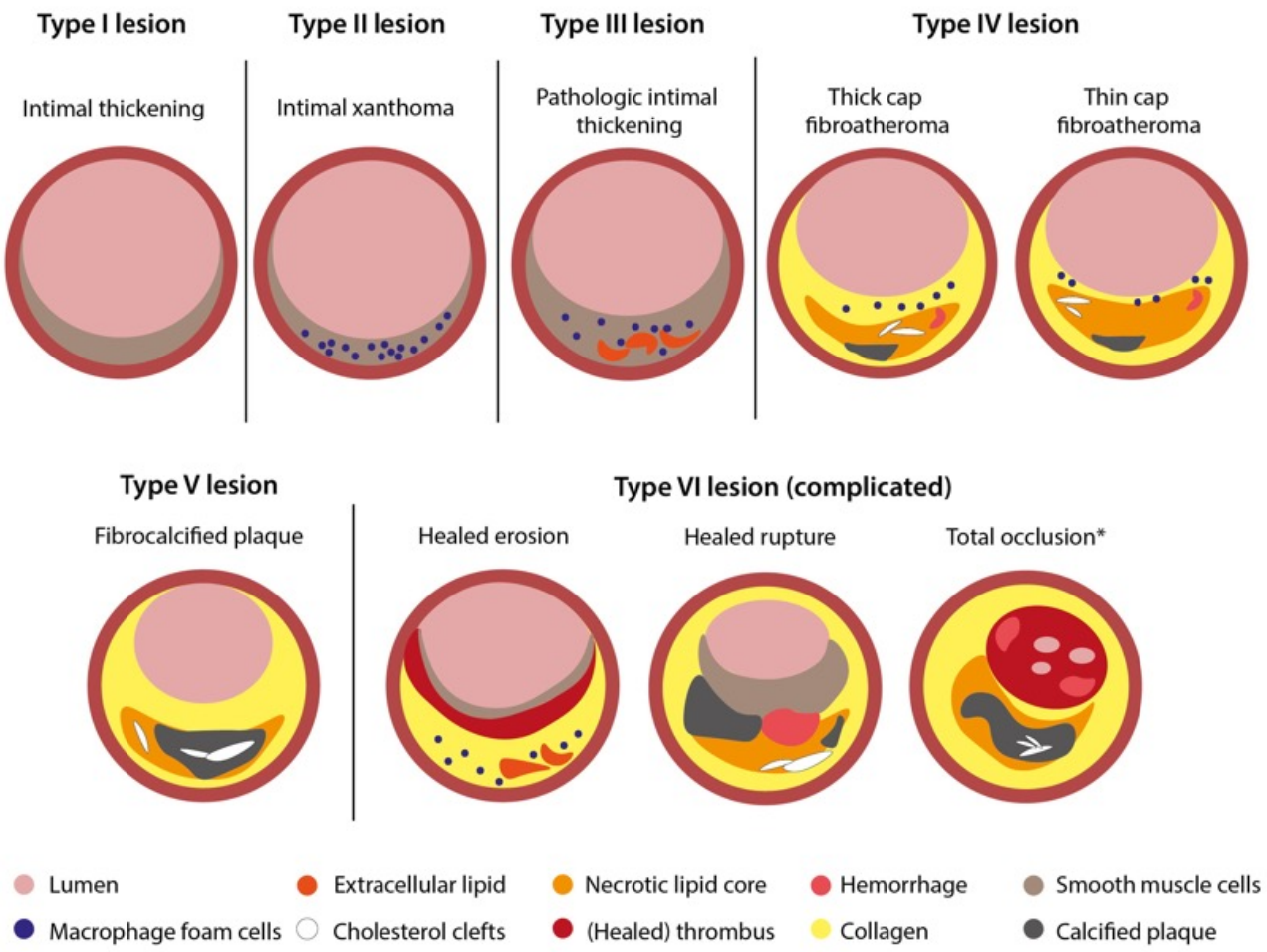
Type I lesion
Intimal thickening
Type II lesion
Intimal xanthoma
Type III lesion
Pathologic intimal thickening
Type IV lesion
Thick cap fibroatheroma
Thin cap fibroatheroma
Type V lesion
Fibrocalcified plaque
Type VI lesion (complicated)
Healed erosion
Healed rupture
Total occlusion*
Lumen
Extracellular lipid
Necrotic lipid core
Hemorrhage
Smooth muscle cells
Macrophage foam cells
Cholesterol clefts
(Healed) thrombus
Collagen
Calcified plaque

CENTRAL ILLUSTRATION **Conceptual Framework for the In Vivo Detection and Focal Passivation of Vulnerable Plaques**

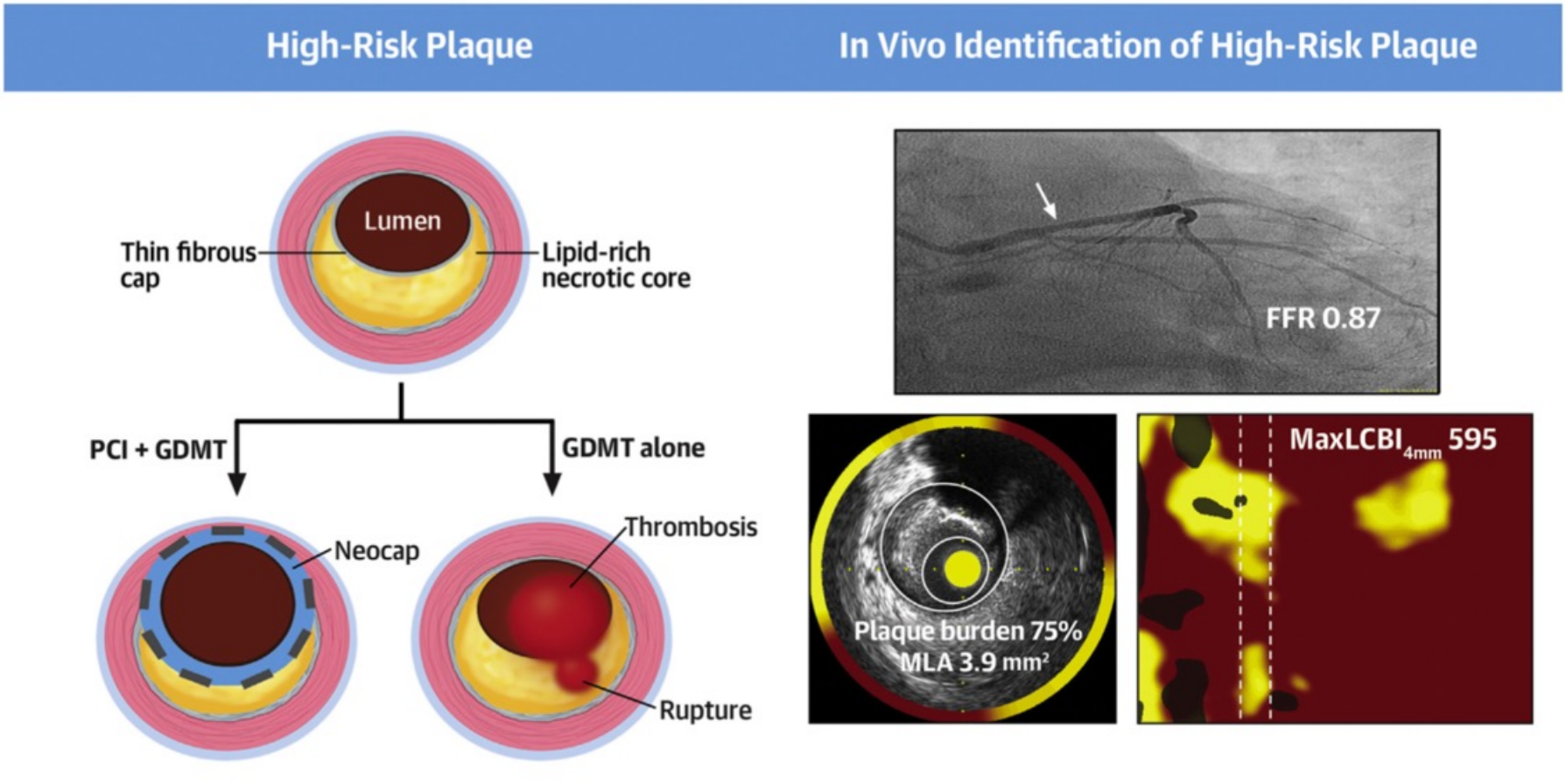

Preventive percutaneous coronary intervention versus optimal medical therapy alone for the treatment of vulnerable atherosclerotic coronary plaques (PREVENT): a multicentre, open-label, randomised controlled trial

Summary

Background Acute coronary syndrome and sudden cardiac death are often caused by rupture and thrombosis of lipid-rich atherosclerotic coronary plaques (known as vulnerable plaques), many of which are non-flow-limiting. The safety and effectiveness of focal preventive therapy with percutaneous coronary intervention of vulnerable plaques in reducing adverse cardiac events are unknown. We aimed to assess whether preventive percutaneous coronary intervention of non-flow-limiting vulnerable plaques improves clinical outcomes compared with optimal medical therapy alone.

Methods PREVENT was a multicentre, open-label, randomised controlled trial done at 15 research hospitals in four countries (South Korea, Japan, Taiwan, and New Zealand). Patients aged 18 years or older with non-flow-limiting (fractional flow reserve >0·80) vulnerable coronary plaques identified by intracoronary imaging were randomly assigned (1:1) to either percutaneous coronary intervention plus optimal medical therapy or optimal medical therapy alone, in block sizes of 4 or 6, stratified by diabetes status and the performance of percutaneous coronary intervention in a non-study target vessel. Follow-up continued annually in all enrolled patients until the last enrolled patient reached 2 years after randomisation. The primary outcome was a composite of death from cardiac causes, target-vessel myocardial infarction, ischaemia-driven target-vessel revascularisation, or hospitalisation for unstable or progressive angina, assessed in the intention-to-treat population at 2 years. Time-to-first-event estimates were calculated with the Kaplan–Meier method and were compared with the log-rank test. This report is the principal analysis from the trial and includes all long-term analysed data. The trial is registered at ClinicalTrials.gov, NCT02316886, and is complete.

Findings Between Sept 23, 2015, and Sept 29, 2021, 5627 patients were screened for eligibility, 1606 of whom were enrolled and randomly assigned to percutaneous coronary intervention (n=803) or optimal medical therapy alone (n=803). 1177 (73%) patients were men and 429 (27%) were women. 2-year follow-up for the primary outcome assessment was completed in 1556 (97%) patients (percutaneous coronary intervention group n=780; optimal medical therapy group n=776). At 2 years, the primary outcome occurred in three (0·4%) patients in the percutaneous coronary intervention group and in 27 (3·4%) patients in the medical therapy group (absolute difference −3·0 percentage points [95% CI −4·4 to −1·8]; p=0·0003). The effect of preventive percutaneous coronary intervention was directionally consistent for each component of the primary composite outcome. Serious clinical or adverse events did not differ between the percutaneous coronary intervention group and the medical therapy group: at 2 years, four (0·5%) versus ten (1·3%) patients died (absolute difference −0·8 percentage points [95% CI −1·7 to 0·2]) and nine (1·1%) versus 13 (1·7%) patients had myocardial infarction (absolute difference −0·5 percentage points [−1·7 to 0·6]).

Interpretation In patients with non-flow-limiting vulnerable coronary plaques, preventive percutaneous coronary intervention reduced major adverse cardiac events arising from high-risk vulnerable plaques, compared with optimal medical therapy alone. Given that PREVENT is the first large trial to show the potential effect of the focal treatment for vulnerable plaques, these findings support consideration to expand indications for percutaneous coronary intervention to include non-flow-limiting, high-risk vulnerable plaques.

Methods

Study design and participants

The Preventive Coronary Intervention on Stenosis with Functionally Insignificant Vulnerable Plaque (PREVENT) trial was an investigator-initiated, multicentre, open-label, randomised controlled trial. The trial was conducted at 15 research hospitals in four countries (South Korea, Japan, Taiwan, and New Zealand). Details regarding the participating investigators and the organisation of the trial are in the appendix (pp 3–7). The trial design and methods have been published previously.[15] The study protocol was approved by the institutional review board (number 2015–1040) and ethics committee at each participating site. An independent data safety and monitoring board approved the initial trial protocol and subsequent amendments and monitored patient safety periodically (appendix pp 6, 113). All patients provided written informed consent. The original and final protocol and a summary of changes are in the appendix (pp 53–137).

Patients aged 18 years or older with stable coronary disease or acute coronary syndromes undergoing cardiac catheterisation were assessed for eligibility. Flow-limiting lesions with a fractional flow reserve of 0·80 or less and lesions causing acute coronary syndrome were treated with percutaneous coronary intervention with metallic drug-eluting stents before randomisation. All untreated, non-culprit lesions (ie, those that were clearly not responsible for the presenting clinical syndrome) with an angiographic diameter stenosis of 50% or more by site visual estimation were functionally assessed by fractional flow reserve. Any intermediate, non-flow-limiting (fractional flow reserve >0·80), non-culprit lesions were then assessed by intracoronary imaging with either grey-scale intravascular ultrasonography, radiofrequency intravascular ultrasonography, a combination of grey-scale intravascular ultrasonography and near-infrared spectroscopy, or optical coherence tomography, at the discretion of the trained interventional cardiologists. Vulnerable plaques were defined as lesions possessing at least two of the following four characteristics: a minimal lumen area of less than 4·0 mm^2 by intravascular ultrasonography or optical coherence tomography; a plaque burden of more than 70% by intravascular ultrasonography; a lipid-rich plaque by near-infrared spectroscopy (defined as maximum lipid core burden index within any 4 mm pullback length [$maxLCBI_{4mm}$] >315); or a thin-cap fibroatheroma detected by radiofrequency intravascular ultrasonography or optical coherence tomography (defined as a ≥10% confluent necrotic core with >30° abutting the lumen in three consecutive frames on radiofrequency intravascular ultrasonography or as a lipid plaque with arc >90° and fibrous cap thickness <65 μm on optical coherence tomography). Major exclusion criteria included previous

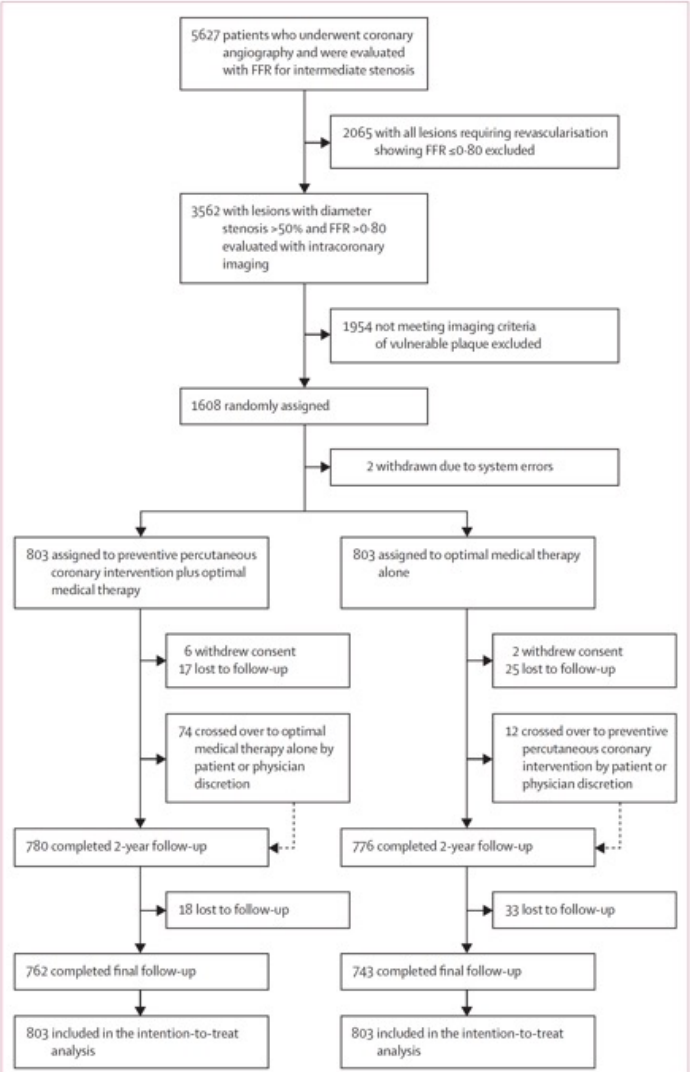

Figure 1: **Trial profile**
FFR=fractional flow reserve.

	Preventive percutaneous coronary intervention plus optimal medical therapy (n=803 [831 lesions])	Optimal medical therapy alone (n=803 [841 lesions])
Age, years	64 (58–71)	65 (59–71)
Sex		
Male	606 (76%)	571 (71%)
Female	197 (25%)	232 (29%)
BMI, kg/m²	24·6 (22·9–26·5)	24·7 (22·9–26·4)
Diabetes		
Any	244 (30%)	246 (31%)
Requiring insulin	16 (2%)	21 (3%)
Hypertension	519 (65%)	536 (67%)
Hyperlipidaemia	721 (90%)	709 (88%)
Current smoker	136 (17%)	139 (17%)
Family history of premature coronary artery disease	95 (12%)	80 (10%)
Previous myocardial infarction	47 (6%)	41 (5%)
Previous percutaneous coronary intervention	109 (14%)	85 (11%)
History of heart failure	5 (1%)	10 (1%)
History of cerebrovascular disease	52 (6%)	50 (6%)
History of peripheral artery disease	21 (3%)	20 (2%)
Atrial fibrillation or atrial flutter	15 (2%)	7 (1%)
Chronic renal insufficiency*	9 (1%)	10 (1%)
Clinical presentation		
Stable angina or silent ischaemia	670 (83%)	677 (84%)
Unstable angina	106 (13%)	91 (11%)
Non-ST-elevation myocardial infarction	18 (2%)	28 (3%)
ST-elevation myocardial infarction	9 (1%)	7 (1%)
Left ventricular ejection fraction†	63 (60–66)	63 (60–66)
Serum cholesterol, mg/dL		
Total cholesterol‡	148 (40)	154 (40)
LDL cholesterol§	88 (34)	93 (34)
HDL cholesterol¶	46 (12)	47 (12)
Triglycerides, mg/dL‖	138 (116)	139 (99)
High-sensitivity C-reactive protein, mg/dL**	0·07 (0·04–0·19)	0·07 (0·04–0·18)
Number of diseased epicardial coronary arteries		
One vessel	327 (41%)	330 (41%)
Two vessels	302 (38%)	307 (38%)
Three vessels	174 (22%)	166 (21%)
Number of target lesions (vulnerable plaques) per patient	1 (1–1)	1 (1–1)
Qualifying criteria for target lesions††		
Minimal luminal area <4·0 mm² by grey-scale IVUS or OCT	809/831 (97%)	817/841 (97%)
Plaque burden >70% by grey-scale IVUS	792/815 (97%)	805/831 (97%)
Large lipid-rich plaque by NIRS ($maxLCBI_{4mm}$ >315)	99/348 (28%)	94/369 (26%)
Thin-cap fibroatheroma defined by OCT or radiofrequency IVUS	39/571 (7%)	40/679 (6%)
Target lesion location		
Left anterior descending artery	416/831 (50%)	400/841 (48%)
Left circumflex artery	170/831 (20%)	147/841 (17%)
Right coronary artery	245/831 (29%)	294/841 (35%)

(Table 1 continues on next page)

(Continued from previous page)

	Preventive percutaneous coronary intervention plus optimal medical therapy (n=803 [831 lesions])	Optimal medical therapy alone (n=803 [841 lesions])
Median FFR values of target lesions	0·87 (0·83–0·90)	0·86 (0·83–0·90)
Quantitative coronary angiography of target lesions		
Diameter stenosis	56·6% (9·2)	52·6% (9·8)
Minimal lumen diameter, mm	1·3 (0·3)	1·5 (0·4)
Reference vessel diameter, mm	3·1 (0·4)	3·1 (0·5)
Lesion length, mm	23·6 (8·5)	19·3 (8·3)
Any percutaneous coronary intervention of target lesion, per patient‡‡	729/803 (91%)	12/803 (1%)
Drug-eluting stent implantation	491/729 (67%)	7/12 (58%)
Bioabsorbable scaffold implantation	237/729 (33%)	5/12 (42%)
Number of stents or scaffolds implanted	1 (1–1)	0 (0–0)
Stent or scaffold diameter, mm	3·5 (3·0–3·5)	3·3 (3·0–3·5)
Total stent or scaffold length, mm	23 (18–28)	23 (18–28)
Intravascular imaging used to optimise stent or scaffold implantation	729/729 (100%)	12/12 (100%)
Any percutaneous coronary intervention of non-target lesions, per patient	290/803 (36%)	286/803 (36%)
Number of lesions treated	0 (0–1)	0 (0–1)
Number of stents implanted	0 (0–1)	0 (0–1)
Stent diameter, mm	3·3 (3·0–3·5)	3·3 (3·0–3·5)
Total stent length, mm	38 (23–51)	38 (28–51)

Data are median (IQR), n (%), mean (SD), or n/N (%). FFR=fractional flow reserve. IVUS=intravascular ultrasonography. $maxLCBI_{4mm}$=maximal lipid core burden index in a 4 mm segment. NIRS=near-infrared spectroscopy. OCT=optical coherence tomography. *Defined as serum creatinine ≥2·0 mg/dL or dependence on chronic haemodialysis. †Preventive percutaneous coronary intervention group n=485; optimal medical therapy group n=358. ‡Preventive percutaneous coronary intervention group n=773; optimal medical therapy group n=760. §Preventive percutaneous coronary intervention group n=733; optimal medical therapy group n=725. ¶Preventive percutaneous coronary intervention group n=732; optimal medical therapy group n=727. ‖Preventive percutaneous coronary intervention group n=732; optimal medical therapy group n=728. **Preventive percutaneous coronary intervention group n=392; optimal medical therapy group n=326. ††The denominators represent the number of lesions that were assessed for these characteristics by one or more of the imaging tests. ‡‡One patient underwent balloon angioplasty only.

Table 1: **Baseline characteristics**

	Preventive percutaneous coronary intervention plus optimal medical therapy (n=803)	Optimal medical therapy alone (n=803)	Difference in event rates, percentage points (95% CI)	Hazard ratio (95% CI)*
Primary composite outcome†	..	..	..	0·54 (0·33 to 0·87)
At 2 years (primary timepoint)	3 (0·4%)	27 (3·4%)	−3·0 (−4·4 to −1·8)	0·11 (0·03 to 0·36), p=0·0003
At 4 years	17 (2·8%)	37 (5·4%)	−2·6 (−4·7 to 0·4)	..
At 7 years	26 (6·5%)	47 (9·4%)	−2·9 (−7·3 to 1·5)	..
Death from any cause	..	..	..	0·61 (0·35 to 1·06)
At 2 years	4 (0·5%)	10 (1·3%)	−0·8 (−1·7 to 0·2)	..
At 4 years	11 (1·8%)	17 (2·6%)	−0·8 (−2·4 to 0·8)	..
At 7 years	20 (5·2%)	32 (7·4%)	−2·3 (−6·0 to 1·5)	..

(Table 2 continues on next page)

	Preventive percutaneous coronary intervention plus optimal medical therapy (n=803)	Optimal medical therapy alone (n=803)	Difference in event rates, percentage points (95% CI)	Hazard ratio (95% CI)*
(Continued from previous page)				
Death from cardiac causes	..	..	..	0·87 (0·31 to 2·39)
At 2 years	1 (0·1%)	6 (0·8%)	−0·6 (−1·3 to 0·02)	..
At 4 years	5 (0·8%)	7 (0·9%)	−0·1 (−1·1 to 0·9)	..
At 7 years	7 (1·4%)	8 (1·3%)	0·1 (−1·4 to 1·5)	..
All myocardial infarctions	..	..	..	0·79 (0·40 to 1·55)
At 2 years	9 (1·1%)	13 (1·7%)	−0·5 (−1·7 to 0·6)	..
At 4 years	14 (2·0%)	15 (2·0%)	−0·1 (−1·5 to 1·4)	..
At 7 years	15 (2·4%)	19 (3·5%)	−1·2 (−3·4 to 1·0)	..
Target-vessel-related myocardial infarction	..	..	..	0·62 (0·20 to 1·90)
At 2 years	1 (0·1%)	6 (0·8%)	−0·6 (−1·3 to 0·02)	..
At 4 years	4 (0·6%)	7 (10%)	−0·3 (−1·3 to 0·6)	..
At 7 years	5 (1·0%)	8 (1·4%)	−0·3 (−1·7 to 1·1)	..
Any revascularisation	..	..	..	0·66 (0·44 to 0·98)
At 2 years	14 (1·8%)	29 (3·7%)	−1·9 (−3·6 to −0·3)	..
At 4 years	31 (4·6%)	42 (6·1%)	−1·5 (−4·0 to 0·9)	..
At 7 years	39 (8·5%)	58 (12·4%)	−3·9 (−8·9 to 1·2)	..
Ischaemia-driven target-vessel revascularisation	..	..	..	0·44 (0·25 to 0·77)
At 2 years	1 (0·1%)	19 (2·4%)	−2·3 (−3·4 to −1·2)	..
At 4 years	10 (1·7%)	29 (4·4%)	−2·7 (−4·6 to −0·8)	..
At 7 years	17 (4·9%)	38 (8·0%)	−3·2 (−7·4 to 1·1)	..
Hospitalisation for unstable or progressive angina	..	..	..	0·19 (0·06 to 0·54)
At 2 years	1 (0·1%)	12 (1·5%)	−1·4 (−2·3 to −0·5)	..
At 4 years	4 (0·7%)	16 (2·4%)	−1·7 (−3·0 to −0·4)	..
At 7 years	4 (0·7%)	21 (4·9%)	−4·2 (−7·2 to −1·4)	..
Death from any cause or target-vessel myocardial infarction	..	..	..	0·62 (0·38 to 1·03)
At 2 years	5 (0·6%)	15 (1·9%)	−1·3 (−2·4 to −0·2)	..
At 4 years	15 (2·4%)	23 (3·4%)	−1·0 (−2·8 to 0·9)	..
At 7 years	25 (6·2%)	39 (8·6%)	−2·4 (−6·4 to 1·6)	..
The composite of death from any cause, all myocardial infarctions, or any revascularisation	..	..	..	0·69 (0·50 to 0·95)
At 2 years	24 (3·0%)	41 (5·2%)	−2·2 (−4·1 to −0·2)	..
At 4 years	48 (7·1%)	61 (8·9%)	−1·8 (−4·7 to 1·2)	..
At 7 years	65 (14·4%)	92 (19·3%)	−4·9 (−10·8 to 1·1)	..

Estimated differences were tabulated at a prespecified timepoint of primary-outcome assessment (2 years), at median follow-up time (4 years), and at maximum follow-up time (7 years). *Hazard ratios are for preventive percutaneous coronary intervention compared with optimal medical therapy alone during the entire follow-up period, other than for the primary composite outcome at 2 years. 95% CIs have not been adjusted for multiple comparisons, and therefore these intervals should not be used to infer definitive treatment effects. †Death from cardiac causes, target-vessel myocardial infarction, ischaemia-driven target-vessel revascularisation, or hospitalisation for unstable or progressive angina at 2 years.

Table 2: Primary composite outcome and key secondary composite outcomes in the intention-to-treat population

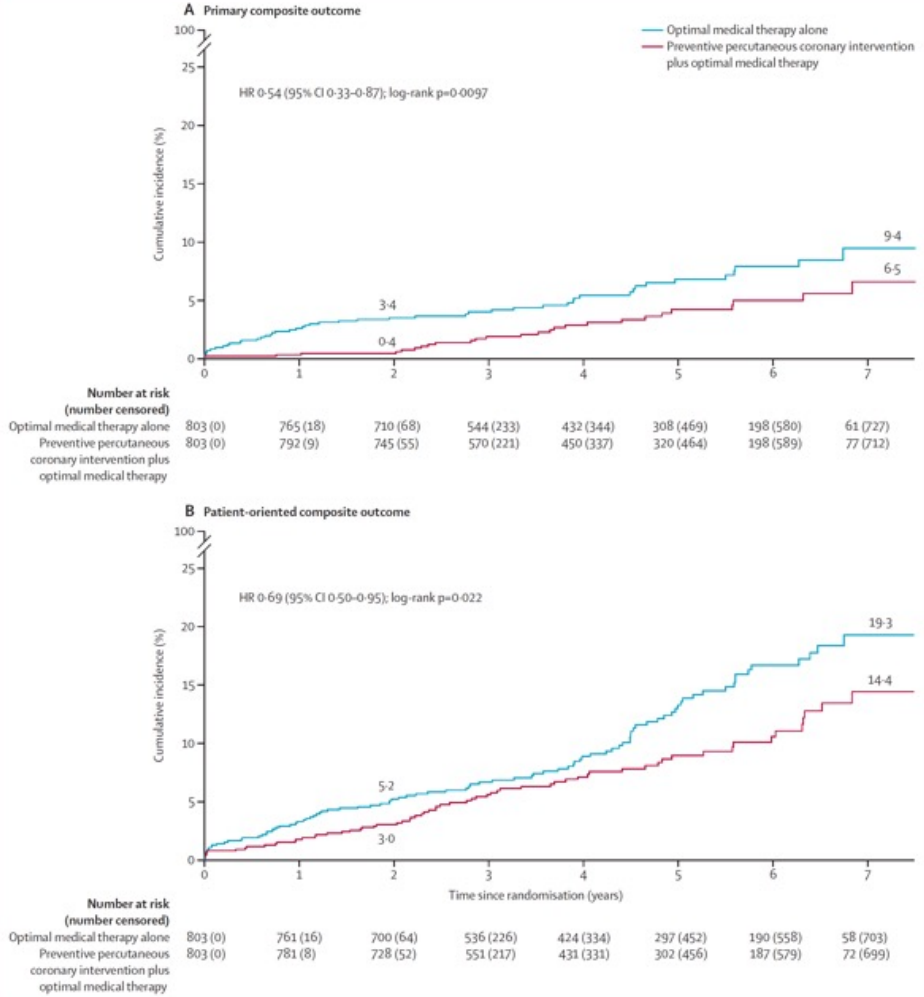

Figure 2: **Time-to-event curves for the primary composite outcome and key secondary patient-oriented composite outcome**
(A) Cumulative incidence of the primary composite outcome of death from cardiac causes, target-vessel myocardial infarction, ischaemia-driven target-vessel revascularisation, or hospitalisation for unstable or progressive angina during the entire follow-up period. (B) Cumulative incidence of the secondary patient-oriented composite outcome of death from any cause, any myocardial infarction, or any repeat revascularisation. Event rates are noted at 2 years (the time of the primary endpoint) and at 7 years (maximum follow-up). HR=hazard ratio.

	Preventive percutaneous coronary intervention plus optimal medical therapy (n=741)	Optimal medical therapy alone (n=865)
Patients without non-target-vessel preventive percutaneous coronary intervention*		
Total percutaneous coronary intervention time, min	29 (18–45)	0
Total amount of contrast media used, mL	150 (120–200)	0
Patients with non-target-vessel percutaneous coronary intervention†		
Total percutaneous coronary intervention time, min	57 (40–73)	46 (25–65)
Total amount of contrast media used, mL	250 (200–300)	200 (150–250)
Any percutaneous coronary intervention-related acute adverse events		
Total	7 (<1%)	3 (<1%)
Acute stent or scaffold thrombosis	1 (<1%)	1 (<1%)
Distal dissection of at least type B	1 (<1%)	0
Side branch occlusion	3 (<1%)	2 (<1%)
Distal embolisation	1 (<1%)	0
Coronary perforation	1 (<1%)	0
Preventive percutaneous coronary intervention-related acute adverse events		
Total	4 (<1%)‡	0
Acute stent or scaffold thrombosis	1 (<1%)	0
Distal dissection of at least type B	1 (<1%)	0
Side branch occlusion	2 (<1%)	0
Distal embolisation	1 (<1%)	0
Coronary perforation	0	0

Data are median (IQR) or n (%). *Preventive percutaneous coronary intervention group n=461; optimal medical therapy group n=569. †Preventive percutaneous coronary intervention group n=280; optimal medical therapy group n=296. ‡One patient has two events.

Table 3: **Procedural safety outcomes in the as-treated population**

A

	Number of events/number of patients (cumulative 2-year incidence)		HR (95% CI)	$P_{interaction}$
	Preventive percutaneous coronary intervention plus optimal medical therapy	Optimal medical therapy alone		
Age (years)				
<65 years	1/408 (0·3%)	15/394 (3·9%)	0·06 (0·01–0·47)	0·44
≥65 years	2/395 (0·5%)	12/409 (3·0%)	0·17 (0·04–0·76)	
Sex				
Male	2/606 (0·3%)	17/571 (3·0%)	0·11 (0·03–0·47)	0·97
Female	1/197 (0·5%)	10/232 (4·4%)	0·11 (0·02–0·89)	
Diabetes				
Yes	0/244 (0%)	9/246 (3·7%)	NC	0·99
No	3/559 (1·2%)	18/557 (3·3%)	0·16 (0·05–0·56)	
Acute coronary syndrome				
Yes	0/133 (0%)	8/126 (6·7%)	NC	0·99
No	3/670 (0·5%)	19/677 (2·8%)	0·16 (0·05–0·53)	
Percutaneous coronary intervention of non-target vessel				
Yes	0/290 (0%)	13/286 (4·6%)	NC	0·99
No	3/513 (0·6%)	14/517 (2·8%)	0·21 (0·06–0·74)	
Median diameter stenosis by QCA				
≥55%	1/491 (0·2%)	14/316 (4·5%)	0·04 (0·01–0·34)	0·18
<55%	2/308 (0·7%)	13/484 (2·7%)	0·24 (0·05–1·07)	
Median fractional flow reserve value				
≤0·86	3/412 (0·7%)	14/395 (3·6%)	0·20 (0·06–0·71)	0·92
>0·86	0/389 (0%)	13/405 (3·3%)	NC	
Intracoronary imaging screening tools				
Grey-scale IVUS only	3/303 (1·0%)	6/261 (2·3%)	0·41 (0·10–1·66)	NA
Radiofrequency IVUS	0/506 (0%)	18/635 (2·9%)	NC	
Near-infrared spectroscopy	1/333 (0·3%)	12/346 (3·5%)	0·09 (0·01–0·66)	
OCT	1/67 (1·5%)	1/20 (5·0%)	0·30 (0·02–4·76)	
Type of stent used for preventive coronary intervention				
BVS	1/265 (0·4%)	12/281 (4·3%)	0·09 (0·01–0·67)	0·77
CoCr-EES	2/538 (0·4%)	15/522 (2·9%)	0·13 (0·03–0·55)	
Overall population	**3/803 (0·4%)**	**27/803 (3·4%)**	**0·11 (0·03–0·36)**	

Favours preventive percutaneous coronary intervention plus optimal medical therapy Favours optimal medical therapy alone

(Figure 3 continues on next page)

B

	Number of events/number of patients (incidence)		HR (95% CI)	$P_{interaction}$
	Preventive percutaneous coronary intervention plus optimal medical therapy	Optimal medical therapy alone		
Age (years)				0·62
<65 years	13/408 (3·2%)	25/394 (6·4%)	0·48 (0·25 to 0·94)	
≥65 years	13/395 (3·3%)	22/409 (5·4%)	0·61 (0·31 to 1·20)	
Sex				1·00
Male	19/606 (3·1%)	32/571 (5·6%)	0·54 (0·31 to 0·96)	
Female	7/197 (3·6%)	15/232 (6·5%)	0·53 (0·22 to 1·31)	
Diabetes				0·70
Yes	8/244 (3·3%)	13/246 (5·3%)	0·62 (0·26 to 1·50)	
No	18/559 (3·2%)	34/557 (6·1%)	0·51 (0·29 to 0·89)	
Acute coronary syndrome				0·38
Yes	4/133 (3·0%)	11/126 (8·7%)	0·33 (0·11 to 1·05)	
No	22/670 (3·3%)	36/677 (5·3%)	0·60 (0·35 to 1·01)	
Percutaneous coronary intervention of non-target vessel				0·0074
Yes	5/290 (1·7%)	24/286 (8·4%)	0·19 (0·07 to 0·51)	
No	21/513 (4·1%)	23/517 (4·4%)	0·91 (0·50 to 1·64)	
Median diameter stenosis by QCA				0·014
≥55%	11/491 (2·2%)	23/316 (7·3%)	0·28 (0·14 to 0·58)	
<55%	15/308 (4·9%)	24/484 (5·0%)	0·95 (0·50 to 1·81)	
Median fractional flow reserve value				0·77
≤0·86	16/412 (3·9%)	25/395 (6·3%)	0·59 (0·32 to 1·11)	
>0·86	10/389 (2·6%)	22/405 (5·4%)	0·46 (0·22 to 0·97)	
Intracoronary imaging screening tools				NA
Grey-scale IVUS only	10/306 (3·3%)	14/261 (5·4%)	0·50 (0·22 to 1·12)	
Radiofrequency IVUS	15/506 (3·0%)	31/635 (4·9%)	0·55 (0·29 to 1·01)	
Near-infrared spectroscopy	15/333 (4·5%)	24/346 (6·9%)	0·63 (0·33 to 1·20)	
OCT	5/67 (7·5%)	3/20 (15·0%)	0·41 (0·10 to 1·71)	
Type of stent used for preventive coronary intervention				0·018
BVS	19/265 (7·2%)	22/281 (7·8%)	0·89 (0·48 to 1·65)	
CoCr-EES	7/538 (1·3%)	25/522 (4·8%)	0·25 (0·11 to 0·59)	
Overall population	**26/803 (3·2%)**	**47/803 (5·9%)**	**0·54 (0·33 to 0·87)**	

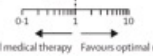

Favours preventive percutaneous coronary intervention plus optimal medical therapy Favours optimal medical therapy alone

Figure 3: **Subgroup analyses of the primary composite outcome at 2-year follow-up and maximal follow-up**
(A) Subgroup analysis for the primary composite outcome (composite of death from cardiac causes, target-vessel myocardial infarction, ischaemia-driven target-vessel revascularisation, or hospitalisation for unstable or progressive angina) at 2 years. (B) Subgroup analysis for the primary composite outcome at maximal follow-up. HRs are for the preventive percutaneous coronary intervention group compared with the optimal medical therapy alone group. CIs have not been adjusted for multiplicity and should not be used to reject or not reject treatment effects. BVS=bioresorbable vascular scaffolds. CoCr-EES=cobalt-chromium everolimus-eluting metallic stents. HR=hazard ratio. NA=not available. NC=not calculated. OCT=optical coherence tomography. QCA=quantitative coronary angiography.

Research in context

Evidence before this study

Optimal medical therapy with pharmacological management is the standard approach to stabilise plaque vulnerability. Theoretically, preventive percutaneous coronary intervention might seal and passivate vulnerable plaques, potentially reducing future acute coronary events. However, the safety and efficacy of revascularisation by percutaneous coronary intervention of non-flow-limiting (non-ischaemic) vulnerable plaques remain uncertain. We searched PubMed and MEDLINE on June 11, 2015, for articles published in English, using the search terms: "coronary artery disease", "vulnerable plaque", "percutaneous coronary intervention", "fractional flow reserve", and "intravascular imaging". We found no randomised clinical trials that assessed the efficacy and safety of localised preventive therapy with percutaneous coronary intervention of non-flow-limiting vulnerable plaques.

Added value of this study

To our knowledge, PREVENT is the first large-scale, randomised controlled trial comparing preventive percutaneous coronary intervention plus optimal medical therapy versus optimal medical therapy alone for the treatment of patients with non-flow-limiting, high-risk, vulnerable plaques identified by intracoronary imaging. In this trial, preventive percutaneous coronary intervention reduced the composite risk of death from cardiac causes, target-vessel myocardial infarction, ischaemia-driven target-vessel revascularisation, or hospitalisation for unstable or progressive angina at 2 years, compared with optimal medical therapy alone. Preventive percutaneous coronary intervention also reduced the composite patient-oriented outcome of risk of all-cause death, any myocardial infarction, or any repeat revascularisation. This benefit was sustained throughout the 7-year follow-up period of the trial.

Implications of all the available evidence

The primary results of PREVENT provide clinical evidence that a preventive percutaneous coronary intervention strategy guided by intravascular imaging plus optimal medical therapy can reduce adverse cardiac events arising from high-risk coronary vulnerable plaques better than optimal medical therapy alone. These findings support an expansion of the indications for percutaneous coronary intervention to include non-flow-limiting, high-risk, vulnerable plaques.

Bei der Amblyopie handelt es sich um eine starke Schwachsichtigkeit, die jedoch auf keiner organischen Ursache beruht. Das heißt, dass die zum scharfen Sehen nötigen Strukturen nicht erkrankt sind. Davon kann sowohl nur ein Auge, aber auch beide betroffen sein.

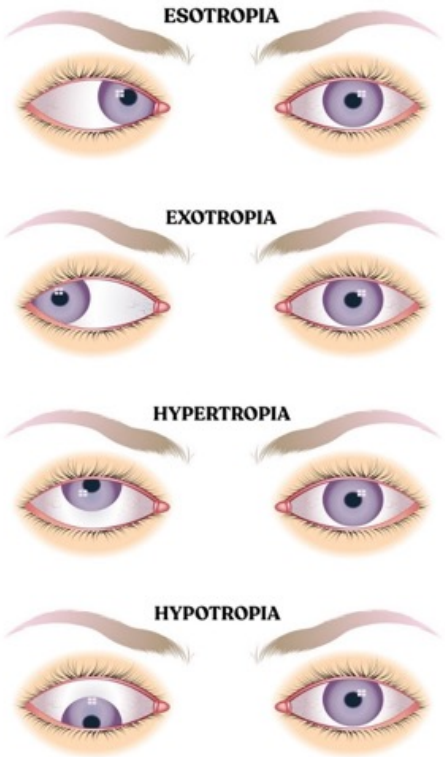

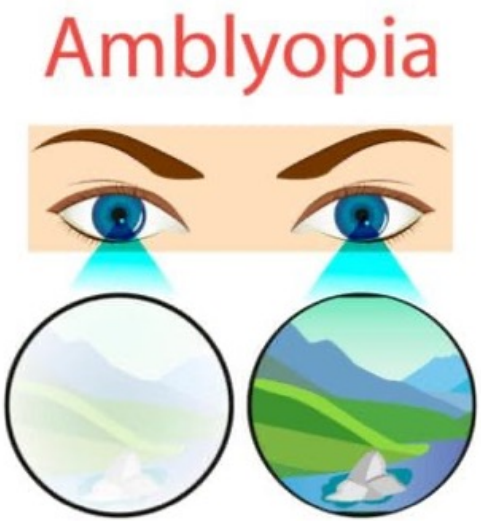

Extended optical treatment versus early patching with an intensive patching regimen in children with amblyopia in Europe (EuPatch): a multicentre, randomised controlled trial

Summary

Background Amblyopia, the most common visual impairment of childhood, is a public health concern. An extended period of optical treatment before patching is recommended by the clinical guidelines of several countries. The aim of this study was to compare an intensive patching regimen, with and without extended optical treatment (EOT), in a randomised controlled trial.

Methods EuPatch was a randomised controlled trial conducted in 30 hospitals in the UK, Greece, Austria, Germany, and Switzerland. Children aged 3–8 years with newly detected, untreated amblyopia (defined as an interocular difference ≥0·30 logarithm of the minimum angle of resolution [logMAR] best corrected visual acuity [BCVA]) due to anisometropia, strabismus, or both were eligible. Participants were randomly assigned (1:1) via a computer-generated sequence to either the EOT group (18 weeks of glasses use before patching) or to the early patching group (3 weeks of glasses use before patching), stratified for type and severity of amblyopia. All participants were initially prescribed an intensive patching regimen (10 h/day, 6 days per week), supplemented with motivational materials. The patching period was up to 24 weeks. Participants, parents or guardians, assessors, and the trial statistician were not masked to treatment allocation. The primary outcome was successful treatment (ie, ≤0·20 logMAR interocular difference in BCVA) after 12 weeks of patching. Two primary analyses were conducted: the main analysis included all participants, including those who dropped out, but excluded those who did not provide outcome data at week 12 and remained on the study; the other analysis imputed this missing data. All eligible and randomly assigned participants were assessed for adverse events. This study is registered with the International Standard Randomised Controlled Trial Number registry (ISRCTN51712593) and is no longer recruiting.

Findings Between June 20, 2013, and March 12, 2020, after exclusion of eight participants found ineligible after detailed screening, we randomly assigned 334 participants (170 to the EOT group and 164 to the early patching group), including 188 (56%) boys, 146 (44%) girls, and two (1%) participants whose sex was not recorded. 317 participants (158 in the EOT group and 159 in the early patching group) were analysed for the primary outcome without imputation of missing data (median follow-up time 42 weeks [IQR 42] in the EOT group *vs* 27 weeks [27] in the early patching group). 24 (14%) of 170 participants in the EOT group and ten (6%) of 164 in the early patching group were excluded or dropped out of the study, mostly due to loss to follow-up and withdrawal of consent; ten (6%) in the EOT group and three (2%) in the early patching group missed the 12 week visit but remained on the study. A higher proportion of participants in the early patching group had successful treatment (107 [67%] of 159) than those in the EOT group (86 [54%] of 158; 13% difference; p=0·019) after 12 weeks of patching. No serious adverse events related to the interventions occurred.

Interpretation The results from this trial indicate that early patching is more effective than EOT for the treatment of most children with amblyopia. Our findings also provide data for the personalisation of amblyopia treatments.

Amblyopia is usually treated first with a period of glasses use to correct for refractive errors, followed by patching of the contralateral eye. Several studies, including a meta-analysis, found a moderate to large effect size from the glasses-only period before commencing patching,[9–15] which significantly decreased for children who commenced treatment when they were older.[9] However, whether parameters such as severity of amblyopia or refractive error and type of amblyopia have a role in the success of treatment with glasses is unclear.

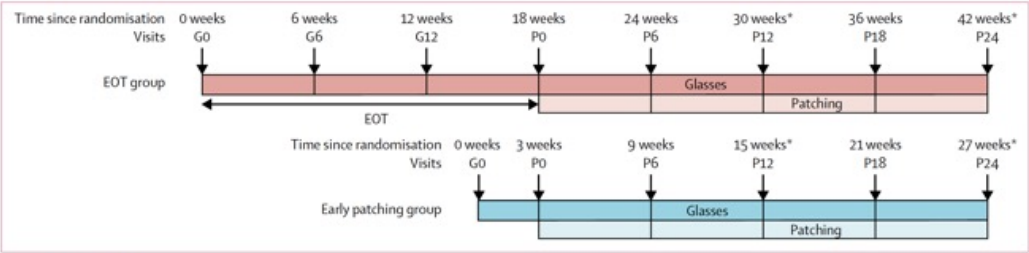

Figure 1: **Study design**
Arrows indicate orthoptic examination timepoints. G0 to G12 indicate the number of weeks of only glasses use and P0 to P24 indicate the numbers of weeks of patching. The primary outcome was assessed at P12 (ie, after 12 weeks of prescribed patching in the two treatment groups). Secondary outcome assessments were performed at P18 and P24. EOT=extended optical treatment. *Timepoints at which questionnaires were administered.

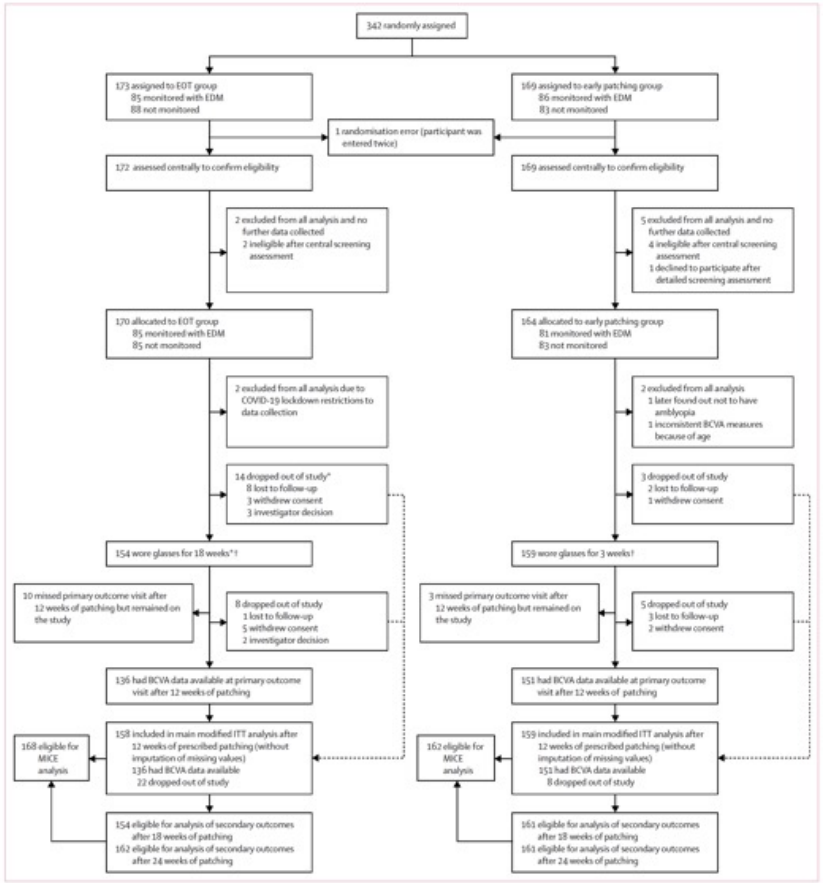

	EOT (n=170)	Early patching (n=164)
Age, years	5·2 (4·2–5·7)	5·4 (4·7–5·9)
Sex		
Female	69 (41%)	77 (47%)
Male	101 (59%)	87 (53%)
Not recorded	1 (1%)	1 (1%)
Type of amblyopia		
Anisometropic	115 (68%)	116 (71%)
Mixed	41 (24%)	34 (21%)
Strabismic	14 (8%)	14 (9%)
Spherical equivalent, dioptres		
Amblyopic eye	4·00 (2·50–5·00)	3·88 (2·75–5·25)
Contralateral (unaffected) eye	1·00 (0·25–2·25)	1·25 (0·38–2·25)
Baseline BCVA, logMAR		
Amblyopic eye	0·675 (0·500–0·800)	0·663 (0·550–0·800)
Contralateral (unaffected) eye	0·100 (0·050–0·180)	0·100 (0·025–0·175)
Baseline interocular visual acuity difference	0·525 (0·400–0·681)	0·550 (0·425–0·700)
Amblyopia severity		
Mild to moderate	66 (39%)	54 (33%)
Severe	104 (61%)	110 (67%)
Ethnicity		
White British	120 (71%)	122 (74%)
White Irish	8 (5%)	3 (2%)
White, other	14 (8%)	5 (3%)
Asian	16 (9%)	17 (10%)
Chinese	0	1 (1%)
Black or Black British	4 (2%)	6 (4%)
Mixed	6 (4%)*	7 (4%)†
Other	1 (1%)‡	1 (1%)§
Not recorded	1 (1%)	2 (1%)
Index of Multiple Deprivation (UK participants only)		
Mean (SD)	5·8 (3·0)	5·8 (2·9)

Data are median (IQR) or n (%), unless otherwise specified. Ethnicity based on parental report. BCVA=best corrected visual acuity. EOT=extended optical treatment. logMAR=logarithm of the minimum angle of resolution. *White and Black African (n=2), Mixed not further specified (n=2), White and Black Caribbean (n=1), and White and Thai (n=1). †White and Asian (n=2), White and Black African (n=1), White and mixed Black Caribbean and Indian (n=1), Arab (n=1), Romany (n=1), and Mixed not further specified (n=1). ‡Iraqi. §Irish Traveller. ¶135 participants in the EOT group and 135 participants in the early patching group were recruited from the UK.

Table: Baseline characteristics

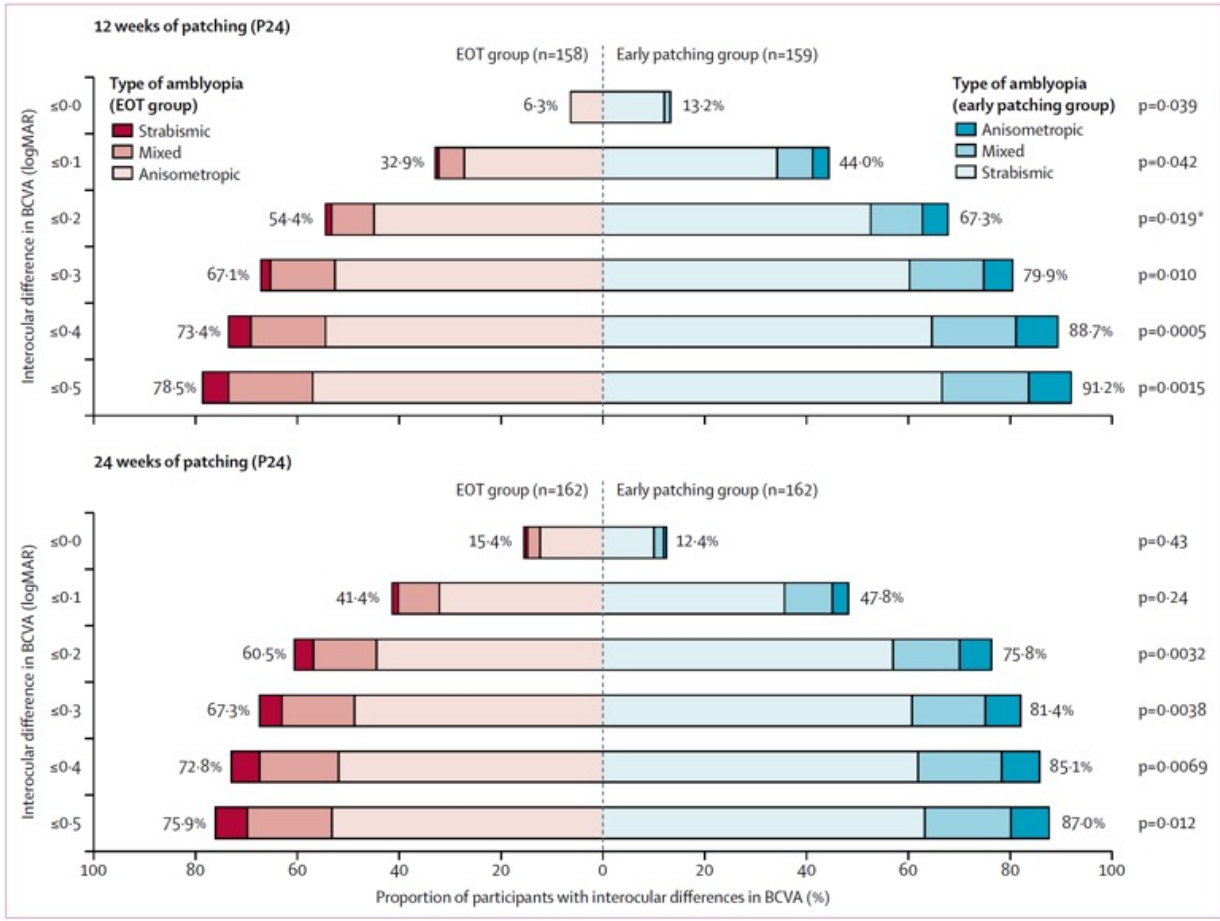

***Figure 3*: Proportion of participants reaching interocular differences in visual acuity at the primary outcome and end of study (without imputation of missing values)**

Different shades of colour show the breakdown by type of amblyopia (anisometropic, mixed, strabismic) for the primary outcome (12 weeks of patching) and the final outcome (24 weeks of patching). Statistical comparisons between the EOT group and the early patching group were done with χ^2 tests. The two panels represent the timepoints indicated by P12 and P24 on figure 1. For each panel, the proportions of participants reaching the thresholds of improvement indicated on the y axis are provided for the EOT group (red) and for the early patching group (blue). The percentage values provided are for all participants in each group. *EOT=extended optical treatment. logMAR=logarithm of the minimum angle of resolution. The primary outcome (ie, ≤0·20 logMAR interocular difference at 12 weeks). BCVA=best corrected visual acuity.

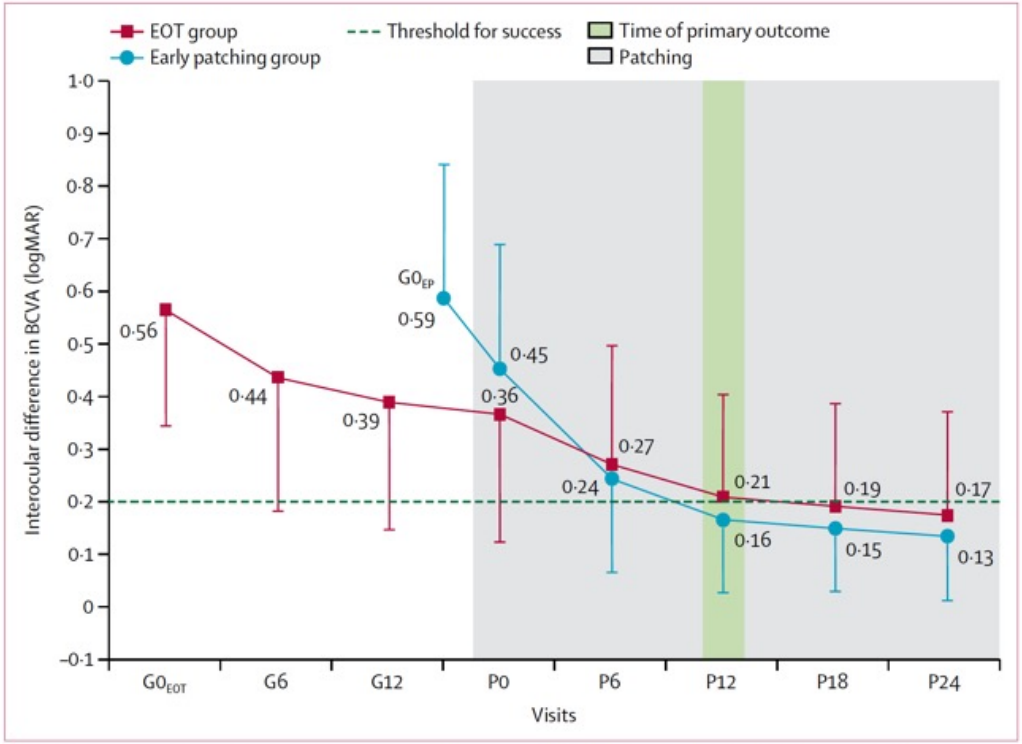

Figure 4: **Time course of changes in interocular differences in BCVA throughout the study, without imputation of missing values and excluding study dropouts**

Means and SDs of interocular differences in BCVA are shown, with the EOT group data shown in red squares and the early patching group data shown in blue circles. G0, G6, and G12 indicate weeks of glasses use; P0, P6, P12, P18, and P24 indicate weeks of patching. The threshold for successful treatment is indicated by the dashed line. BCVA=best corrected visual acuity. EOT=extended optical treatment. $G0_{EP}$=week 0 of glasses use in the early patching group. logMAR=logarithm of the minimum angle of resolution.

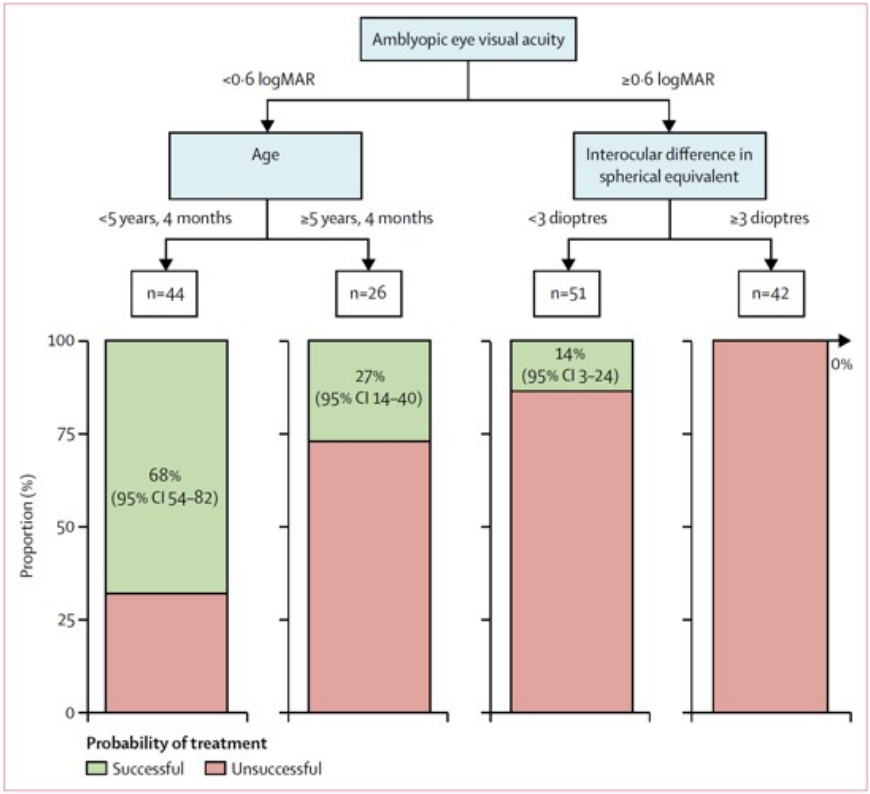

Figure 5: **Decision tree for probability of treatment success with EOT**

To assist in future clinical decision making, this decision tree shows the probability of successful treatment (with 95% CIs) with EOT only (before patching) on the basis of study participants' demographic and clinical characteristics. We included 163 children in the EOT group and used the recursive partitioning method. The sample of 163 participants included 149 children who had BCVA measurements available after 18 weeks of glasses use (including two participants who continued to wear glasses for 23 weeks and 24 weeks and were excluded from the primary outcome analysis after 12 weeks of patching) and 14 children who had dropped out before measurements were obtained at 18 weeks of glasses use. Using recursive partitioning, we identified the optimal split of predictor variables that would partition the data into outcome groups (successful treatment *vs* unsuccessful treatment). Finally, sensitivity and specificity of the decision tree for predicting successful treatment during the EOT period was calculated. Age, amblyopic eye BCVA at baseline, and interocular difference in spherical equivalent remained in the model. BCVA=best corrected visual acuity. EOT=extended optical treatment. logMAR=logarithm of the minimum angle of resolution.

Research in context

Evidence before this study

Amblyopia is the most common childhood visual disease, affecting 1–5% of the global population. If left untreated, amblyopia can lead to life-long serious visual impairment as well as lead to negative experiences for children receiving treatment (eg, bullying), which can affect children psychologically and socially at the time of treatment and even later in life. Optimal treatment regimens for amblyopia are far from established. Before this study, several clinical trials were published by multicentre collaboratives showing the efficacy of an extended period of glasses use only (of 4–6 months or more), called extended optical treatment, in improving vision before start of patching therapy. These studies have led to extended optical treatment becoming a mainstay of treatment for amblyopia. Extended optical treatment is included in clinical guidelines in several countries, including guidelines from the American Academy of Ophthalmology and the UK Royal College of Ophthalmologists. We searched all PubMed research articles, in any language, listed from database inception up to June 12, 2012, using the search terms "amblyopia (tiab)" OR "anisometropia (tiab)" OR "strabismus (tiab)" AND "optical (tiab)" OR "refractive (tiab)" OR "glasses". We found no published randomised controlled trials comparing extended optical treatment to a treatment group in which patching was begun earlier. In addition, a search of clinical trials registries, including ClinicalTrials.gov, the EU Clinical Trials Register, and the International Standard Randomised Controlled Trial Number registry found no planned randomised controlled trials investigating this question. A similar search was also done at the trial's midpoint on June 14, 2016. Subsequently, a similar study prescribing 2-h patching per day was launched by the Pediatric Eye Disease Investigator Group in 2020 (NCT04378790).

Added value of this study

Currently, the use of glasses for 4–6 months or more before children start patching is widely prescribed. This recommendation is based on the assumption that improving vision before patching reduces the overall amount of patching required, improving the treatment experience. This approach, however, could have the opposite effect, resulting in an extended treatment period, reducing motivation, and leading to worse visual outcomes and patient satisfaction. To our knowledge, this study is the first randomised controlled trial comparing extended glasses use before patching for the treatment of amblyopia with a control group for whom patching was begun earlier. Extended glasses use was more successful in younger children with mild amblyopia than in older children and those with more severe amblyopia. In contrast, in most children with severe amblyopia, children with larger differences in refractive errors between the eyes, and older children benefitted from starting patching early because, overall, early patching accelerated improvement in their vision. The attitudes of parents or guardians of children with amblyopia towards patching were more favourable for children patched earlier than those who underwent extended optical treatment.

Implications of all the available evidence

A systematic review and meta-analysis based on 20 publications by Asper and colleagues in 2018 showed unequivocally that vision improves during 4–6 months or more of glasses use, but not whether this improvement is better than that caused by earlier patching. The evidence from our study indicates that a personalised approach to extended glasses use is preferred. In our study, prescriptions of extended glasses use were favourable in younger children with mild amblyopia. Children with severe amblyopia, large differences in refractive errors between the eyes, and older children were less likely to benefit from glasses use alone, and the majority benefitted from early patching. We prescribed intense patching (ie, 10 h/day, 6 days per week) in our study. Future studies, comparing treatments with and without extended glasses use, are needed to establish whether the same conclusions can be drawn for different patching regimens.

Rates and causes of death after release from incarceration among 1 471 526 people in eight high-income and middle-income countries: an individual participant data meta-analysis

Summary

Background Formerly incarcerated people have exceptionally poor health profiles and are at increased risk of preventable mortality when compared with their general population peers. However, not enough is known about the epidemiology of mortality in this population—specifically the rates, causes, and timing of death in specific subgroups and regions—to inform the development of targeted, evidence-based responses. We aimed to document the incidence, timing, causes, and risk factors for mortality after release from incarceration.

Methods We analysed linked administrative data from the multi-national Mortality After Release from Incarceration Consortium (MARIC) study. We examined mortality outcomes for 1 471 526 people released from incarceration in eight countries (Australia, Brazil, Canada, New Zealand, Norway, Scotland, Sweden, and the USA) from 1980 to 2018, across 10 534 441 person-years of follow-up (range 0–24 years per person). We combined data from 18 cohort studies using two-step individual participant data meta-analyses to estimate pooled all-cause and cause-specific crude mortality rates (CMRs) per 100 000 person-years, for specific time periods (first, daily from days 1–14; second, weekly from weeks 3–12; third, weeks 13–52 combined; fourth, weeks 53 and over combined; and fifth, total follow-up) after release, overall and stratified by age, sex, and region.

Findings 75 427 deaths were recorded. The all-cause CMR during the first week following release (1612 [95% CI 1048–2287]) was higher than during all other time periods (incidence rate ratio [IRR] compared with week 2: 1·5 [95% CI 1·2–1·8], I^2=26·0%, weeks 3–4: 2·0 [1·5–2·6], I^2=53·0%, and weeks 9–12: 2·2 [1·6–3·0], I^2=70·5%). The highest cause-specific mortality rates during the first week were due to alcohol and other drug poisoning (CMR 657 [95% CI 332–1076]), suicide (135 [36–277]), and cardiovascular disease (71 [16–153]). We observed considerable variation in cause-specific CMRs over time since release and across regions. Pooled all-cause CMRs were similar between males (731 [95% CI 630–839]) and females (660 [560–767]) and were higher in older age groups.

Interpretation The markedly elevated rate of death in the first week post-release underscores an urgent need for investment in evidence-based, coordinated transitional healthcare, including treatment for mental illness and substance use disorders to prevent post-release deaths due to suicide and overdose. Temporal variations in rates and causes of death highlight the need for routine monitoring of post-release mortality.

Chief investigator(s)	Country (state/province)	Study dates	Sample size	Female population (%)	Male population (%)	Age at release, median (IQR)	Length of follow-up in years, median (IQR); range	Length of follow-up in person-years, total	Deaths (%)
Binswanger	USA (Washington)	1999–2009	76 208	12 229 (16·0%)	63 979 (84·0%)	32 (25–40)	4·7 (2·4–7·2); 0·0–10·5	370 100	2507 (3·3%)
Bukten and Clausen	Norway	2000–2016	96 170	9902 (10·3%)	86 268 (89·7%)	31 (23–42)	10·1 (5·9–13·8); 0·0–17·0	929 809	7975 (8·3%)
Cunningham and King	New Zealand	1998–2016	91 632	11 610 (12·7%)	80 022 (87·3%)	27 (21–37)	10·7 (5·9–15·3); 0·0–19·0	951 846	4803 (5·2%)
Fazel and Chang	Sweden	2000–2009	47 326	3846 (8·1%)	43 480 (91·9%)	36 (26–45)	5·3 (2·7–7·6); 0·0–10·0	242 967	2874 (6·1%)
Giles	Australia (Western Australia)	2005–2014	13 282	1661 (12·5%)	11 621 (87·5%)	31 (25–38)	6·9 (5·2–8·3); 0·0–9·5	89 103	541 (4·1%)
Graham	Scotland	1996–2007	75 033	8181 (10·9%)	66 852 (89·1%)	26 (21–35)	6·5 (3·3–9·6); 0·0–12·0	478 891	4404 (5·9%)
Kariminia	Australia (New South Wales)	1988–2002	82 669	8667 (10·5%)	74 002 (89·5%)	28 (22–35)	7·4 (3·6–11·1); 0·0–15·0	614 569	5000 (6·0%)
Kinner	Australia (Queensland)	1994–2007	42 015	4976 (11·8%)	37 039 (88·2%)	28 (22–37)	7·6 (3·5–10·3); 0·0–14·0	297 223	2203 (5·2%)
Kouyoumdjian (A)	Canada (Ontario)	2000–2009	31 183	2780 (8·9%)	28 403 (91·1%)	32 (25–40)	8·2 (5·8–9·0); 0·0–12·5	220 157	1723 (5·5%)
Kouyoumdjian (B)	Canada (Ontario)	2010–2015	52 307	6357 (12·2%)	45 950 (87·8%)	32 (24–43)	5·5 (5·2–5·7); 0·0–7·2	270 569	2034 (3·9%)
Lim	USA (New York)	2001–2005	244 274	29 650 (12·1%)	214 624 (87·9%)	31 (23–40)	3·1 (1·7–4·2); 0·0–5·0	702 455	1657 (0·7%)
Liu	Brazil (Mato Grosso do Sul)	2009–2018	62 425	7215 (1·6%)	55 210 (88·4%)	31 (26–39)*	5·0 (2·3–7·7); 0·0–10·0	311 069	2402 (3·8%)
Pizzicato and Viner	USA (Pennsylvania)	2010–2016	82 780	16 371 (19·8%)	66 409 (80·2%)	31 (24–43)	4·4 (2·5–5·9); 0·0–7·0	342 616	2516 (3·0%)
Preen (A)	Australia (Western Australia)	1994–2003	16 160	1930 (11·9%)	14 230 (88·1%)	28 (22–36)	6·1 (3·6–8·9); 0·0–10·0	97 767	673 (4·2%)
Preen (B)	Australia (Western Australia)	1985–2008	6375	666 (10·4%)	5709 (89·6%)	27 (22–37)	18·1 (14·8–21·2); 0·0–24·0	111 638	674 (10·6%)
Ranapurwala	USA (North Carolina)	2000–2018	258 617	36 278 (14·0%)	222 339 (86·0%)	30 (24–39)	10·8 (6·3–15·2); 0·0–19·0	2 708 859	17 422 (6·7%)
Rosen	USA (North Carolina)	1980–1999	113 079	0	113 079 (100%)	31 (25–39)	8·2 (4·8–13·0); 0·0–20·0	1 010 760	9001 (8·0%)
Somers	Canada (British Columbia)	2001–2018	79 991	10 245 (12·8%)	69 746 (87·2%)	33 (25–42)	10·2 (5·3–14·7); 0·0–17·2	784 268	7018 (8·8%)
Total	NA	1980–2018	1 471 526	172 204 (11·7%)	1 299 322 (88·3%)	NA	NA	10 534 441	75 427 (5·1%)

Study dates are from the beginning of recruitment until the end of follow-up. NA=not applicable. *Information on age at release was only available for a subset of participants (n=2393) in the Liu cohort.

Table 1: **Summary of the 18 included cohorts from the Mortality After Release from Incarceration Consortium**

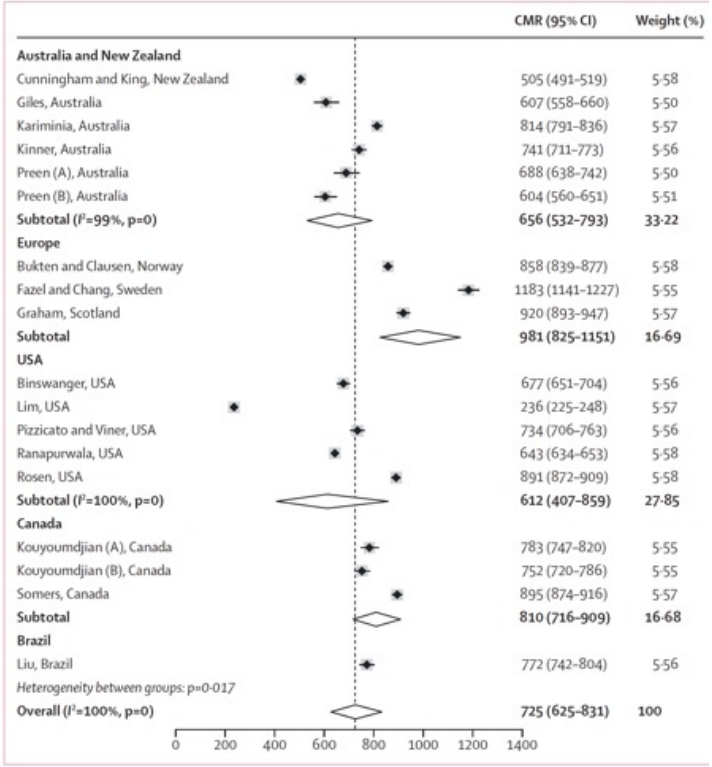

Figure 1: **Forest plot of overall CMRs for people released from incarceration, by region**
I^2 and p-value calculated for regions with four or more cohorts. CMR=crude mortality rate.

Cause of death category	N dea
All-cause	7542
Maternal, nutritional, and infectious diseases	367
HIV	204
Respiratory infections*	91
Tuberculosis*†	8
Maternal*†‡	1
Other and ill-defined infectious and nutritional diseases*†	55
Non-communicable diseases	2973
Cardiovascular diseases	1131
Cancer and other neoplasms	892
Liver disease	379
Chronic respiratory diseases	192
Diabetes	101
Other and ill-defined non-communicable diseases	276
Injuries	3742
Alcohol and other drug poisoning (unintentional and undetermined intent)	1612
Suicide	619
Interpersonal violence	636
Transport-related accidents	516
Other and ill-defined injuries	357
Other and ill-defined	394
Intermediate and immediate causes of death§	112
Ill-defined or unknown causes of death	281
Missing cause of death*	64

CMR=crude mortality rate. *Binswanger could not provid
from these analyses. †Cunningham and King could not pr
excluded from these analyses. ‡Rosen was excluded from
Due to these exclusions, the number of deaths in the caus
deaths. §An intermediate cause of death is a condition tha
in the immediate cause of death or another intermediary

Table 2: **Pooled all-cause and cause-specific crude m**

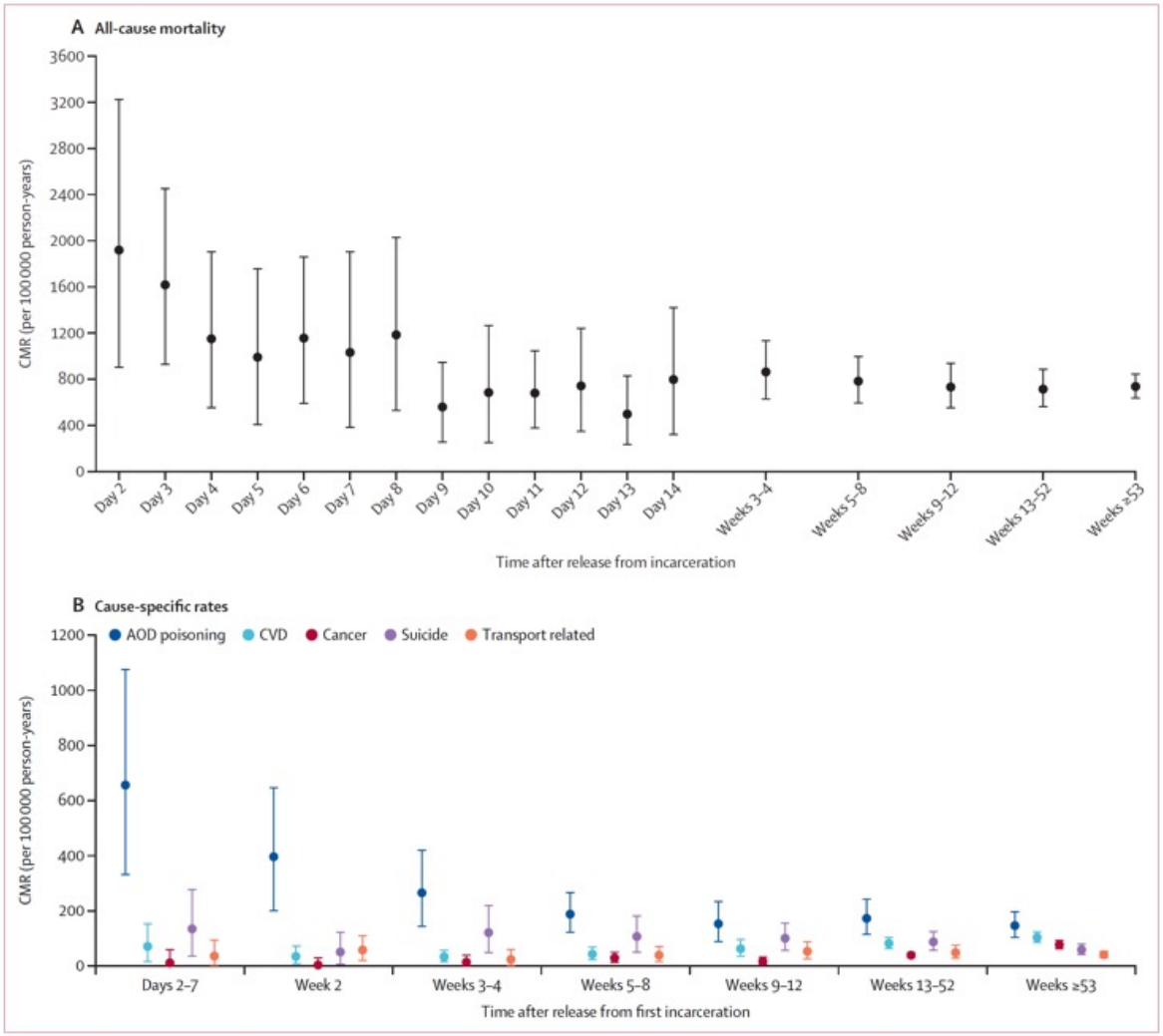

Figure 2: **Piecewise pooled mortality rates after release from incarceration**
The cohorts from Cunningham and King and from Binswanger could not provide deaths by day data and were excluded from these analyses. AOD=alcohol and other drugs. CMR=crude mortality rate. CVD=cardiovascular disease.

Research in context

Evidence before this study

We sought to identify relevant cohort studies that examined the epidemiology of mortality due to any cause(s) following release from prison or jail internationally. We searched MEDLINE, PsycINFO, and Embase for studies published in English from database inception (1966, 1978, and 1975, respectively) until Feb 1, 2023, using a combination of terms: "prison", "jail", "release", "mortality", "death", "suicide", "overdose", "HIV", "longitudinal", and "cohort". While many studies identified an increased rate of death relative to the surrounding population in the period immediately following release from incarceration, most studies were limited by: first, small sample sizes; second, focusing solely on the first 2 weeks or first month after release; third, studying cohorts created on the basis of a specific health condition (eg, HIV) or cohort members having been convicted of a particular offence (eg, violent offences); and fourth, focusing on only one cause of death (eg, opioid overdose).

Added value of this study

Our combined sample size (N=1 471 526) is orders of magnitude larger than most previous studies, and our use of two-step individual participant data meta-analyses and a standardised data analysis plan used by 18 cohorts ensured, for the first time, consistency of analysis and aggregate outputs across cohorts. We include all causes of death during discrete time periods for up to 24 years following release from incarceration and include data from cohort studies conducted in eight countries. Our findings demonstrate that the leading causes of death after release from incarceration vary across demographic subgroups, geographical regions, and the length of time between release from incarceration and subsequent death. Additionally, our analyses provide new and compelling evidence that the previously documented spike in deaths on day 1 following release is likely a partial artefact of the miscoding of administrative data.

Implications of all the available evidence

There is a high rate of death from numerous preventable causes after release from incarceration internationally, with rates and causes of death varying across demographic subgroups, geographical regions, and time since release from incarceration. These variations highlight the need for prevention that is socio-demographically, geographically, and temporally tailored, and for effective, sustained health promotion for people who experience incarceration. In addition, routine monitoring of post-release mortality is essential to inform ongoing, country-specific prevention efforts. There is a crucial need for greater investment in evidence-based transitional and post-release support to prevent further unnecessary deaths in vulnerable individuals who have been released from incarceration.

Visualising the dynamic morphology of stuttering using real-time MRI

A 42-year-old man with a history of an intermittent disorder of speech fluency beginning around the age of 4 years without any obvious triggers attended our unit for further investigation; he had agreed to participate in our MRI study on speech production.

The patient had no medical history and on clinical examination we found him to be fit and well.

However, he had moments when his speech fluency was lost; these were episodic, brief—rarely lasting longer than 30 secs—and occurring mostly, but not exclusively, at the beginning of words, and usually, but not always, with consonants rather than vowels. The episodes were markedly exacerbated by environmental stressors and were attenuated by cueing and external rhythms. Previously, several attempts had been made to treat and improve speech fluency with no lasting effect; the speech difficulty remained.

Notably, in his personal history, the patient had left school early to take up a technical apprenticeship. He had avoided professions which were more language-related and obtained an academic degree in engineering after 4 years of evening school.

More recently, he had just participated in speech therapy focusing on different kinds of block releasing techniques, combined with anti-anxiety training. An uncle and his daughter—the patient's cousin—had shown similar speech dysfluencies since they were children.

For our study, we used real-time MRI to non-invasively visualise the movements of the tongue and the oropharynx while the patient read a specially selected piece of text from a screen positioned in his field of vision as he was in the scanner.

The video clip, with 55 MRI images per second, showed a midsagittal cross-sectional plane covering the mouth, mandibular nasal cavities, pharynx, and larynx (figure; video). The intermittent repetitions of syllables and sounds, prolongations of sounds, and audible or silent blockings were visible as spasms and repetitive movements in parts of the tongue, lips, and velum. The video also showed fluent sounding segments of speech, thereby ruling out permanent speech disorders. A speech-language pathologist confirmed the diagnosis of stuttering and categorised it as moderate.

The patient was reassured that the visualisation had delineated his condition clearly and it enabled him to gain a greater understanding into its mechanics.

Stuttering affects about 1% of the adult population, mostly males, and has a high heritability. Relapse after therapy—which includes fluency shaping and block modification techniques—is frequent and often results in the condition continuing for many years. Stuttering can impair social development. Attempts to stop or to avoid stuttering may result in verbal, visual, or situational avoidance, and not speaking in circumstances where the patient would be expected to may be misinterpreted as inappropriate behaviour. Anxiety disorders—including social anxiety disorder and generalised anxiety disorder—are present in about half of the affected individuals and addressing them improves therapy outcomes.

The real-time MRI, which demonstrated the mechanical pathogenesis of the primary symptoms, has improved our understanding of and updates our thinking about stuttering; it gives a better understanding of what the inner articulators do wrong during this type of dysfluent speech.

Additionally, in clinical practice the method may be useful in identifying dysfunctional motor behaviour in speech production disorders. Further, it could potentially be used in visual biofeedback settings to aid in the acquisition and reinforcement of new speech patterns. We acknowledge that the use of a single slice MRI is a limitation that may possibly be overcome with future advances in MRI technology.

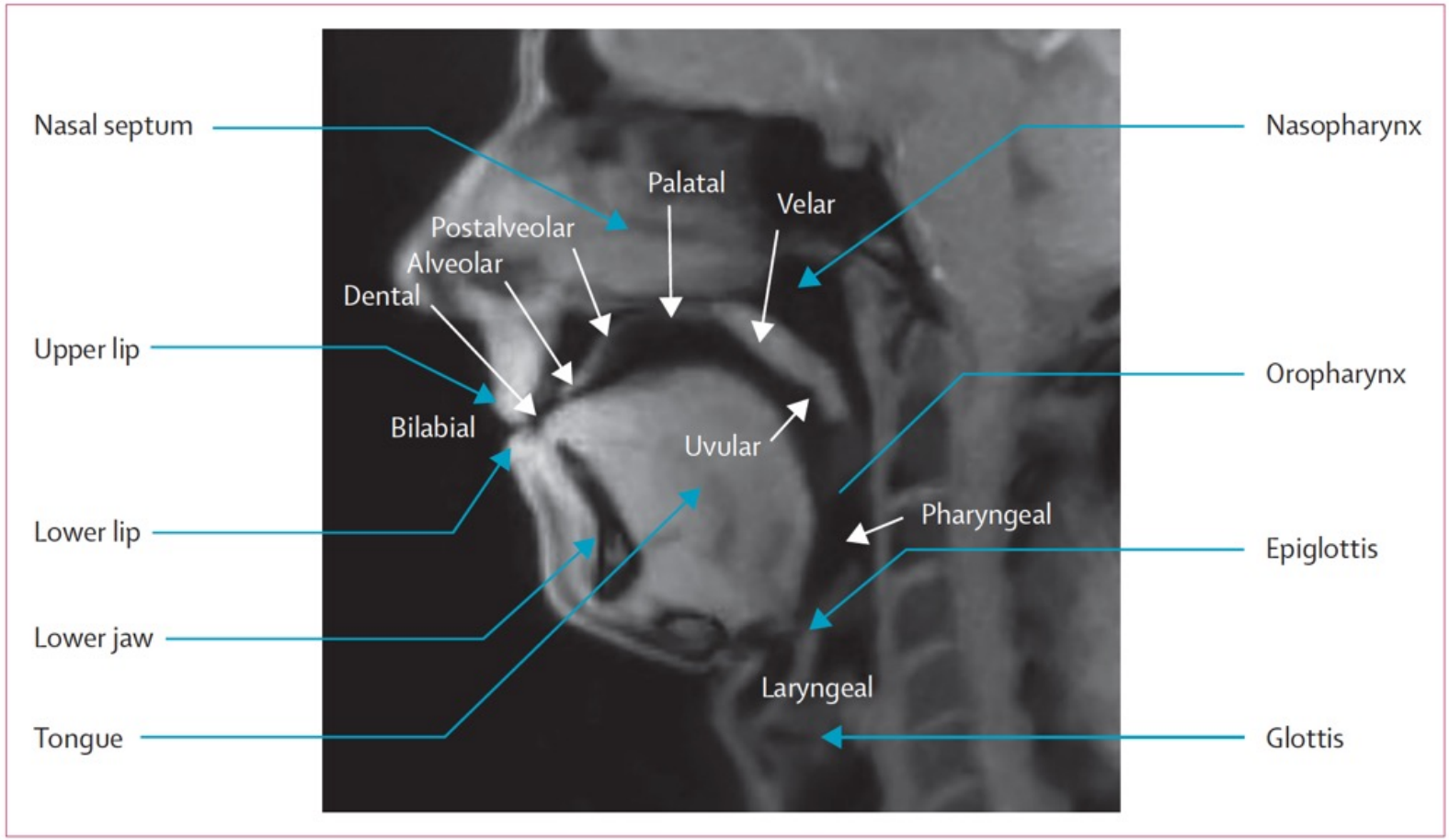

Figure: **Visualising the dynamic morphology of stuttering**
Image of the first frame from a video of the real-time MRI shows a midsagittal cross-sectional plane of the patient's head with vocal tract structures (white arrows) and places of articulation (blue arrows).

B-cell non-Hodgkin lymphomas

B-cell lymphomas occur with an incidence of 20 new cases per 100 000 people per year in high-income countries. They can affect any organ and are characterised by heterogeneous clinical presentations and courses, varying from asymptomatic, to indolent, to very aggressive cases. Since the topic of B-cell non-Hodgkin lymphomas was last reviewed in *The Lancet* in 2017, a deeper understanding of the biological background of this heterogeneous group of malignancies, the availability of new diagnostic methods, and the development and implementation of new targeted and immunotherapeutic approaches have improved our ability to treat patients. This Seminar provides an overview of the pathobiology, classification, and prognostication of B-cell non-Hodgkin lymphomas and summarises the current knowledge and standard of care regarding biology and clinical management of the most common subtypes of mature B-cell non-Hodgkin lymphomas. It also highlights new findings in deciphering the molecular background of disease development and the implementation of new therapeutic approaches, particularly those targeting the immune system.

Panel: Mature B-NHL subtypes as classified by the International Consensus Classification and WHO Classification 5th edition (selection including those discussed in this Seminar)

Small B-cell lymphomas

International Consensus Classification

- Chronic lymphocytic leukaemia and small lymphocytic lymphoma
- Monoclonal B-cell lymphocytosis
- B-cell prolymphocytic leukaemia*†
- Splenic marginal zone lymphoma
- Hairy cell leukaemia
- Splenic B-cell lymphoma or leukaemia, unclassifiable‡
  - Splenic diffuse red pulp small B-cell lymphoma‡
  - Hairy cell leukaemia-variant†‡
- Lymphoplasmacytic lymphoma
  - Waldenström macroglobulinaemia
- IgM MGUS
  - IgM MGUS, plasma cell type*†§
  - IgM MGUS, NOS*†§
- Primary cold agglutinin disease§

WHO Classification

- Chronic lymphocytic leukaemia or small lymphocytic lymphoma
- Monoclonal B-cell lymphocytosis
- B-cell prolymphocytic leukaemia deleted
- Splenic marginal zone lymphoma
- Hairy cell leukaemia
- Splenic diffuse red pulp small B-cell lymphoma
- Splenic B-cell lymphoma or leukaemia with prominent nucleoli.†§ Encompasses hairy cell leukaemia-variant and some cases of B-cell prolymphocytic leukaemia
- Lymphoplasmacytic lymphoma
  - Waldenström macroglobulinaemia
- IgM monoclonal gammopathy of undetermined significance
- Cold agglutinin disease§

Nodal and extranodal neoplasms

International Consensus Classification

- Extranodal marginal zone lymphoma of mucosa-associated lymphoid tissue (MALT lymphoma)
- Primary cutaneous marginal zone lymphoproliferative disorder†§
- Nodal marginal zone lymphoma
  - Paediatric nodal marginal zone lymphoma
- Follicular lymphoma
  - Grade 1–2 and 3A
  - Grade 3B
  - In situ follicular neoplasia
- Duodenal-type follicular lymphoma
- BCL2-R negative, CD23-positive follicle centre lymphoma (related but not equivalent to the diffuse variant of follicular lymphoma in the WHO classification)*†‡§
- Primary cutaneous follicle centre lymphoma
- Paediatric-type follicular lymphoma
- Testicular follicular lymphoma†§
- Large B-cell lymphoma with IRF4 rearrangement (listed with follicular lymphoma)†§‡
- Mantle cell lymphoma
  - In situ mantle cell neoplasia
  - Leukaemic non-nodal mantle cell lymphoma

WHO Classification

- Extranodal marginal zone lymphoma of mucosa-associated lymphoid tissue (MALT lymphoma)
- Primary cutaneous marginal zone lymphoma†§
- Nodal marginal zone lymphoma
- Paediatric nodal marginal zone lymphoma
- Follicular lymphoma
  - Classic follicular lymphoma†§
  - Follicular large B-cell lymphoma†§
  - In situ follicular B-cell neoplasm
  - Duodenal-type follicular lymphoma
  - Testicular follicular lymphoma†
    - Follicular lymphoma with uncommon features†§
    - Follicular lymphoma with blastoid or large centrocytes†§
- Diffuse follicular lymphoma†§
- Primary cutaneous follicle centre lymphoma
- Paediatric-type follicular lymphoma
- Mantle cell lymphoma
  - In situ mantle cell neoplasm
  - Leukaemic non-nodal mantle cell lymphoma

Large B-cell lymphomas

International Consensus Classification

- DLBCL, NOS
  - Germinal centre B-cell subtype
  - Activated B-cell subtype
- Large B-cell lymphoma with 11q aberration†§
- Nodular lymphocyte predominant B-cell lymphoma (no longer considered a Hodgkin subtype of lymphoma)†§
- T-cell or histiocyte-rich large B-cell lymphoma
- Primary DLBCL of the CNS†
- Primary DLBCL of the testis†§
- Primary cutaneous DLBCL, leg type
- Intravascular large B-cell lymphoma
- HHV-8 and EBV-negative primary effusion-based lymphoma†§‡
- EBV-positive mucocutaneous ulcer
- EBV-positive DLBCL, NOS
- DLBCL associated with chronic inflammation
  - Fibrin-associated DLBCL
- Lymphomatoid granulomatosis

(Continues on next page)

(Panel continued from previous page)

- EBV-positive polymorphic B-cell lymphoproliferative disorder, NOS*†§
- ALK-positive large B-cell lymphoma
- Burkitt lymphoma
- High-grade B-cell lymphoma, with *MYC* and *BCL2* rearrangements†§
- High-grade B-cell lymphoma with *MYC* and *BCL6* rearrangements†§‡
- High-grade B-cell lymphoma, NOS
- Primary mediastinal large B-cell lymphoma
- Mediastinal grey-zone lymphoma§
- Plasmablastic lymphoma
- HHV-8-associated lymphoproliferative disorders
  - Multicentric Castleman disease
  - HHV-8-positive germinotropic lymphoproliferative disorder
  - HHV-8-positive DLBCL, NOS
  - Primary effusion lymphoma

WHO Classification

- Diffuse large B-cell lymphoma, NOS
  - Germinal centre B-cell subtype
  - Activated B-cell subtype
- High-grade B-cell lymphoma with 11q aberration†§
- T-cell or histiocyte-rich large B-cell lymphoma
- Large B-cell lymphoma with IRF4 rearrangement (listed with large B-cell lymphomas)†§
- Primary large B-cell lymphoma of immune-privileged sites (includes CNS, testis, and vitreoretinal)†§
- Primary cutaneous DLBCL, leg type
- Intravascular large B-cell lymphoma
- Fluid overload-associated large B-cell lymphoma†§
- EBV-positive mucocutaneous ulcer
- EBV-positive DLBCL
- DLBCL associated with chronic inflammation
- Fibrin-associated large B-cell lymphoma
- Lymphomatoid granulomatosis
- ALK-positive large B-cell lymphoma
- Burkitt lymphoma
- Diffuse large B-cell lymphoma or high-grade B-cell lymphoma with *MYC* and *BCL2* rearrangements†§
- Cases with *MYC* and *BCL6* rearrangements are classified either as a subtype of DLBCL NOS, or high-grade B-cell lymphoma NOS, according to their cytomorphological features†§
- High-grade B-cell lymphoma, NOS
- Primary mediastinal large B-cell lymphoma
- Mediastinal grey-zone lymphoma§
- Plasmablastic lymphoma
- KSHV or HHV-8-associated B-cell lymphoid proliferations and lymphomas
  - KSHV or HHV-8-associated multicentric Castleman disease
  - KSHV or HHV-8-positive germinotropic lymphoproliferative disorder
  - KSHV or HHV-8-positive DLBCL
  - Primary effusion lymphoma

Adapted from Campo et al.[7] B-NHL=B-cell non-Hodgkin lymphomas. DLBCL=Diffuse large B-cell lymphoma. EBV=Epstein-Barr virus. HHV-8=human herpesvirus-8. KSHV=Kaposi sarcoma associated herpesvirus. MALT=mucosa-associated lymphoid tissue. MGUS=monoclonal gammopathy of undetermined significance. NOS=not otherwise specified. *Entities only present in the International Consensus Classification. †Entities that differ between the International Consensus Classification and WHO 5th edition. ‡Provisional entities from the International Consensus Classification. §Entities that introduce substantial changes compared with the WHO 4th edition revised classification.

	IPI (DLBCL)	NCCN-IPI (DLBCL)	FLIPI (follicular lymphoma)	MIPI (simplified; MCL)
Age	>60 years=1	40–60 years=1; 61–74 years=2; ≥75 years=3	>60 years=1	50–59 years=1; 60–69 years=2; ≥70 years=3
Lactate dehydrogenase	>1 ULN=1	≤3 ULN=1; >3 ULN=2	>1 ULN=1	0·67–0·99 ULN=1; 1–1·49 ULN=2; ≥1·5 ULN=3
Eastern Cooperative Oncology Group Performance status ≥2	1	1	..	1
Ann Arbor stage 3–4	1	1	1	..
Extranodal disease presence* >1	1	1	..	..
Haemoglobin concentration (g/dL)	..	..	<12= 1	..
Number of nodal sites	..	..	>4=1	..
White blood cells (g per L)	..	..	..	6·7–9·9=1; 10–14·9=2; ≥15=3
Risk categories				
Low	0–1	0–1	0–1	0–3
(Low-) Intermediate	2	2–3	2	4–5
(High-) Intermediate	3	4–5	..	..
High	4–5	≥6	3–5	6–11

DLBCL=diffuse large B-cell lymphoma. FLIPI=Follicular Lymphoma International Prognostic Index. IPI=International Prognostic Index. MCL=mantle cell lymphoma. MIPI=Mantle Cell Lymphomas International Prognostic Index. NCCN-IPI=National Comprehensive Cancer Network International Prognostic Index. ULN=upper limit of normal. *Including bone marrow, gastrointestinal tract, liver, lung, CNS, and other sites.

Table 1: **Subtype-specific risk scores and their relation to risk categories on each measure**

	First-line approved	First-line off-label	Relapse approved	Relapse off-label
Waldenström macroglobulinaemia				
BTK inhibitor	Ibrutinib or zanubrutinib with or without rituximab*	..	Ibrutinib or zanubrutinib with or without rituximab	Acalabrutinib
Proteasome inhibitor	..	Bortezomib plus rituximab	..	Bortezomib plus rituximab
Others	..	..	..	Venetoclax
Marginal zone lymphoma				
BTK inhibitor	..	..	Ibrutinib; zanubrutinib	Acalabrutinib
Immune modulator	..	..	Rituximab plus lenalidomide†	..
Follicular lymphoma				
BTK inhibitor	..	Rituximab plus lenalidomide	Rituximab plus lenalidomide	..
Immunotherapy	..	..	Axicabtagene ciloleucel‡; tisagenlecleucel‡; mosunetuzumab‡	Glofitamab; epcoritamab
Others	..	..	Tazemetostat§	..
Mantle cell lymphoma				
BTK inhibitor	..	Rituximab plus ibrutinib§	Ibrutinib¶; zanubrutinib§; acalabrutinib§; pirtobrutinib||§	..
Immune modulator	..	..	Lenalidomide with or without rituximab||	..
Immunotherapy	..	..	Brexucabtagene autoleucel||	Glofitamab
Others	..	..	..	Venetoclax
Diffuse large B-cell lymphoma				
BTK inhibitor	..	Ibrutinib (plus R-CHOP; molecular subtype)	..	..
Proteasome inhibitor	..	Bortezomib (plus R-CHOP; ABC subtype)	..	..
Immune modulator	..	..	Tafasitamab plus lenalidomide	..
Immunotherapy	..	..	Axicabtagene ciloleucel; lisocabtagene maraleucel; tisagenlecleucel‡; glofitamab‡§ ; epcoritamab‡§	..
Others	..	..	Selinexor||; loncastuximab tesirine	Venetoclax (ViPOR)

BTK inhibitor. ABC=activated B cell. BTK=Bruton tyrosine kinase. R-CHOP=rituximab plus cyclophosphamide, doxorubicin, vincristine, and prednisone or prednisolone. ViPOR=venetoclax, ibrutinib, prednisone, obinutuzumab, and revlimid. *For patients not qualifying for immunochemotherapy. †Only USA. ‡For higher relapse. §For patients with indolent forms. ¶Only EU. ||After previous BTK inhibitor.

Table 2: **Recommended targeted therapies**

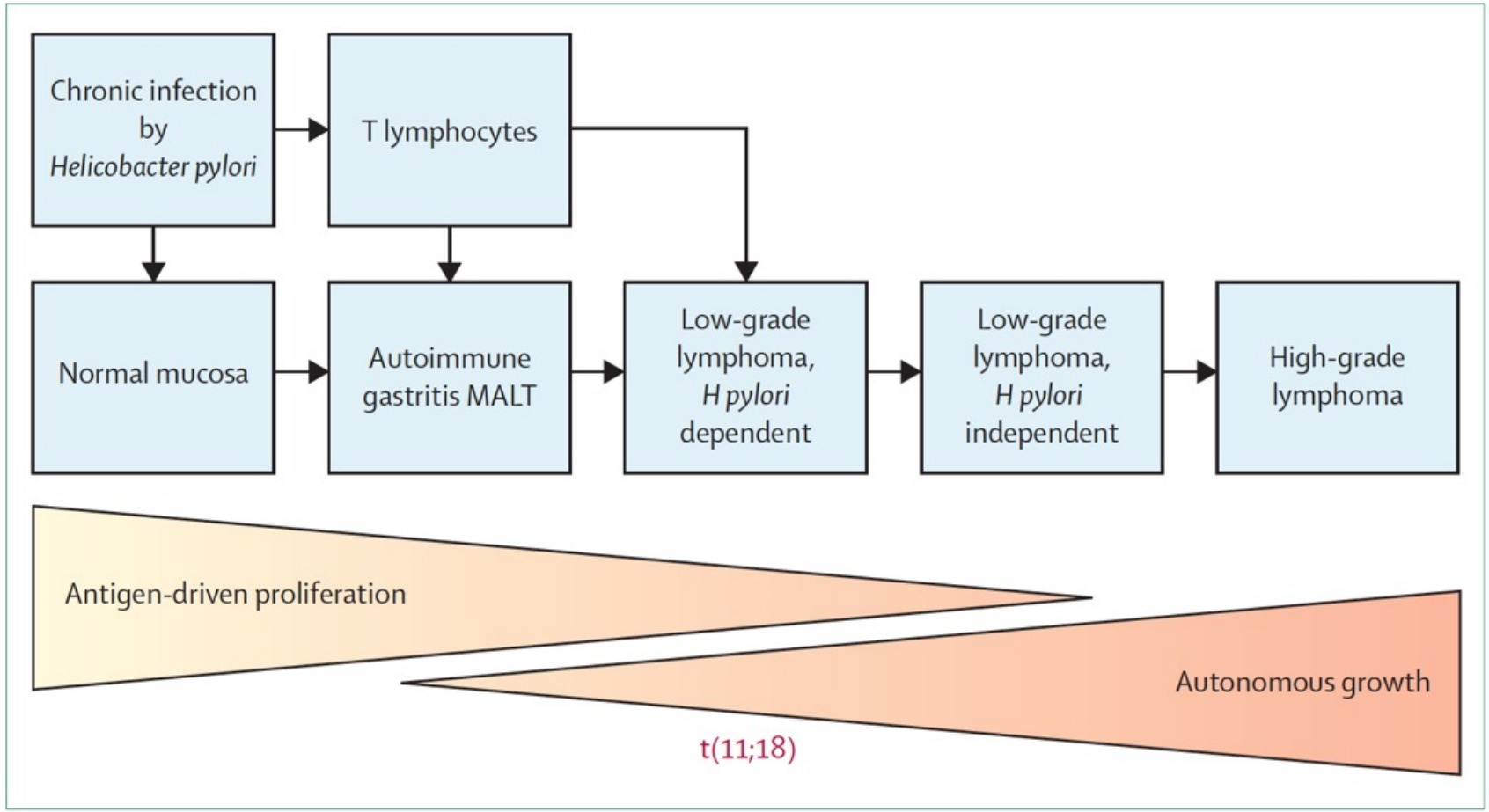

Figure 1: **Pathogenesis of gastric MALT lymphoma**
Reproduced from Fischbach.[44] MALT=mucosa-associated lymphoid tissue.

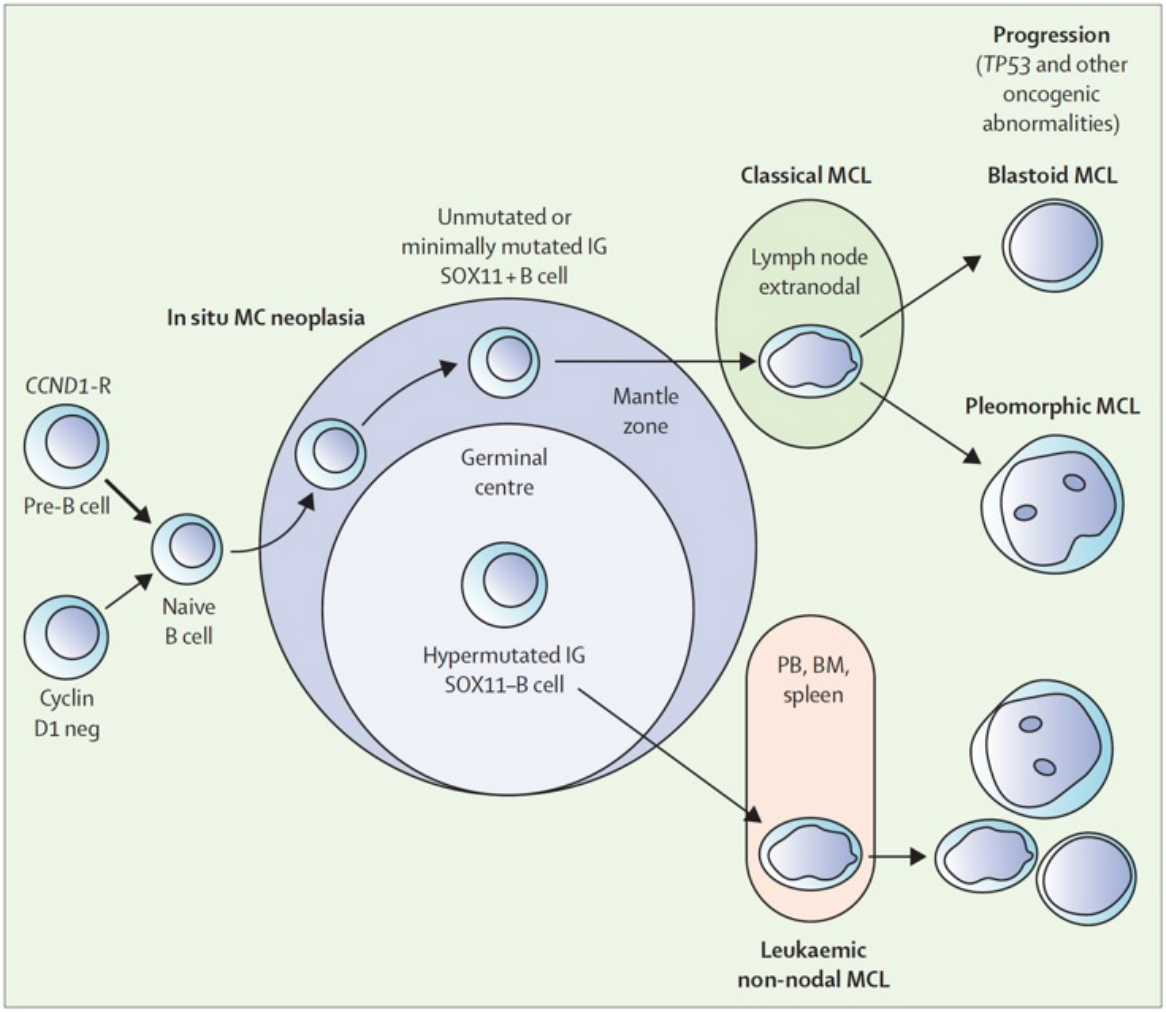

Figure 2: **Pathogenesis of mantle cell lymphoma**
Reproduced from Dreyling et al.[93] BM=bone marrow. MC=mantle cell. MCL=mantle cell lymphoma. PB=peripheral blood.

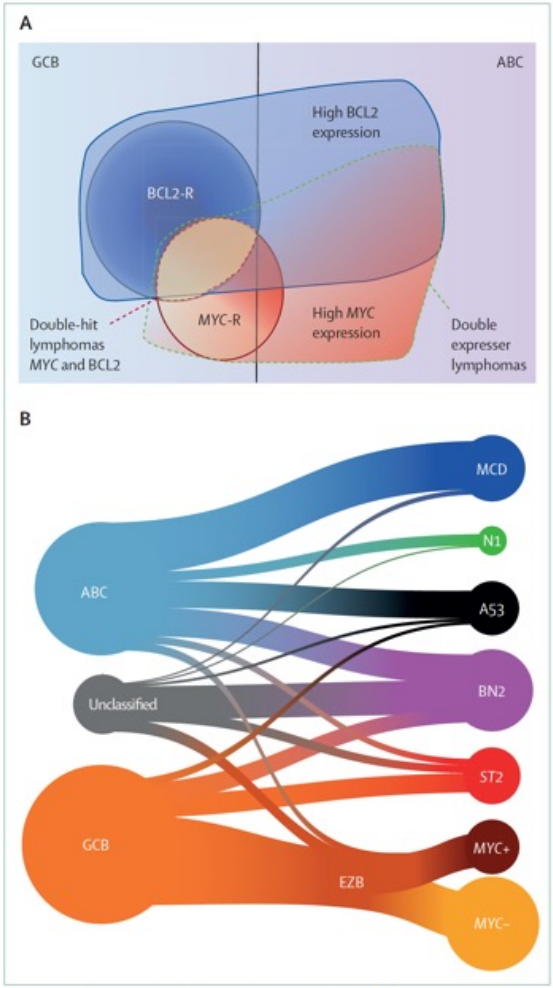

Figure 3: **DLBCL: Double-hit and double-expresser lymphomas and genetic subtyping**
(A) Reproduced from Dunleavy.[124] (B) Reproduced from Wright et al.[125] ABC=activated B cell-like. GCB=germinal centre B cell. All elements of the right side and EZB are the names of the subtypes as defined by the LymphGen algorithm.

Conclusion

Our understanding of the biological basis of B-cell lymphomas has greatly improved during the past decade, paving the way for numerous new developments in diagnosis, prognostication, and therapeutic management of this heterogeneous group of diseases. This increased understanding has led to revised classifications of B-NHL, considering the increasing importance of genetic and other molecular data in the evaluation of lymphoid neoplasia. The use of in-depth genetic analyses has resulted in the identification of prognostically relevant genetic profiles defining high-risk disease. However, except for *TP53* mutations in mantle cell lymphoma, none of these prognostic scores has entered diagnostic routine yet and improvement of the clinical applicability of these scores is warranted.

Current investigations continue to evaluate targeted approaches in molecularly characterised subsets of DLBCL. In indolent lymphomas, chemotherapy-based first-line approaches are increasingly challenged by targeted therapies. Finally, immunotherapeutic approaches, mostly with adoptive T-cell therapy, are becoming the standard of care for relapsed disease in several lymphoma subtypes including DLBCL (CAR T-cells) as well as indolent lymphomas (bispecific antibodies). This knowledge could lead to more risk-based and individualised treatment strategies that benefit patients.

Two types of B cell in the tumor microenvironment modulate antitumor immunity

An effective humoral response is associated with the formation of GCs in the follicles of secondary lymphoid organs, such as the lymph nodes, and the production of highly specific antibodies. However, B cells can also be generated by an extrafollicular (EF) pathway that directs the cells away from the GC and mutation-driven increases in BCR affinity. Tumors can also support an organized cluster of immune cells termed tertiary lymphoid structures (TLSs), which resemble those found in the secondary lymphoid organs. Although the most mature TLSs often correlate with a good patient prognosis, many tumors with B cell infiltrates display only disorganized or no TLSs, implying the existence of alternative differentiation pathways

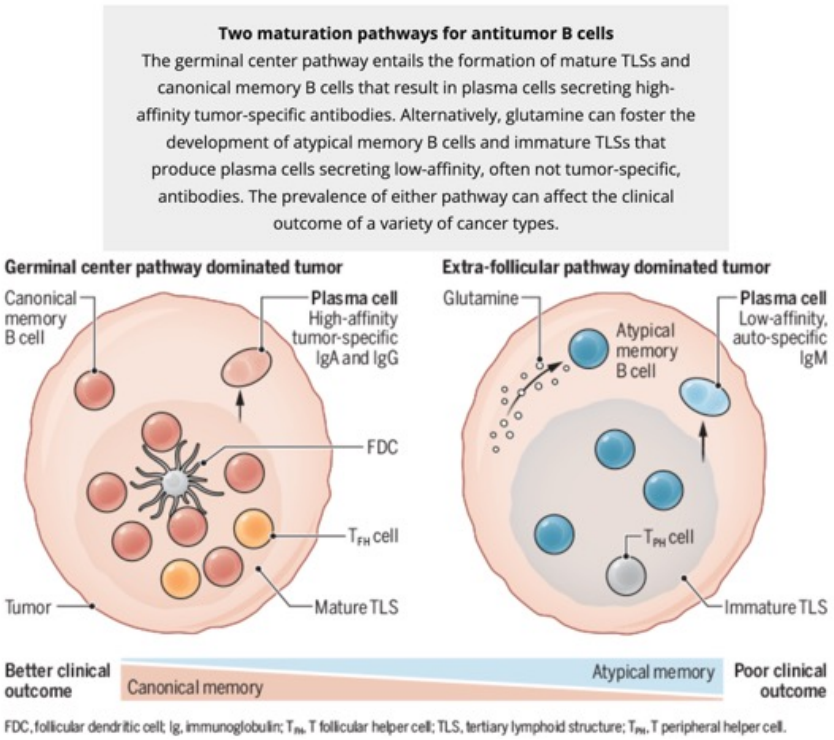

A blueprint for tumor-infiltrating B cells across human cancers

INTRODUCTION: Tumor-infiltrating B cells have emerged as important players in cancer immunity and served as predictors of response to immunotherapy. These B cells display multiple functions, primarily through their ability to differentiate into plasma cells to produce antibodies, but vary spatiotemporally across different cancer types. Dissecting the abundance and differentiation states of B cells across diverse cancer types holds promise for improving the immunotherapeutic response.

RATIONALE: To compile a comprehensive pan-cancer B cell landscape, we performed single-cell RNA sequencing (scRNA-seq) on paired tumors, lymph node metastases, adjacent normal tissues, and peripheral blood from patients with various cancer types, as well as incorporating substantial published scRNA-seq datasets. After correction of the batch effect, this atlas consists of scRNA-seq data from 269 patients across 20 cancer types. We assembled B cell receptor (BCR) sequencing of individual B cells with gene-expression profiles to characterize the dynamic transition between B cells and antibody-secreting cells (ASCs). We integrated the single-cell chromatin accessibility landscape of B cells from different cancers to dissect the epigenomic regulation networks that function in fine-tuning B cell development. We spatially localized B cells in mature versus immature tertiary lymphoid structures (TLSs) and investigated the potential regulators that direct B cells into specific responses.

RESULTS: We revealed substantial heterogeneity within B and plasma cells, identifying 15 B cell subsets and 10 plasma cell subsets. We computationally derived and validated two independent developmental pathways to ASCs through canonical germinal center (GC) and alternative extrafollicular (EF) pathways and demonstrated an apparent cancer-type preference. Colon adenocarcinoma and liver hepatocellular carcinoma were the two representative types of cancer enriched for GC and EF pathways, respectively. We affirmed that EF-dominant cancers correlate with dysregulated immune responses and worse clinical outcomes. We then identified the dynamic metabolic-epigenetic signaling networks engaged in fine-tuning tumor-infiltrating B cell differentiation and managing the balance between the EF and GC pathways. Atypical memory (AtM) B cells, the primary progenitors of EF-derived ASCs, exhibit an exhausted and bystander phenotype and develop independently of the GC pathway. We found that the AtM B cells reside in the center of immature TLSs and spatially relocate to the periphery during TLS maturation. Last, we mechanistically linked these findings to specific transcription factors and epigenomic regulations. We demonstrated that the glutamine-derived metabolite α-ketoglutarate (α-KG) could increase the expression of AtM B cell– associated transcription factors *T-bet* and *BATF* and promote their differentiation, accompanied by the activation of mammalian target of rapamycin complex 1 (mTORC1) signaling. Consequently, AtM B cells acquire an immunoregulatory function that dampens antitumor T cell responses and fosters an immunosuppressive microenvironment.

CONCLUSION: We compiled the blueprint of B cell heterogeneity and two dynamic differentiation pathways in human cancers, providing a fundamental reference of ASC differentiation trajectory for future studies. The systematic comparison between EF and GC pathways reveals the similarities and differences of B cell states across different cancer types, highlighting the unfavorable clinical outcome linked to the immunosuppressive microenvironment of EF pathway–associated AtM B cells. Metabolicepigenetic networks are remarkably flexible and can reconfigure B cell fates in a way that will facilitate the development of B cell–targeted immunotherapies.

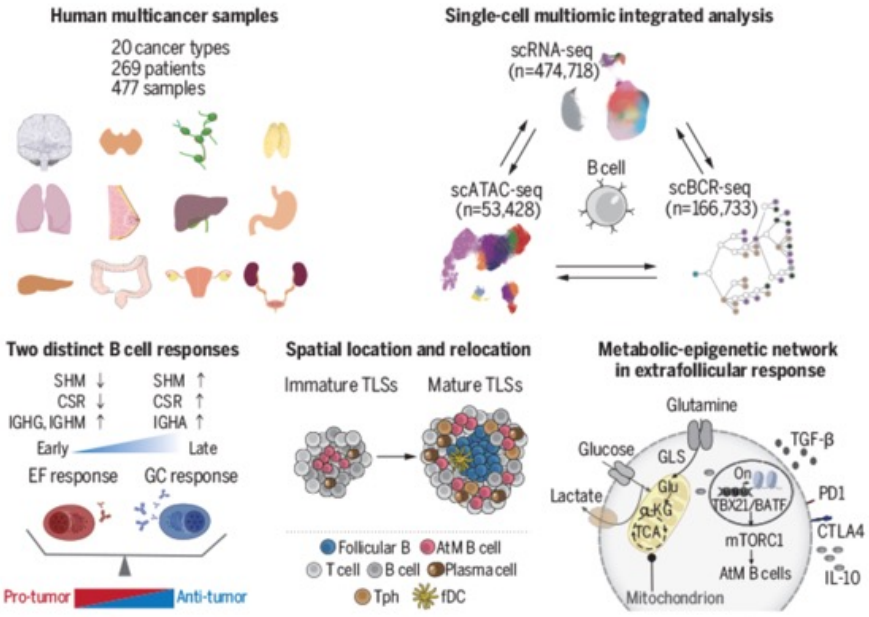

Systematic analysis of a human pan-cancer B cell atlas. We analyzed 474,718 B cells from 269 patients across 20 cancer types using single-cell sequencing data. By combining gene expression profiles, BCR sequences, and chromatin accessibility, we investigated the diversity and plasticity of tumor-infiltrating B cells and performed a multilevel comparison of EF- and GC-responsive plasma cells among cancer types. We visualized their dynamic spatial locations along the maturation of TLSs and identified potential metabolicepigenetic mechanisms in regulating B cell differentiation.

Senior homes refuse to pick up fallen residents, dial 911. ‘Why are they calling us?’

“It doesn’t make sense,” Callison said. “Why are they calling us?”

The answer, according to industry critics and fire officials, is that companies want to avoid the risk and expense associated with picking someone up off the floor. Like many cities, Rockford provides lift assists free.

Some senior-care homes say they don’t have the ability to lift fallen residents. Many have adopted “no lift” policies to avoid the risk of back injuries for staff and other potential liabilities. But firefighters and other experts say there are tools to make lifting easier and safer, ranging from $70 cloth straps with handles to $1,500 hydraulic lifts.

“If you’re on the floor, period, you’d have to call,” said the nurse, who left her position last year. She said residents were often embarrassed by the lift-assist calls. Some begged her not to dial 911. She said she had no choice.